Universidad de Valladolid

Doctoral Program of
Information and Telecommunication Technologies

Doctoral Thesis

Analysis and correlation between brain signals and genetic data for the characterization of the Alzheimer's disease

Thesis presented by **D. Aarón Maturana Candelas**
to apply for the *Ph.D. degree*
from the *University of Valladolid*

Directed by:
Dr. Carlos Gómez Peña and Dr. Roberto Hornero Sánchez

2024
Valladolid, Spain

"Is there anything that we associate more closely with intelligence than curiosity?"
Alexandra Drennan - The Talos Principle

Universidad de Valladolid

Escuela Técnica Superior de Ingenieros de Telecomunicación
Dpto. de Teoría de la Señal y Comunicaciones e Ingeniería Telemática

Research Stay for the International Mention

City:	Stockholm (Sweden)
Faculty:	Department of Neurobiology, Care Sciences and Society (NVS)
Institution:	Karolinska Institutet
Research group:	Division of Clinical Geriatrics
Dates:	25/03/2022 - 25/06/2022
Duration:	90 days (3 months)
Supervisor:	Dra. Vesna Jelic

Agradecimientos

Deseo expresar mi gratitud de manera especial a mis directores de Tesis, los Drs. Carlos Gómez y Roberto Hornero; incluyendo aquí también al Dr. Jesús Poza. Por un lado, por darme la oportunidad de incorporarme a este grupo de investigación sin pruebas de mi valía y, además, por su infinita paciencia soportando la tortura de revisar mis artículos. Sin la interminable serie de segundas oportunidades que me ofrecieron, este trayecto se habría visto posiblemente truncado muy prematuramente.

Por supuesto, amplío mis agradecimientos a los miembros del Grupo de Ingeniería Biomédica. Cuando me preguntan qué tal son mis compañeros de trabajo, suelo decir que me sentía listo hasta que entré aquí. Pero no sólo se caracterizan todos ellos por un intelecto brillante, sino también por un insólito afán de prestar ayuda a quien lo necesita. Cualquier problema que pudiera tener, ya fuera técnico o emocional, era invitado a ser expresado libremente para buscar solución inmediata. Además, cada logro que cumplía, por nimio que fuera, era celebrado como propio (con su correspondiente tortilla de patata). Ello resultaba en una agradable sensación de camaradería que me hacía incluso olvidar (a veces) el punzante y siempre presente síndrome del impostor. Especial mención al bobo de Víctor y al gigachad de Pablo, los cuales tuvieron que llevarme del carrito los primeros años sufriendo preguntas tan pertinentes e interesantes como "¿qué es la potencia relativa esa?". Os debo una por sacarme a pulso del fondo de ese oscuro pozo de viscosa ignorancia en el que me hallaba.

Por último, destacar mi familia como el pilar fundamental que ha sostenido mi determinación a lo largo de todo este proyecto. Cuando te alejas de tus seres queridos, realmente aprecias tener un lugar al que volver, un lugar en el que te esperan incondicionalmente. Un lugar en el que reafirmarte, en el que recuperar fuerzas y valor para volver a enfrentarte a lo desconocido.

Abstract

Alzheimer's disease (AD) is a neurodegenerative disorder characterized by disabling symptomatology that aggravates gradually along its progression in the form of dementia. This syndrome greatly affects cognitive capabilities that involve memory, behavior, and thinking. The more advanced states of dementia are accompanied by devastating deterioration in overall brain functions including language and movement, bringing the patient to a fully-dependent condition. The increase in life expectancy has resulted in a higher prevalence of neurodegenerative diseases, such as AD, which has become a public health concern. For this reason, an understanding of the mechanisms that lead to AD is of paramount importance. Although the current state of the art associates AD with a compilation of biochemical and functional changes in the brain, the actual causes that originate AD are yet to be discerned.

In the present Doctoral Thesis, the electroencephalography (EEG) activity in AD has been characterized using different frameworks that incorporate genetic aspects. These perspectives are aimed at obtaining new insights into the relation between EEG alterations and neurodegeneration caused by AD. They include a multiscale entropy analysis to estimate EEG complexity; a bispectral analysis in order to quantify non-linear interactions between specific frequency components; a spectral analysis in carriers of risk and protective alleles of two genes implicated in cell debris clearance; and finally, a multiplex network analysis in carriers of risk and protective alleles in seven variants of the tau-encoding gene, a protein closely related with AD. These procedures were applied to the resting-state EEG acquired from participants previously categorized in five study groups describing the AD continuum, from healthy control (HC) subjects to severe AD patients.

In the first study, a multiplex entropy analysis was carried out in order to examine the changes in the irregularity and complexity of brain activity along the AD continuum. To investigate these aspects, entropy-based measures were utilized

across various temporal scales. Specifically, multiscale sample entropy (MSE) and refined multiscale spectral entropy (rMSSE) were computed from the EEG. These metrics reported significant differences in slope values and areas under the curve, which have been previously considered complexity estimators. The results of this study demonstrate that both MSE and rMSSE capture the neuronal disruptions linked to the progression of dementia and have the potential to serve as valuable tools in monitoring AD progression.

Subsequently, the study of the non-linear interactions between frequency components allocated in different frequency bands was conducted using a bispectral analysis. Bispectral matrices were obtained in each progression stage in the AD continuum, which showed a decrease in overall frequency interactions in the more advanced phases. Additionally, this study revealed an increase in bispectral interactions between slower frequency bands and the rest of the spectrum with the AD progression, while the opposite pattern was observed for faster frequency bands. Furthermore, the distribution of these interactions was more widespread among frequency components in HC subjects than in AD patients. These findings suggest a progressive decline in inter-band interactions, particularly involving high-frequency components, in correlation with the severity of the disease. Given that inter-band coupling oscillations are associated with intricate and multi-scaled brain processes, these observed alterations likely reflect divergences from normal brain functioning.

Finally, two studies were oriented to evaluate the association of genetic variations in the brain electrical activity. First, the risk and protective alleles of the phosphatidylinositol binding clathrin assembly protein (*PICALM*) and clusterin (*CLU*) genes were established as genotypes of interest, as they are implicated in beta-amyloid clearance from the brain tissue. Subsequently, their association with relative power (RP) in the classical frequency bands was computed. Statistically significant differences in both RP values and their spatial distribution were observed in AD patients between carriers of risk and protective alleles in the beta band. These findings indicate that *PICALM* and *CLU* AD-inducing variants are implicated in physiological mechanisms connected to the disruption of beta power. This observation suggests that alterations in beta-amyloid metabolism are likely to be associated with disturbances in brain function at higher frequencies.

In the second study involving genetic data, microtubule associated protein tau (*MAPT*) was established as the gene of interest. *MAPT* encodes tau, which is a highly relevant protein that contributes to the structural integrity of the microtubules of the neuron. Since differences in *MAPT* sequence can affect the

translational processes, these may ultimately disrupt tau function. The brain functional network was assessed in relation to the risk and protective alleles from 7 *MAPT* variants by applying a multiplex approach in order to evaluate the contribution of each frequency band to the brain functional network. This aspect was assessed using the participation coefficient (P). In most genotypes, significant differences in P disruption (*i.e.* P in AD patients minus P in HC subjects) were observed between risk and protective carriers, especially in the left default mode network. In addition, the node degree in theta and beta bands reported statistically significant differences in most of the SNPs. These findings indicate that diverse variants of the *MAPT* gene could lead to tau species that may affect brain functioning, particularly within regions specialized in information management during preclinical stages.

To sum up, the results obtained along the Doctoral Thesis revealed several insights about the association between AD and alterations in brain electrical activity. First, it was confirmed that AD is associated with continuous deterioration in brain mechanisms that involve information processing. This can be suggested by the significant changes in EEG complexity and bispectral features as AD severity increases. And secondly, it has been demonstrated that brain electrical activation is sensitive to minimal genetic variations associated with AD biochemical biomarkers. In addition, these implications may be more notorious in different cognitive conditions depending on the affected neurophysiological mechanism. Based on the aforementioned findings, this work represents an advance in the understanding of AD at an essential level. Besides, it contributes to elucidating significant relationships between brain electrical activation and aspects, both biological and computational, that could inspire future work in the field of AD prevention.

Acronyms

$A\beta$	Amyloid-beta
AD	Alzheimer's Disease
AD_{MIL}	Mild Alzheimer's Disease Patients
AD_{MOD}	Moderate Alzheimer's Disease Patients
AD_{SEV}	Severe Alzheimer's Disease Patients
AP	Action Potential
APOE	Apolipoprotein E (gene)
ApoE	Apolipoprotein E (protein)
APP	Amyloid Precursor Protein
AUC	Area Under The Curve
CLU	Clusterin (gene)
CLU	Clusterin (protein)
CR1	Complement Receptor Type 1
BispEn	Bispectral Entropy
BispMF	Bispectral Median Frequency
BispRP	Bispectral Relative Power
CAR	Center of Alzheimer Research
CEGEN	Spanish National Center for Genotyping
CK	Cohen-Kappa
ClC	Clustering Coefficient
CSF	Cerebrospinal Fluid
DMN	Default Mode Network
EEG	Electroencephalography
EOAD	Early-Onset Alzheimer's Disease
eQTL	Expression Quantitative Trait Loci
FDR	False Discovery Rate

FIR	Finite Impulse Response
GABA	γ-Aminobutyric Acid
GDS	Global Deterioration Scale
GRCh37	Genome Reference Consortium Human Build 37
GWAS	Genome-Wide Association Study
HC	Healthy Control
HOS	Higher Order Spectra
p-tau	Hyperphosphorylated Tau
ICA	Independent Component Analysis
JCR	Journal Citation Reports
LD	Linkage Disequilibrium
LDA	Linear Discriminant Analysis
LOAD	Late-Onset Alzheimer's Disease
MAPT	Microtubule Associated Protein Tau
MCI	Mild Cognitive Impairment
MMSE	Mini-Mental State Examination
MNA	Multiplex Network Analysis
MSE	Multiscale Entropy
MEG	Magnetoencephalography
MRI	Magnetic Resonance Imaging
NFT	Neurofibrillary Tangles
NIA-AA	National Institute of Aging and Alzheimer's Association
nPSD	Normalized Power Spectral Density
NVS	Neurobiology, Care Sciences, and Society
P	Participation coefficient
PET	Positron Emission Tomography
PICALM	Phosphatidylinositol Binding Clathrin Assembly Protein (gene)
PICALM	Phosphatidylinositol Binding Clathrin Assembly Protein (protein)
PLI	Phase Lag Index
PS	Power Spectrum
PSD	Power Spectral Density
PSEN1	Presenilin 1
PSEN2	Presenilin 2
PSP	Postsynaptic Potential
QC	Quality Control

QDA	Quadratic Discriminant Analysis
QTL	Quantitative Trait Loci
rMSSE	Refined Multiscale Spectral Entropy
RP	Relative Power
ROI	Region Of Interest
SampEn	Sample Entropy
SCI	Subjective Cognitive Impairment
SE	Spatial Entropy
sLORETA	Standardized Low Resolution Brain Electromagnetic Tomography
SMR	Stepwise Multilinear Regression
SNP	Single Nucleotide Polymorphisms
SP	Senile Plaques
SpecEn	Spectral Entropy
sQTL	Splicing Quantitative Trait Loci

Contents

List of Figures

List of Tables

Chapter 1

Introduction

The present Doctoral Thesis focuses on the characterization of Alzheimer's disease (AD) based on the brain electrical activity and genetic variations associated with biomarkers typically involved with neuronal alterations. Although AD has been previously characterized for multiple changes in brain function in isolation, their associations and potential causal relationships with biological aspects are yet to be discerned. For this reason, this Thesis aims to explore these relations analyzing brain electrical activity data from multiple perspectives along the AD progression. For this purpose, the resting-state electroencephalogram (EEG) was acquired from AD patients in diverse stages of severity and age-matched healthy subjects. Subsequently, these data were analyzed to obtain a wide range of features that expressed discordance between study groups or trends in the AD continuum. Finally, a set of physiological interpretations that may cause these disruptions was proposed and discussed. The findings obtained throughout the Doctoral Thesis resulted in the publication of three articles in journals indexed in the Journal Citation Reports (JCR) from the Web of Science^{TM} between May 2019 and October 2021, plus an additional article currently under review. Each manuscript is thematically consistent in the context of bringing new insights into AD characterization. For this reason, this Doctoral Thesis is presented as a compendium of publications.

Section 1.1 comprises the thematic consistency of the Doctoral Thesis. Additionally, the basic principles needed to understand the hypotheses and objectives proposed in this manuscript are briefly mentioned. A summary of the published articles is also included at the end of this section. The general context in which this work is supported is elaborated in section 1.2, describing the

notions of neural signal processing and genetic analyses. Section 1.3 is focused on AD, its etiology, treatment, and the biomolecular principles associated with its progression. The basis of genetic information, analysis, and state of art about early onset (EOAD) and late-onset AD (LOAD) genetic expression are detailed in Section 1.4. Subsequently, Section 1.5 explains the fundamentals of neural activity, detailing the principles of action and postsynaptic potentials and how these phenomena are reflected in the EEG. In addition, the classical frequency bands and the levels of EEG analysis commonly used in research are described. Finally, the state of the art regarding the use and analysis of the EEG and genetics in the AD characterization is explained in Section 1.6.

1.1 Compendium of publications: Thematic consistency

Throughout evolution, the nervous system is one of the most sophisticated structures that living beings have ever developed. This intricate network of cells called neurons, capable of precise and high-speed transmission of information across the body, has become essential in animal organisms. Neurons activate synchronously using voltage-dependent mechanisms that result in chain reactions of ionic flows, which manifest macroscopically as fluctuations of electric potentials (Im, 2018). As multicellular beings evolved into bigger and more complex entities, the processing of information, such as external stimuli, became crucial for understanding the environmental context (Arendt, 2021). The ability to process larger amounts of information allowed organisms to conduct a proper reaction and increase the chances of survival (Arendt, 2021). For this reason, a vast variety of living beings in the animal kingdom were involved in an "arms race" for better and more efficient intra-organism communication systems. One could say that the paramount of this process culminates in the development of the human brain. This organ is composed of more than 86 billion neurons (Azevedo et al., 2009) allocated in several lobes specialized in a wide diversity of functions (Schoenemann, 2006). The most sophisticated processing capabilities of the human brain, namely the *higher brain functions*, involves mechanisms such as cognition, which includes language, complex perception, judgment, and decision making; and behavior, which is the manifestation of these cognitive functions (Tranel et al., 2003). However, like any other biological system, the chance of malfunctioning or deterioration due to disease or trauma is always present.

Medical advances have contributed to eradicating or, at least, diminishing the effect of uncountable ailments. Human beings have achieved overcoming infectious diseases, one of the main causes of death in the past (Shaw-Taylor, 2020). However, this leads nowadays to a greater challenge: Dealing with neuropathologies. With the unavoidable aging of the population, the degradation of the central nervous system has become one of the main concerns for public health (Gauthier et al., 2021). The diagnosis and effective treatment of brain pathologies require understanding the fundamentals of neurodegeneration, especially at early stages (Gauthier et al., 2021). This is a complicated task due to the convoluted nature of the brain and its highly non-linear behavior. Since we are not even close to comprehending the nuances of brain functioning, every piece of research aimed at this cause is of great value.

This Doctoral Thesis aims to contribute to the existing literature regarding the characterization of AD, which is one of the main causes of neurodegeneration. To this end, brain electrical activity and genetic features were extracted, compared, and discussed in the different stages of AD severity. The obtained data were reported in four articles consistent with the theme of defining new physiological features in AD. The insights proposed in these documents could be potentially useful to establish new hallmarks of AD in order to improve diagnostic procedures. The thematic consistency that encompasses these works is illustrated in Figure 1.1.

The papers included in this compendium of publications are listed in chronological order. The initial two manuscripts exclusively comprised analyses of EEG features, while the last two integrated genetic information into these data. The first paper (Maturana-Candelas et al., 2019) focused on the effects of neurodegeneration on EEG entropy. In signal theory, entropy measures the irregularity (or unpredictability) of a time series (Shannon, 1948). In addition, this study implemented a multiscale approach. This means that the calculations of entropy were considered in different temporal scales. Multiscale entropy has been previously used to estimate complexity (Costa et al., 2005), which is also related to the amount of "meaningful" information that a physical object is able to store (Grassberger, 1991). In this regard, AD patients showed lower levels of complexity in their EEGs compared with healthy subjects. This study was conducted taking the AD continuum into account, which allowed visualizing entropy alterations along AD progression, including its prodromal forms. The second paper (Maturana-Candelas et al., 2020) focused on bispectral analysis in order to characterize the inter-band interactions in AD patients compared with healthy controls. Bispectrum is the higher order spectra (HOS) of the

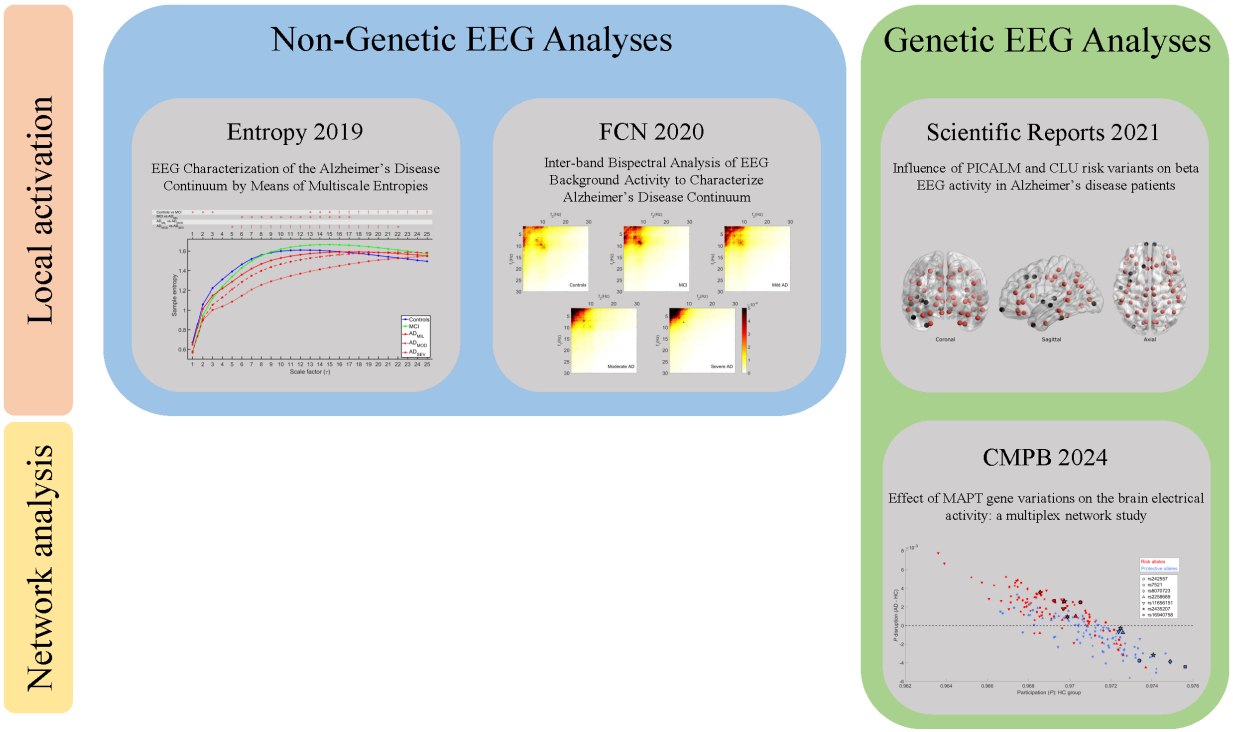

Figure 1.1: Schematic diagram displaying each published contribution included in the compendium of publications. Two grand groups were established distinguishing between non-genetic (Maturana-Candelas et al. (2019, 2020)) and genetic (Maturana-Candelas et al. (2021, 2024)) EEG analyses. Also, upper row encompasses local activation studies, while the lower row includes a network analysis.

third-order statistics or "cumulants" (Nikias and Mendel, 1993). This metric is sensitive to divergences from Gaussianity of the series distributions, which is able to reflect non-linear interactions. This is a great advantage compared to the power spectrum density, in which these elements are suppressed. Bispectrum was used to calculate three novel features in inter-band ranges, namely, those matrix locations that reflected interactions between components from strictly different frequency bands (*i.e.*, delta-theta, alpha-beta, etc.). We obtained significant tendencies in each feature along the AD continuum, especially those involving high-frequency components. The third paper (Maturana-Candelas et al., 2021) was the first that was centered on studying genotype populations. In this work, relative power (RP) in each classical frequency band was calculated in each brain region of interest (ROI). This calculation was performed in the EEG of healthy controls and AD patients, classified as well as carriers of risk and protective alleles of phosphatidylinositol binding clathrin assembly protein (*PICALM*) and clusterin (*CLU*) genes. The beta band showed significant differences between AD patients carrying different genotypes, with those carrying protective alleles showing greater resemblance to subjects at earlier stages of neurodegeneration. Finally, the fourth paper (Maturana-Candelas et al., 2024) studied the differences in brain electrical activity between carriers of microtubule associated protein tau (*MAPT*) risk and protective alleles. In this case, several genetic variants were integrated in order to ensure that the results were associated with *MAPT* and not with other causes. This work incorporated a parameter derived from multiplex analysis (participation coefficient, P) to examine the homogeneity of inter-band interactions. The disruption in P values between healthy controls and AD patients was different between genotypes. Furthermore, the left default mode network (DMN) showed greater differences than any other region. This is evidence that tau expression and structure could have an impact on the brain functional network, even in preclinical states.

Given these manuscripts are essential to understand the insights provided by this Doctoral Thesis, they have been included in Appendix 8. More information regarding each published paper along with each abstract are displayed below:

EEG characterization of the Alzheimer's disease continuum by means of multiscale entropies (Maturana-Candelas et al., 2019)

Aarón Maturana-Candelas, Carlos Gómez, Jesús Poza, Nadia Pinto, and Roberto Hornero. *Entropy*, vol. 21(6), p. 544, 2019. Impact factor in 2019: 2.494, Q2 in "PHYSICS, MULTIDISCIPLINARY" (Journal Citation Reports - Clarivate Analytics).

Alzheimer's disease (AD) is a neurodegenerative disorder with high prevalence, known for its highly disabling symptoms. The aim of this study is to characterize the alterations in the irregularity and the complexity of the brain activity along the AD continuum. Both irregularity and complexity can be studied applying entropy-based measures throughout multiple temporal scales. In this regard, multiscale sample entropy (MSE) and refined multiscale spectral entropy (rMSSE) were calculated from electroencephalographic (EEG) data. Five minutes of resting-state EEG activity were recorded from 51 healthy controls, 51 mild cognitive impaired (MCI) subjects, 51 mild AD patients (AD_{MIL}), 50 moderate AD patients (AD_{MOD}), and 50 severe AD patients (AD_{SEV}). Our results showed statistically significant differences (p-values < 0.05, FDR-corrected Kruskal-Wallis test) between the five groups in every temporal scale. Additionally, average slope values and areas under MSE and rMSSE curves revealed significant changes in complexity for controls vs. MCI, MCI vs. AD_{MIL} and AD_{MOD} vs. AD_{SEV} comparisons (p-values < 0.05, FDR-corrected Mann-Whitney U-test). These findings indicate that MSE and rMSSE reflect the neuronal disturbances associated with the development of dementia, and may contribute to the development of new tools to track the AD progression.

Inter-band bispectral analysis of EEG background activity to characterize Alzheimer's disease continuum (Maturana-Candelas et al., 2020)

Aarón Maturana-Candelas, Carlos Gómez, Jesús Poza, Saúl J. Ruiz-Gómez, and Roberto Hornero. *Frontiers in Computational Neuroscience*, vol. 14, p. 70, 2020. Impact factor in 2020: 2.380, Q2 in "MATHEMATICAL & COMPUTATIONAL BIOLOGY" (Journal Citation Reports - Clarivate Analytics).

The aim of this study was to characterize the EEG alterations in inter-band interactions along the Alzheimer's disease (AD) continuum. For this purpose, EEG background activity from 51 healthy control subjects, 51 mild cognitive impairment patients, 50 mild AD patients, 50 moderate AD patients, and 50 severe AD patients was analyzed by means of bispectrum. Three inter-band features were extracted from bispectrum matrices: bispectral relative power (BispRP), cubic bispectral entropy (BispEn), and bispectral median frequency (BispMF). BispRP results showed an increase of delta- and theta-interactions with other frequency bands, and the opposite behavior for alpha, beta-1 and beta-2. Delta- and theta-interactions with the rest of the spectrum also experimented a decrease of BispEn with the disease progression, suggesting these bands interact with a reduced variety of components in advanced stages of dementia. Finally, BispMF showed a consistent reduction along the AD continuum in all bands, which reflects an interaction of the global spectrum with lower frequency bands as the disease develops. Our results indicate a progressive decrease of inter-band interactions with the severity of the disease, especially those involving high frequency components. Since inter-band coupling oscillations are related with complex and multi-scaled brain processes, these alterations likely reflect the neurodegeneration associated with AD continuum.

Influence of *PICALM* and *CLU* risk variants on beta EEG activity in Alzheimer's disease patients (Maturana-Candelas et al., 2021)

Aarón Maturana-Candelas, Carlos Gómez, Jesús Poza, Víctor Rodríguez-González, Víctor Gutiérrez-de Pablo, Alexandra M. Lopes, Nadia Pinto, and Roberto Hornero. *Scientific Reports*, vol. 11(1), p. 1-11, 2021. Impact factor in 2021: 4.996, Q2 in "MULTIDISCIPLINARY SCIENCES" (Journal Citation Reports - Clarivate Analytics).

PICALM and *CLU* genes have been linked to alterations in brain biochemical processes that may have an impact on Alzheimer's disease (AD) development and neurophysiological dynamics. The aim of this study is to analyze the relationship between the electroencephalographic (EEG) activity and the *PICALM* and *CLU* alleles described as conferring risk or protective effects on AD patients and healthy controls. For this purpose, EEG activity was acquired from: 18 AD patients and 12 controls carrying risk alleles of both *PICALM* and *CLU* genes, and 35 AD patients and 12 controls carrying both protective alleles. Relative power (RP) in the conventional EEG frequency bands (delta, theta, alpha, beta, and gamma) was computed to quantify the brain activity at source level. In addition, spatial entropy (SE) was calculated in each band to characterize the regional distribution of the RP values throughout the brain. Statistically significant differences in global RP and SE at beta band (p-values < 0.05, Mann-Whitney U-test) were found between genotypes in the AD group. Furthermore, RP showed statistically significant differences in 58 cortical regions out of the 68 analyzed in AD. No statistically significant differences were found in the control group at any frequency band. Our results suggest that *PICALM* and *CLU* AD-inducing genotypes are involved in physiological processes related to disruption in beta power, which may be associated with physiological disturbances such as alterations in beta-amyloid and neurotransmitter metabolism.

Effect of MAPT gene variations on the brain electrical activity: a multiplex network study (Maturana-Candelas et al., 2024)

Aarón Maturana-Candelas, Roberto Hornero, Jesús Poza, Víctor Rodríguez-González, Víctor Gutiérrez-de Pablo, Nadia Pinto, Miguel A. Rebelo, Carlos Gómez. (UNDER REVIEW in *Computer Methods and Programs in Biomedicine*).

Background and Objective: Tauopathies are usually related to anomalies in brain connectivity patterns. These signs of neurophysiological alterations are associated with disturbances in information flow and processing. However, the implications of genetic variations associated with the tau protein in the brain functional network are not clearly understood. Hence, the aim of this study is to examine how variations in the microtubule-associated protein tau (*MAPT*) gene affect neural dynamics. Methods: Resting-state electroencephalogram (EEG) data from 155 participants were acquired, including healthy controls and Alzheimer's disease patients carrying *MAPT* alleles associated with risk or protective effects against the development of neuropathologies or abnormal tau presence in cerebrospinal fluid. Particularly, seven single nucleotide polymorphisms (SNPs) associated with *MAPT* were analyzed. In order to identify the effects of each genotype on neural activity, we performed a multiplex network analysis on the EEG data. Specifically, the connectivity contribution of each node in the frequency-dependent multiplex network was quantified using the participation coefficient (P). This parameter was obtained calculating the phase lag index (PLI) from the EEG previously filtered in the conventional frequency bands: delta, theta, alpha, and beta. The PLI adjacency matrices in each frequency band corresponded to the layers conforming the multiplex network. Subsequently, P was computed from the PLI distributions across layers in every brain region corresponding to the Yeo-7 atlas, reflecting node degree diversification among frequency bands. Results: Carriers of risk and protective alleles exhibited distinct values of P, especially in healthy controls at the left default mode network. In general, carriers of the risk alleles also presented higher network disruptions. In addition, significant differences in node degree values were observed across SNPs in the theta and beta frequency bands. Conclusions: Different *MAPT* variants may lead to diverse tau species that influence brain function, specifically in the brain regions involved in information flow management in preclinical states. These insights may help understanding network disturbances caused by molecular factors.

1.2 Context: Neural signal processing and genetic analyses

Brain processes are underpinned by electrical dynamics. Brain alterations that diverge from healthy states are reflected in neural activation and signaling. With the advances in technology and computation in the last century, numerous techniques aiming to study the disruptions of brain functioning have been developed. These have allowed not only the acquisition of neurophysiological data, but also their processing in order to extract meaningful information. On this line, abundant neurological disorders have been recently characterized through biosignal analysis (Bai et al., 2017; Newson and Thiagarajan, 2019; Stam, 2014). However, the fundamentals of brain processes are also biological and biochemical. Neurotransmitters play an essential role in the brain electrical activity and disturbances in their release, uptake, and synthesis are associated with deterioration of multiple brain subsystems (Kandimalla and Reddy, 2017). Other biochemical alterations can contribute to anomalies in neural behavior in the form of byproducts yielded by disrupted metabolic pathways (Carrillo-Mora et al., 2014; Hyman, 2023). Neural malfunctioning can also be aggravated by indirect causes, such as changes in cellular adhesion, autophagy, or endocytosis (Bao et al., 2015; Kimura and Yanagisawa, 2018; Nixon, 2013). All these aspects could be affected by genetic expression and anomalies in this mechanism can result in severe physiological disruption that leads to disease.

In this Doctoral Thesis, neuronal signaling and genetic analyses are applied together to characterize the neurodegeneration process that accompanies AD. Brain electrical activity data were obtained in the form of resting-state EEG in noise-free environments from healthy subjects and AD patients. On the other hand, the genetic data were obtained from the genotyping of either saliva or mucosa samples collected from each participant. This process resulted in a collection of 692359 single nucleotide polymorphisms (SNP) located in all 23 chromosome pairs. The genotyping procedure was performed at the Spanish National Center for Genotyping (CEGEN, Santiago de Compostela, Spain), whilst the subsequent genetic analyses were carried out by our collaborators in Portugal. The integration of both perspectives allowed us to obtain a compilation of features that could be potentially useful in the development of diagnostic bio-computational devices.

1.3 The Alzheimer's disease

Alzheimer's disease (AD) is a neurological disorder, characterized by biochemical and structural changes in the brain which culminate in neuronal damage and, eventually, cognitive impairment. AD is the most common cause of dementia, accounting for 60-80% of cases (Alzheimer's Association, 2022). The main risk factor of AD is age, which increases exponentially as the subject gets older (Gauthier et al., 2021). However, other elements such as genetics and habits have a significant impact on the development of the disease (Gauthier et al., 2021). Since AD is so disruptive physically and mentally, families and caregivers need to implicate in common tasks on a daily basis to ensure the well-being of the patient. For this reason, AD not only affects the individual but also disrupts the lives of the relatives.

In the last decades, AD has become one of the main concerns to public health since 55 million people have developed some form of dementia (Gauthier et al., 2021). This number is expected to increase because of the gradual aging of the population worldwide, estimating around 78 million dementia patients by 2030 (Gauthier et al., 2021). Treatment and caregiving costs for society were expected to reach an economic burden of US$321 billion in 2022 (Alzheimer's Association, 2022). Hence, the development of new bio-computational tools in order to obtain more accurate AD diagnoses at the early stages of neurodegeneration is of great interest. Although the cure for the disease is hard to imagine in the near future, this approach could be decisive in enhancing therapy effectiveness.

1.3.1 Etiology

AD pathogenesis can be identified in two clinical conditions: Early-onset AD (EOAD) and late-onset AD (LOAD). EOAD is defined as AD occurring under age 65 and its causes are primarily genetic (Cacace et al., 2016). Highly penetrant mutations in amyloid precursor protein (*APP*) and the presenilins 1 and 2 (*PSEN1* and *PSEN2*) have been robustly associated with EOAD (Cacace et al., 2016). However, EOAD only comprises 1% of AD cases (Gauthier et al., 2021), which mostly expresses in its LOAD form. LOAD is also associated with genetic expression, especially with the $\epsilon 4$ variant of apolipoprotein E (APOE) (Farrer, 1997), but its etiology is much more diverse. For the aforementioned reasons, this Doctoral Thesis is specific to LOAD when referring to AD.

According to the National Institute of Aging and Alzheimer's Association (NIA-AA) (Jack et al., 2018), the biological hallmark of AD includes the

histological presence of senile plaques (SP) and neurofibrillary tangles (NFT) in the neural tissue. SPs are insoluble aggregates of oligomerized fibrils of beta-amyloid ($A\beta$), the result of an altered cleavage of the transmembrane protein APP. The participation of β-secretase in the proteolysis, followed by γ-secretase, yields a residue consisting of a peptide up to 42 amino acids long (Carrillo-Mora et al., 2014). This pathogenic sequence constitutes what is called amyloidogenesis (Kisilevsky, 2000). Subsequently, due to its high hydrophobicity, this molecule tends to aggregate, finally resulting in SP formation. Initially, SPs were considered the central cause of AD pathogenesis (Glenner and Wong, 1984). However, that thesis was later reinterpreted as the "amyloid cascade hypothesis" of AD, suggesting that alternative potential causes for neuronal damage may exist (Hardy and Higgins, 1992). Indeed, more recent studies have suggested that the soluble $A\beta$ oligomers, and not their deposition in the form of SPs, is the original source of neurotoxicity (Haass and Selkoe, 2007; Kirkitadze et al., 2002; Klein et al., 2004). Besides, this interpretation has been further challenged, suggesting that $A\beta$ fibrillation may even be a protection mechanism (Carrillo-Mora et al., 2014; Cheng et al., 2007). Among the variety of $A\beta$ alloforms previously observed, the peptide $A\beta 42$ expresses the greatest association with AD (Mitternacht et al., 2010). Nonetheless, $A\beta 42/A\beta 40$ ratios have been found to predict AD with higher accuracy than with just $A\beta 42$ (Janelidze et al., 2016).

NFTs are located in the cytoplasm and accompany their presence with SPs in AD. NFTs are composed of agglutinated hyperphosphorylated tau (p-tau) fibrils that have detached from the cytoskeleton (Chi et al., 2019). The tau protein is codified by the microtubule-associated protein tau (*MAPT*) gene (Chi et al., 2019). Tau consists of a sequence from 352 to 441 amino acids, and it is crucial in providing motility and stability to the neuron, specifically contributing to the integrity and spacing of microtubules (Drubin and Kirschner, 1986). This is thought to prevent or, at least, slow microtubule depolymerization (Drubin and Kirschner, 1986). In addition, tau is also involved in axonal transport, which when compromised can affect APP metabolism, synaptic functioning, and NFT formation itself (Terwel et al., 2002). In its normal form, tau is subject to a balance between phosphorylation and dephosphorylation processes (Terwel et al., 2002). When this balance breaks, tau hyperphosphorylates and changes its conformational configuration (Hallinan et al., 2019). This alteration results in detachment from the microtubules, not only generating diverse inflammatory responses (Hyman, 2023), but also compromising axonal functions and integrity resulting in its eventual degradation (Terwel et al., 2002). Tau anomalies have

been even suggested to be the "central executer" in the chain of events, leading to neurophysiological and biochemical disruptions associated with neurodegeneration (also called tauopathies, see Chi et al. (2019)), questioning the cause-effect relation with amyloid neurotoxicity (Terwel et al., 2002). Furthermore, a recent review indicates that NFTs are not even the real cause of inflammatory processes, but soluble and not yet aggregated fibrils and oligomers of hyperphosphorylated tau, which comprise a dominant driver of AD neurodegeneration (Hyman, 2023). However, the actual causation process that leads to AD is not clearly understood and is not devoid of controversy. NFTs and SPs have been associated with chronic inflammatory responses and the disruption of other physiological mechanisms (Carrillo-Mora et al., 2014; Farias et al., 2011). Nonetheless, these anomalies might turn out to be secondary processes not necessarily related to the primary cause. Previously, it has been suggested that some of these biochemical changes may be attributed to purely physiological factors or even to neuroprotective responses (Carrillo-Mora et al., 2014). In addition, research aimed at detecting causative factors in AD indicates external aspects as possible origins of the disease, such as infectious agents (Sochocka et al., 2017) or metallic contamination (Shcherbatykh and Carpenter, 2007).

Another pathological hallmark in AD is neurotransmitter deficits, which have been associated with impairments in numerous cognitive processes, such as memory and learning (Kandimalla and Reddy, 2017). Among the wide variety of neurotransmitters that regulate brain functioning, acetylcholine exhibits the greatest anomalies and the highest association with the severity of the disease (Ferreira-Vieira et al., 2016). However, other systems, such as dopaminergic (Pan et al., 2019), glutaminergic (Zádori et al., 2014), and serotonergic (Chakraborty et al., 2019), are disturbed in AD. Disruptions in these neural populations are also subject to genetic expression. For instance, noradrenergic signaling has been suggested to be affected by the deregulation of certain genes, and polymorphisms in these loci could alter AD risk (Belbin et al., 2019).

1.3.2 Diagnosis and treatment

The definite AD diagnosis, according to Jack et al. (2016), is defined by the presence of 7 biomarkers which can be organized into three main categories: The first one is amyloid-related biomarkers, which comprises positron emission tomography (PET) amyloid and cerebrospinal fluid (CSF) $A\beta 42$. The second one is tau-related biomarkers, which include CSF p-tau and PET tau. The

third one combines biomarkers related to neurodegeneration and neural injury, which are [^{18}F]-fluorodeoxyglucose–PET, structural magnetic resonance imaging (MRI), and CSF total tau. This framework is known as the A/T/N system (Jack et al., 2016, 2018), which provides an unbiased diagnostic criterion. However, biopsies of brain tissue are extremely invasive, and obtaining medical images is often unaffordable. For this reason, alternative means to discern the severity of the disease are currently applied. A variety of cognitive tests are usually used to assess dementia, such as Clinical Dementia Rating (Hughes et al., 1982) and Mini-Mental State Examination (MMSE) (Folstein et al., 1975). Noteworthy, these methods ascertain cognitive impairment, which is an indirect means to estimate neurodegenerative severity. Therefore, these methods come with limitations, such as the subjectivity of the interpretations of some of the test responses. Besides, these tests do not disregard factors not necessarily related to neurodegeneration, such as blindness or essential tremor. Hence, the results must be adjusted in order to minimize bias.

Diagnosing AD carries an additional challenge, which is called mixed dementia. First, it is important to discern between AD and dementia. AD is referred to the changes that the brain experiments regarding the three categories aforementioned, also being the main cause of dementia. On the other hand, dementia is an overall term that describes a particular group of symptoms. These symptoms include impairments in memory, language, problem-solving, and other cognitive abilities (Alzheimer's Association, 2022). Causes that lead to dementia are diverse, such as AD, cerebrovascular disease, Lewy body disease, Parkinson's disease, and many others (Alzheimer's Association, 2022). In general, AD is expressed combined with other types of neurodegenerative disorders. In fact, only 3% cases of possible AD patients are "pure" AD, while 82% express changes of, at least, one additional cause of dementia (Alzheimer's Association, 2022). The remaining 15% have alterations related to other kinds of dementia (Alzheimer's Association, 2022). For the aforementioned reasons, one could understand the importance of developing diagnostic tools to ease the characterization of neurodegenerative states.

The treatment of dementia due to AD is carried out pharmacologically and non-pharmacologically. Although no treatment currently exists to completely arrest or reverse the effects of neurodegeneration, some interventions have proven effective in slowing the pathological cascade that leads to neuronal dysfunction. On one hand, a variety of drugs have been developed in this regard, showing limited effectiveness in improving cognition (Long and Holtzman, 2019; Marucci et al., 2021) or being not fully validated (Alexander and Karlawish, 2021). Among

them, only six have been approved by the U.S. Food and Drug Administration. These are Aduhelm (aducanumab-avwa), ARICEPT (donepezil hydrochloride), Exelon Patch (rivastigmine transdermal system), Namenda (memantine HCl), Namzaric (memantine hydrochloride extended-release + donepezil hydrochloride), and Reminyl (galantamine hydrobromide) (National Institute of Aging, 2023) (CenterWatch, 2023). These drugs may even help alleviate some of the behavioral and psychiatric symptoms that are commonly expressed in moderate-to-severe AD, such as depression, apathy, and anxiety (Massoud and Léger, 2011). However, they have been associated with frequent and severe side effects, such as nausea, anorexia, vomiting, and diarrhea, as well as weight loss, insomnia, abnormal dreams, muscle cramps, bradycardia, syncope, and fatigue (Bianchetti et al., 2006). For this reason, their prescription must be conducted with extreme caution.

On the other hand, therapeutic strategies have been applied from non-pharmacological approaches. Non-drug interventions are based on cognitive stimuli and tasks with the aim of reducing cognitive and behavioral symptoms (Alzheimer's Association, 2022). Examples of these applications are art and music therapies, and cognitive training and stimulation (Alzheimer's Association, 2022). Exercise and nutrition interventions have been proven to have positive effects in maintaining cognitive functions, which are recommended to be applied to supporting other therapeutic procedures (Alzheimer's Association, 2022).

1.3.3 Mild cognitive impairment: The Alzheimer's disease as a continuum

AD is a neurodegenerative disorder that is characterized by its gradual symptomatic progression. The pathological changes that occur in the brain are also gradual and begin up to 20 years before the first symptoms appear (Alzheimer's Association, 2022). At the beginning, the subject experiments an insidious cognitive deficit caused by progressive neuronal damage. Despite being potentially frequent, symptoms in this stage are nothing more than an annoyance and the subject's daily tasks are practically unaltered. This pre-clinical condition is called subjective cognitive impairment (SCI) (Stewart, 2012). Although this state does not necessarily lead to neurodegeneration, SCI is considered a marker of risk for dementia (Stewart, 2012). This would be the first step of what is called the AD continuum. AD continuum describes a continuous deterioration of cognitive abilities over time, from slight memory loss to severe impairments in basic functions leading to total disability or even death. The second step towards

definite AD is mild cognitive impairment (MCI). MCI is the first clinical state, in which patients are diagnosed with slight cognitive deficits but insufficient to categorize them as dementia symptoms (Petersen, 2004).

MCI is a clinical condition that is considered separate from AD. The categorization of MCI has been a controversial topic, starting from being considered a prodromal state of AD to a more heterogeneous construct (Wolk and Vaishnavi, 2016). Nowadays, MCI subtypes are described based on the biomarkers present. Thus, "MCI due to AD" may exist if a particular subject has brain changes with typical AD characteristics (Wolk and Vaishnavi, 2016). Despite being considered a preceding stage of AD, MCI does not necessarily lead to dementia. In fact, some patients do not progress to any state of greater deterioration and there are even reversions to normal cognition (Wolk and Vaishnavi, 2016). Unfortunately, the most common scenario is clinical progression to a definite neurodegenerative disorder.

As greater levels of AD biomarkers are reached, dementia due to AD can be diagnosed. In this stage, cognitive skills, behavior, and memory are significantly altered. Reisberg (1986) contemplated the continuous nature of the cognitive decline from degenerative dementia in different steps, which can be grouped into mild, moderate, and severe dementia. This classification was determined by means of the Global Deterioration Scale (GDS), which reflects an overview of cognitive function (Reisberg, 1986). Adjusting the Reisberg's scale to the context of this Doctoral Thesis, three groups of AD severity can be established: Mild AD (AD_{MIL}), moderate AD (AD_{MOD}), and severe AD (AD_{SEV}). AD_{MIL} patients show relatively high performance in tasks, such as working, driving, or leisure activities. Although requiring some assistance and vigilance, AD_{MIL} patients are generally independent on a daily basis. In the stage of AD_{MOD}, patients can no longer survive without assistance and are usually unable to recall relevant aspects of their life. Furthermore, patients tend to show significant behavioral changes, such as agitation and suspiciousness. Finally, AD_{SEV} patients become completely dependent on fundamental routines, such as toileting and feeding. During this stage, basic psychomotor skills and the ability to speak are also lost.

1.4 The genetics of the Alzheimer's disease

Sometimes, the biochemical unbalances observed in AD have a foundation in genetics. Genetic expression has proved to be strongly associated with AD and other types of neurodegenerative disorders (Bellenguez et al., 2020; Tanzi, 2012).

The most straightforward genetic features related to AD are those characteristic of EOAD, as mentioned in Section 1.3.1. Mutations in the *APP*, *PSEN1*, and *PSEN2* genes are, although rare, highly penetrant and virtually guarantee familial EOAD (Tanzi, 2012). To date, 73 mutations have been registered for *APP*, 350 for *PSEN1*, and 87 for *PSEN2* (Alzforum, 2023). In the case of LOAD, the genetic feature showing the highest association with the disease is the allele $\epsilon 4$ of the apolipoprotein E (*APOE*). This gene is located at chromosome 19q13.2 and encodes a plasma protein (ApoE) involved in cholesterol transport (Strittmatter et al., 1993). ApoE is implicated in nervous growth and repair mechanisms during development and its synthesis is increased as a response to injury (Strittmatter et al., 1993). Farrer (1997) found that subjects with one $\epsilon 4$ allele were 4 times more likely to develop AD than individuals carrying the most common genotype $\epsilon 3/\epsilon 3$. Furthermore, homozygous $\epsilon 4/\epsilon 4$ subjects were exposed to about 15 times the risk when compared with subjects with genotype $\epsilon 3/\epsilon 3$. For this reason, *APOE* $\epsilon 4$ was originally established as the main risk factor for AD. Additionally, other studies have identified genotypes affecting numerous physiological mechanisms, such as autophagy (Nixon, 2013), cell adhesion (Bao et al., 2015), and endocytosis (Kimura and Yanagisawa, 2018). These processes eventually compromise neuronal stability contributing to brain damage and potentially exacerbating AD pathogenesis.

The technical improvements in genomics achieved throughout the 2000s allowed the characterization of other genetic risk factors. In particular, genome-wide association studies (GWASs) made possible to unveil significant associations between gene expression and AD by studying millions of genetic variations (Abdellaoui et al., 2023). Two of these GWASs were published in 2009 with the discovery of several new genetic loci associated with AD, among which Clusterin (*CLU*), complement receptor type 1 (*CR1*) and phosphatidylinositol binding clathrin assembly protein (*PICALM*) genes were revealed (Harold et al., 2009; Lambert et al., 2009). *CLU* and *PICALM* have been also related to Aβ clearance and SP formation (DeMattos et al., 2002; Xu et al., 2015; Zhao et al., 2015; Zlokovic et al., 1994), which may have an impact on neurodegenerative processes and brain functioning. In this Doctoral Thesis, efforts have been focused on studying the implications of *CLU*, *PICALM*, and *MAPT* genetic variations in the EEG. These genes and proteins led by their expression are briefly described below:

- Clusterin (**CLU**, or apolipoprotein J) is a heterodimer associated with various functions, including apoptotic cell death, membrane lipid recycling, and acting as a stress-induced secreted chaperone protein, among others (Jones, 2002). In humans, its encoding gene, ***CLU***, is located on chromosome

8p21 and contains 9 exons, 8 introns, and a terminal 3'-untranslated region (Koltai, 2014; Yu and Tan, 2012). *CLU* exhibits alternative splicing at the first exon, giving rise to three protein isoforms (Yu and Tan, 2012). The three isoforms of CLU are directed to discrete subcellular locations, with one isoform being situated in the nucleus, another in the cytoplasm, and the third secreted from the cell (Koltai, 2014; Yu and Tan, 2012). As a chaperone protein, CLU supports the correct folding of secreted proteins. Its three isoforms are differentially linked to pro- or anti-apoptotic processes and are involved in oxidative stress-related pathways (Trougakos et al., 2004).

- Phosphatidylinositol binding clathrin assembly protein (**PICALM**) is encoded by ***PICALM***, located in chromosome 11q14 which contains 112 kb (Xu et al., 2015). PICALM is present in a wide variety of vertebrate organisms, tissues, and cells, including neurons, astrocytes, and oligodendrocytes in the central nervous system (Xu et al., 2015). PICALM plays a major role in clathrin-mediated endocytosis, which transports ligands binding the receptor to the cytoplasm from the extracellular matrix. These ligands are varied and can include lipids, proteins, neurotransmitters, and growth factors (Xu et al., 2015). In the case of AD, PICALM has been suggested to be crucial in amyloidogenesis, Aβ clearance, synaptic function, lipid metabolism, immune disorders, and iron homeostasis (Xu et al., 2015).

- **Tau** is encoded by the ***MAPT*** gene, which is located in chromosome 17q21, containing 16 exons (Sergeant et al., 2005) and resides within a ~900 kb inversion polymorphism (Allen et al., 2014). Tau is assembled in six major isoforms as a result of alternative splicing of exons 2, 3, and 10 of *MAPT* (Goedert et al., 1989). Depending on the inclusion or exclusion of exon 10, tau can be built with three (3R-tau) or four (4R-tau) microtubule-binding domains. The longest tau isoform in the central nervous system consists of four repeats (R1, R2, R3, and R4) and two inserts, adding up to a total of 441 amino acids. On the other hand, the shortest isoform has three repeats (R1, R3, and R4) and lacks any inserts, totaling 352 amino acids. The *MAPT* gene has two known haplotypes, called H1 and H2. H1 has been strongly associated with increased risk of progressive supranuclear palsy and corticobasal degeneration (Allen et al., 2014). On the other hand, H2 is associated with higher expression levels of exon 3 and, although it is commonly expressed in Europe and in people with European ancestry, H2 has been associated with AD (Allen et al., 2014).

1.4.1 Single nucleotide polymorphisms

Many of the genetic variations explored by means of GWASs come in the form of single nucleotide polymorphisms (SNPs). SNPs are substitutions of a single base at a specific locus of the genome (namely; adenine, thymine, cytosine, or guanine) for another one. However, it is generally considered that changes in a few nucleotides, as well as small insertions and deletions (indels), can be considered SNPs (Sherry, 2001). SNPs are the simplest and the most frequent changes of DNA sequence (Fadason et al., 2022), and a multitude of them have been associated with specific genotypes that contribute to neurodegeneration (for a review, see Tábuas-Pereira et al. (2020)). SNPs may be associated with molecular outcomes depending on the locus of the variation. For instance, genetic variations in non-coding regions mapped as quantitative trait loci (QTL) can have an impact on gene regulation (Aguet et al., 2020). Changes in these QTL may affect mRNA sequence due to disruptions in the splicing process, which are called splicing QTL (sQTL) (Aguet et al., 2020). These anomalies may result in the inclusion of fragments of intronic code as pseudo-exons during mRNA maturation (Vaz-Drago et al., 2017). On the other hand, intronic substitutions at expression QTL (eQTL) can lead to alterations in protein synthesis (Aguet et al., 2020), which have been previously associated with increasing risk of several types of cancer (Li et al., 2014).

Secondly, SNPs in coding regions are modifications in the DNA sequences that translate directly into protein. These exonic substitutions may be synonymous or non-synonymous, whether the SNP modifies a base in a codon associated with the same amino acid, which is also called "silent mutation", or not. Changes in a single base can lead to a variation in a single amino acid or to a premature stop of the translational process (Mathur et al., 2018). The former are called *missenses* and generally result in physiological malfunctions, whilst the latter are called *nonsenses* and normally produce completely nonfunctional proteins (Mathur et al., 2018). These variations have been commonly related to disease, such as mandibuloacral dysplasia and progeria syndrome (Al-Haggar et al., 2012), and cystic fibrosis (Cordovado et al., 2012).

In the present Doctoral Thesis, an examination was conducted on the association between SNP variations located at *PICALM*, *CLU*, and *MAPT* (see previous subsection) and diverse parameters extracted from brain electrical activity. This approach aims to elucidate the impact of genetic expression on several aspects of neural function.

1.5 Electroencephalography

The EEG is a neuroimaging technique that records the electrical activity of the brain. These electrical fluctuations are mainly constituted by postsynaptic potentials (PSPs) triggering in the pyramidal neurons. These cells exhibit long straight apical dendrites that extend along external cortical layers (Im, 2018). PSPs are changes in membrane potential as a consequence of neurotransmitter release from a presynaptic neuron, affecting membrane permeability and, thus, transmembrane ionic gradients (Im, 2018). PSPs are classified as either excitatory or inhibitory, which tend to depolarize or hyperpolarize the neuron, respectively. Whether the membrane potential reaches a certain threshold, the neuron triggers an action potential (AP) that travels through the axon. However, APs are fast and fleeting, while PSPs slowly decay over time. This is the reason why PSPs changes, when generated synchronously in large populations of neurons, result in electrical fluctuations that are large enough to surpass the attenuation induced by the different tissue layers of the head and be acquired by an EEG device (Im, 2018).

The EEG was first discovered in 1924 by Hans Berger, a German psychiatrist, who used it to study brain activity in humans (Berger, 1929). Since then, EEG has become an important tool in neuroscience, as it provides a means to explore the electrical activity of the brain. This technique enables the investigation of brain function and dysfunction in a wide range of contexts (Babiloni et al., 2021; Jeong, 2004; Vecchio et al., 2013). EEG acquisition begins with the placement of electrodes on the scalp, which are usually set according to two systems (international 10-20 or 10-10 systems) (Chatrian et al., 1985; Nunez and Srinivasan, 2006). Electrical activity is then amplified, digitized, stored, and monitored in real-time as a continuous record displayed as a series of waveforms, typically measured in microvolts (μV). This procedure has been conducted under a variety of circumstances, such as during cognitive tasks (Amin et al., 2012), auditory and visual stimulation (Creel, 2019; Paulraj et al., 2015), and resting state (Bai et al., 2017; Cassani et al., 2018).

EEG systems have many advantages over other medical imaging techniques, such as portability, low cost, and non-invasiveness (Im, 2018). In addition, their exceptionally high temporal resolution permits keeping track of the rapid and transient nature of neural oscillations (Im, 2018). This property makes EEG more suitable in the study of brain functionality than other relatively slower measures, such as hemodynamic response (Cohen, 2014). Furthermore, EEG can

be analyzed from several complementary dimensions: Space, time, and frequency. This multifaceted nature is useful to formulate physiological interpretations since the brain is a complex organ that works in multidimensional spaces (Cohen, 2014).

Although the EEG is a valuable neuroimaging technique, it is not without limitations. The primary drawbacks are the source effect and volume conduction, which arise from the non-homogeneity of the brain and its surrounding layers (Schomer and Lopes da Silva, 2017). EEG electrodes record field potentials that traverse the brain, CSF, skull, and scalp (Im, 2018), each with varying conductivity values that can distort and attenuate signals (source effect). Consequently, EEG sensitivity is restricted to the synchronized activity of billions of neurons, and EEG distribution over the scalp can become blurred due to differences in conductivity between layers and anisotropy in some tissues (volume conduction) (Schomer and Lopes da Silva, 2017). It should be noted, however, that volume conduction is not necessarily a limitation, as it is the mechanism by which currents flow through tissues, enabling EEG measurement from the scalp.

Another limitation of EEG is the potential for recording electrical activity from various sources, such as eye movement, muscle contractions, or cardiac activity (Nunez and Srinivasan, 2006). Thus, techniques as independent component analysis (ICA) must be employed to differentiate the actual neuronal field potentials from other sources (Schomer and Lopes da Silva, 2017), though it is not always evident whether ICA can effectively separate distinct physiological sources. Nonetheless, despite these limitations, EEG remains a cost-effective and widely used neuroimaging tool in clinical settings with the ability to capture dynamic neuronal behavior, rendering it an invaluable research tool.

1.5.1 Neural oscillations

EEG manifest as an amalgam of many different waveforms with no clear pattern. In order to find sequences significantly associated with neurological processes, the EEG has been deconstructed in oscillations situated at multiple frequency bands. It turns out certain spectral ranges have been related to specific functional roles (Knyazev, 2007; Saby and Marshall, 2012), being the interactions between them of particular interest in brain processes, such as working memory (Axmacher et al., 2010; Palva et al., 2005), behavior (Knyazev, 2007; Schutter et al., 2006), and reward stimulation (Cohen et al., 2009; Putman et al., 2010). For this reason, frequency bands are useful for detecting signs of brain dysfunction (Babiloni et al., 2021; Jeong, 2004; Vecchio et al., 2013). The most typical ones broadly used in

the literature are described as delta, theta, alpha, beta, and gamma (Newson and Thiagarajan, 2019), as shown in Figure 1.2. However, these designations are not immutable, and alternative frequency bands have been proposed based on diagnostic optimization criteria (Elgendi et al., 2011).

- **Delta (δ, 1-4 Hz):** Delta oscillations are slow waves usually related to sleep and anesthesia (Amzica and Steriade, 1998). Traditionally, anomalous presence of delta waves is indicative of brain injury due to its association with pathological potentials derived from tumors (Amzica and Steriade, 1998) and neurodegeneration (Jeong, 2004). Delta oscillations have also been linked to glial and thalamic activation, the latter being suggested as a clock-like "master" oscillator of the brain (Amzica and Steriade, 1998).

- **Theta (θ, 4-8 Hz):** This oscillatory activity is typically associated with hippocampal functioning (Vinogradova, 1995). However, the contribution of other limbic structures is crucial for the production of theta activity as a whole (Vinogradova, 1995). Theta waves are strongly correlated with processes, such as memory, spatial navigation, and other aspects of cognition and behavior (Uhlhaas et al., 2008; Zhang and Jacobs, 2015). Also, it is implicated in the modulation of synaptic plasticity and the coordination of brain-wide neuronal networks (Zhang and Jacobs, 2015).

- **Alpha (α, 8-13 Hz):** Cortical alpha rhythms are the result of synergistic interactions within thalamo-cortical-thalamic networks and subcortical areas, such as the hippocampus and the reticular formation (Uhlhaas et al., 2008). This activity is more evident at the occipital brain regions while a subject remains in a relaxed state with the eyes closed, being for this reason associated with cortical idling (Uhlhaas et al., 2008). Since opening the eyes induces alpha blockade, these oscillations have been linked to active stimulus processing (Uhlhaas et al., 2008). However, whether alpha activity is a product of inhibition of task-irrelevant processes or it contributes actively to functional networks is still under debate (Uhlhaas et al., 2008).

- **Beta (β, 13-30 Hz):** Beta waves originate in a variety of cortical areas (Uhlhaas et al., 2008). These oscillations have been related to several neurotransmitter systems, among which the dopaminergic one is of particular importance (Uhlhaas et al., 2008). Beta activity is implicated in multiple cognitive tasks, such as learning, novelty detection, and reward evaluation; being thus associated with wakefulness and attention (Uhlhaas et al., 2008).

Also, these oscillations have been suggested to evoke the maintenance of the current sensorimotor or cognitive state, that is, the predicted or intended *status quo* (Engel and Fries, 2010). In some cases, the beta band is subdivided into two frequency bands, generally ranged between 13 and 19 Hz ($\boldsymbol{\beta}_1$), and between 19 and 30 Hz ($\boldsymbol{\beta}_2$). Previous research suggests the association between $\boldsymbol{\beta}_1$ frequency components with the deactivation of the motor cortex after movement offset, whereas $\boldsymbol{\beta}_2$ rhythms have been related to voluntary motor programming (Schomer and Lopes da Silva, 2017).

- **Gamma ($\boldsymbol{\gamma}$, $>$ 30 Hz):** The fastest frequency rhythms are widespread across the brain, even in the olfactory bulb and the retina (Uhlhaas et al., 2008). Gamma activity ranges in a very wide frequency spectrum (up to 200 Hz) and it is dependent upon several neurotransmitter systems (Uhlhaas et al., 2008). In addition, it has been mostly associated with states of high alertness (Schomer and Lopes da Silva, 2017), as well as cognitive and sensory processing (Uhlhaas et al., 2008).

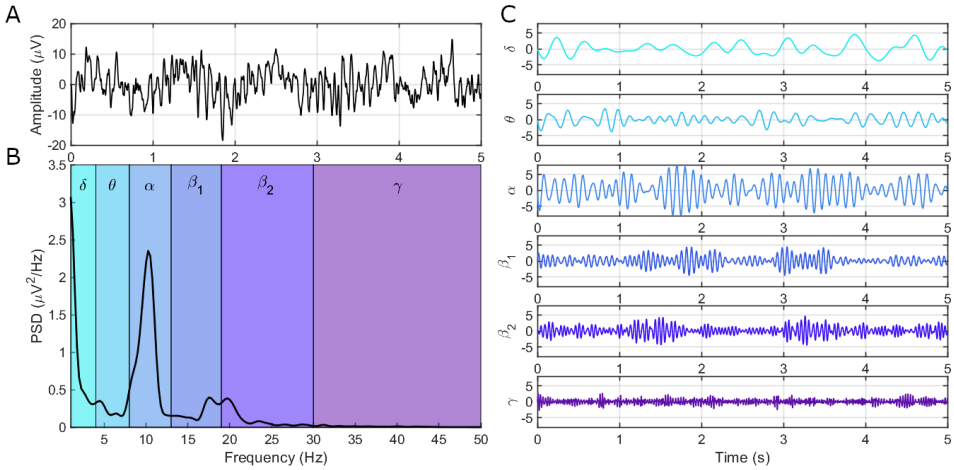

Figure 1.2: Resting-state electroencephalogram (EEG) oscillations obtained from a healthy subject with eyes closed while awake. A) EEG segment of 5 seconds recorded at the Pz location; B) power spectral density of the EEG signal; C) decomposition of the EEG in the six principal frequency bands: δ (1-4 Hz), θ (4-8 Hz), α (8-13 Hz), β_1 (13-19 Hz), β_2 (19-30 Hz), and γ ($>$ 30 Hz).

1.5.2 Levels of EEG analysis

EEG has been traditionally studied in several hierarchical levels of analysis depending on the spatial scale of the components under examination. These levels are defined as i) local activation, ii) pairwise interaction, and iii) global network (Engels et al., 2017; Stam and van Straaten, 2012).

- **Local activation.** In the first hierarchical level, the electrical activity acquired from single neuronal groups is analyzed in isolation. Regarding EEG, each metric is applied to each series obtained from each channel. Then, the values can be averaged or their distribution shown. This level allows simple and immediate comparison between neuronal populations. However, the relationships among them are disregarded and it can result in interpretational bias. It is necessary to mention that this approach can be extrapolated to brain activity sources, not just channels ("nodes" will be used indiscriminately from now on). In order to estimate source-level EEG data, a source localization method has to be previously applied (see Section 3.3).

- **Pairwise interaction (connectivity).** Connectivity metrics take the interactions between nodes into account in order to reveal relationships of interdependence. There are four types of brain connectivity: Structural connectivity, structural co-variance, functional connectivity, and effective connectivity (Yu et al., 2021). The former two types relate to anatomical and morphological characteristics of the brain tissue microstructure, which are examined through magnetic resonance imaging. On the other hand, effective connectivity reveals causal influence on neural functioning among nodes. In some models, this metric can be polysynaptic (Park and Friston, 2013), which may be able to integrate the influence of the variation that other nodes exert to the relationship between each pair of nodes. Furthermore, the computation of effective connectivity requires more sophisticated approaches. In the present Doctoral Thesis, when mention is made of "connectivity", it will refer to functional connectivity, which reveals statistical dependencies between data series of neuronal activity without any causality assumptions (Yu et al., 2021).

- **Global network analysis.** Network analysis is the highest level of brain activity analysis and it describes the brain connectivity configuration as a whole. This perspective derives from connectivity analysis resulting in

multiple types of networks. For instance, structural connectivity brings the structural brain connectome, which consists in an integrated model that reveals the particularities of cytoarchitecture configuration (Yeh et al., 2021). In the case of functional connectivity, statistical associations from data series obtained in different nodes are displayed. Generally speaking, a brain network is described as a graph exhibiting each region of interest (ROI) of the brain as a node and the significant connections between them (structural or functional) as edges (Rubinov and Sporns, 2010). Then, the topological properties of these graphs can be characterized by means of graph-theory metrics (Yu et al., 2021).

1.5.3 The resting state

The brain is an incredibly complex and flexible organ capable of processing a vast array of stimuli and carrying out diverse cognitive and autonomous tasks simultaneously. While brain wave patterns can provide valuable insights into brain behavior, it is challenging to isolate and identify which pattern is associated with each specific brain function. For this reason, research has been focused on studying neurophysiological behavior in controlled environments. In this line, brain activity examinations and EEG devices are designed in such a way as to isolate the process from any external element that may disturb the EEG (Im, 2018). This approach allows to reveal the associations between specific brain operations and EEG changes. However, when studying the impact of AD on neural dynamics during specific tasks, these could be subject to bias due to numerous disrupting factors not necessarily related to neurodegeneration, such as bad eyesight and essential tremor. This factor contributes to the widespread popularity that resting-state studies have gained in the last decade, not only to improve our understanding of AD, but also of many other neurological disorders (Cassani et al., 2018; Khanna et al., 2015; Newson and Thiagarajan, 2019; Wang et al., 2013), highlighting its potential clinical value.

Resting-state brain activity refers to the spontaneous neural activity that occurs in the brain when a person is not actively engaged in a task or receiving external sensory inputs (Vecchio et al., 2013). During resting state, the brain is not inactive but rather exhibits a complex pattern of neural activity comprising multiple interconnected brain regions (Deco et al., 2013). These regions form functional networks that are involved in sensory, motor, and cognitive tasks (Seitzman et al., 2019). Biswal et al. (1995) are credited for identifying these

anatomical structures for the first time using echo-planar MRI. One of the most prominent resting-state networks is the default mode network (DMN), which is active during periods of internal reflection, mind wandering, and self-referential processing (Raichle, 2015). The DMN includes brain regions such as the medial prefrontal cortex, the posterior cingulate cortex, and the inferior parietal lobule; and manages high-level cognitive functions, such as emotion processing and memory evocation (Raichle, 2015). Additionally, the DMN displays a high centrality in the brain functional network (Smitha et al., 2017), and it is considered a brain anatomical "hub", which constitutes a connector that links core cortico-cortical axonal pathways (Raichle, 2015).

1.6 State of the art

This doctoral thesis is dedicated to extracting indicators through various analytic approaches, aiming to establish relationships that could contribute to the characterization of AD. Previously, a large piece of literature has reported EEG and genetic alterations associated with AD, which were consulted to establish feasible hypotheses. This section provides a brief review of the state of the art in this regard.

The EEG is known for exhibiting substantial differences as AD exacerbates. The most known issues to date are its slowing, represented as a shift in the power spectrum (PS) to lower frequencies; reduced complexity, and disruption in connectivity patterns. The first two aspects are quantifiable through local activation exploration, while the third one needs a pairwise connectivity or functional network approach.

1.6.1 Local activation

The slowing and complexity reduction of resting-state EEG are the local activation hallmarks of AD. First, PS shifting to lower frequency bands has been observed by means of relative power in each classical frequency band (see Section 1.5.1). Specifically, along AD progression, theta power increases while beta power decreases, which is followed by a decrease of alpha power (Jeong, 2004). Then, when AD develops to further stages of severity, delta band shows a power increase (Jeong, 2004). This progressive accentuation of EEG alterations is shown along the AD continuum. However, the case of MCI is different, since this condition very often does not conform to the usual trends obtained along AD development.

For instance, MCI patients and preclinical subjects have been found to display increased EEG high-frequency power and decreased low-frequency power. This phenomenon has been associated with initial compensatory mechanisms, being overwhelmed when higher levels of neurodegeneration are reached (Gaubert et al., 2019). However, these indicators have been proposed not as a means for the brain to compensate the effects induced by neural injury, but as directly pathological (de Haan et al., 2012). In any case, they have been associated with changes in brain physiological behavior which can be studied through a variety of local activation metrics. Articles regarding power shifting to characterize brain electrical activity in either AD or MCI subjects have been included in Table 1.1.

Table 1.1: Summary of the main results obtained in previous local activation studies focusing on power shifting in MCI and AD.

Study	Data set	Methods	Results
Prinz and Vitiell (1989)	41 early AD patients and 50 control subjects	DOF	DOF values observed in the AD group were significantly lower than in the control group
Prichep et al. (1994)	40 control subjects, 41 SCI patients, 48 MCI patients, and 140 DAT patients	RP, MF	Theta changes at earliest stages which enlarges with deterioration. Delta changes in subsequent stages of decline. MF shows a negative correlation with the degree of deterioration
Jelic et al. (2000)	27 MCI patients and 16 control subjects	RP, MF	After follow-up, MCI subjects that progressed to AD showed higher theta RP and lower beta RP and mean frequency
van der Hiele et al. (2007)	22 control subjects, 18 MCI patients, and 16 probable AD patients	RP, AR	Theta RP was increased in AD patients as compared with controls and MCI patients. AR was decreased in AD patients as compared with controls
Moretti et al. (2014)	74 MCI patients	RP	Temporoparietal cortical thinning in MCI subjects was associated with high EEG upper/low alpha frequency power ratio
Benwell et al. (2020)	18 AD patients and 27 control subjects	RP, SPR	Reduced alpha and beta power, and increased delta and theta power in AD patients with respect to control subjects. Cognitive dysfunction was closely associated with the $(\alpha+\beta)/(\delta+\theta)$ ratio

DOF: Dominant occipital frequency; SCI: Subjective cognitive impairment; DAT: Dementia of the Alzheimer's type; RP: Relative power; MF: Median frequency; AR: Alpha reactivity; SPR: Spectral power ratio.

The information contained in the spectrum of an EEG signal can be further inspected with more sophisticated techniques. The PS exploration of the EEG is

unable to measure non-linear interactions between frequency components. This limitation can be overcome by HOS analyses, which are defined in terms of higher order statistics or "cumulants" (Nikias and Mendel, 1993). The HOS of third-order cumulants is called bispectrum (Nikias and Mendel, 1993), which is calculated through the Fourier transform of third-order statistics. Exploring the EEG bispectrum involves identifying non-linear interactions between different frequency components of the signal. This is crucial as it allows to reveal divergences from Gaussianity derived from these interactions, such as phase coupling, which are suppressed under PS analyses (Nikias and Mendel, 1993). Although PS analyses are generally sufficient to statistically describe any temporal series (Nikias and Mendel, 1993), the identification of non-linear elements may play a decisive role in revealing physiological abnormalities from biomedical signals. In fact, bispectrum has been previously used to characterize perturbations in brain electrical activity caused by AD. Examples of this approach have been included in Table 1.2.

Table 1.2: Summary of the main results obtained in previous local activation studies focusing on bispectral analysis in MCI and AD.

Study	Data set	Methods	Results
Renna et al. (2003)	19 AD patients and 36 control subjects	BIS	Dementia patients showed decreased BIS values
Wang et al. (2015)	14 probable AD patients and 14 control subjects	WCOB, P_1, P_2	Higher concentration of the WCOB and lower bispectral entropy
Nasrolahzadeh et al. (2018)	30 AD patients and 30 control subjects	B_{avg}, B_{max}, B_{min}, H, P_h, P_1, P_2, P_3	The classification system was able to diagnose the early stage of AD with an accuracy of 95%
Ieracitano et al. (2020)	63 AD patients, 63 MCI patients, and 63 control subjects	P_1, P_2, H, H_d, FOS_d, SOS_d	Multi-Layer Perceptron classifier outperforms other models when combining bispectral and wavelet features
Klepl et al. (2023)	20 AD patients and 20 control subjects	CSB multilayer analysis	Low-frequency coupling strength is increased and high-frequency coupling is decreased in AD patients in comparison to healthy controls

BIS: Bispectral index; WCOB: Weighted center of bispectrum; P_1: Bispectral entropy; P_2: Bispectral cuadratic entropy; B_{avg}: Mean of bispectral magnitude; B_{max}: Maximum of bispectral magnitude; B_{min}: Minimum of bispectral magnitude; H: Sum of logarithmic amplitudes of the bispectrum; P_h: Bispectral phase entropy; P_3: Bispectral cubic entropy; H_d: Sum of logarithmic amplitudes of diagonal elements of the bispectrum; FOS_d: First-order spectral moment of the amplitudes of diagonal elements of the bispectrum; SOS_d: Second-order spectral moment of the amplitudes of diagonal elements of the bispectrum; CSB: Cross-bispectrum.

The brain is a complex organ characterized by electrical function based on

intricate activation patterns. This behavior leads to large-scale, convoluted interactions that transcend linearity, which is a property of systems that are capable of self-organization (Pritchard and Duke, 1992). In order to explore features comprised by such chaotic systems, non-linear analyses are required. These methods can provide insights into the dynamic behavior of the brain and its underlying functional architecture. Some common non-linear analysis methods used in EEG research include the study of the irregularity of the signal in the time domain, which estimates the degree of uncertainty. This is quantified by processing techniques based on Shannon's definition of entropy in signal theory (Shannon, 1948). In this regard, several methods have been developed, such as mutual information (Fraser and Swinney, 1986), approximate entropy (Pincus, 1995), and sample entropy (SampEn) (Richman and Moorman, 2000). Other metrics, such as the central tendency measure (Cohen et al., 1996), have been designed to estimate the variability of a time series. However, although higher signal variation or irregularity are apparently indicators of data complexity, some authors disagree. Indeed, higher levels of entropy have been suggested not to be equivalent to meaningful "structural richness" (Costa et al., 2005), and in order to study the actual complexity of the information stored in a physical object, other means are needed (Grassberger, 1991). From the physiological standpoint, biosignal complexity establishes the adaptation capability of a living being in a changing environment (Costa et al., 2005), being this the reason why several temporal scales must be considered in the analyses. Thus, with the aim to estimate the complexity of a signal, the application of temporal multiscale approaches was proposed in the form of multiscale entropy (MSE) (Costa et al., 2002, 2005) and multiscale Lempel-Ziv complexity (Ibáñez-Molina et al., 2015), among others. Some examples of the most relevant pieces of literature regarding non-linear analysis are shown in Table 1.3.

1.6.2 Connectivity and multi-layer analysis

When it comes to ascertaining relationships between different EEG sources, connectivity methods have to be conducted. Generally speaking, the study of EEG connectivity allows identifying statistically significant synchronization between EEG signals obtained from two or more activity sources (Miljevic et al., 2022). This element of study is also called functional connectivity (or rather effective connectivity if determining causal flow of information (Miljevic et al., 2022)) as opposed to structural connectivity, which describes actual connections between

Table 1.3: Summary of the main results obtained in previous non-linear studies from local activation EEG focusing on MCI and dementia due to AD.

Study	Data set	Methods	Results
Jeong et al. (2001b)	12 AD patients, 12 VaD patients, and 14 controls subjects	L1	Lower L1 values in AD patients compared to controls in most electrodes
Jeong et al. (2001a)	15 AD patients and 15 controls subjects	CMI, AMI	Local CMI in AD patients was lower compared to controls. AMI decreased significantly slower with delay in AD patients than in controls
Abásolo et al. (2006b)	11 AD patients and 11 control subjects	SampEn	Lower SampEn values in patients with AD compared to controls
Abásolo et al. (2006a)	11 AD patients and 11 control subjects	CTM, LZC	Lower LZC values in patients with AD compared to controls
Escudero et al. (2006)	11 AD patients and 11 control subjects	MSE	Less complex EEG background activity in patients with AD compared to controls
Abásolo et al. (2008)	11 AD patients and 11 control subjects	AMI, ApEn	Increased resting-state EEG regularity in AD patients compared to controls
Mizuno et al. (2010)	15 pre-senile AD patients and 18 control subjects	MSE	AD group showed lower complexity at smaller scales and higher complexity at larger scales compared to controls
Yang et al. (2013)	108 AD patients in different states of severity	MSE	Increased severity of AD was associated with decreased MSE complexity in short-time scales, and with increased MSE complexity in long-time scales
Coronel et al. (2017)	79 probable AD patients in diverse severity states	AMI, MSE, and other entropy metrics	Classification models with AMI and MSE were significant in predicting severity. Reductions in complexity were observed as MMSE score decreased
Azami et al. (2023)	19 mild AD patients, 23 MCI patients, and 35 control subjects	MFDE, SFAR-entropy	SFAR-entropy measured in REM sleep is able to distinguish between AD, MCI, and healthy states

VaD: Vascular dementia; L1: First Lyapunov exponent; CMI: Cross-mutual information; AMI: Auto mutual information; SampEn: Sample entropy; CTM: Central tendency measure; LZC: Lempel-Ziv complexity; MSE: Multiscale entropy; ApEn: Approximate entropy; MMSE: Mini-Mental State Examination; MFDE: Multiscale fluctuation dispersion entropy; SFAR-entropy: Slow-to-fast-activity ratio of entropy.

neuronal populations (Yeh et al., 2021). However, the latter can only be studied by means of more sophisticated medical image techniques, such as MRI-based

tractography (Yeh et al., 2021). Functional connectivity can be estimated by numerous metrics, such as phase lag index (PLI) (Stam et al., 2007), coherence (Roach and Mathalon, 2008), and amplitude envelope correlation (O'Neill et al., 2015).

In addition to these methods, several network-based approaches have been developed to study connectivity in EEG data as a whole. These approaches involve the construction of networks based on the correlation or coherence between EEG sources using graph theory metrics. Network measures such as clustering coefficient (Watts and Strogatz, 1998) and betweenness centrality (Barthélemy, 2004) can be used to identify the most important and interconnected brain regions in the network. In addition, graph theoretical measures can also be used to study the topological properties of the network, such as small-worldness (Watts and Strogatz, 1998), path length (Stam et al., 2006), and the degree distribution (Lacasa and Toral, 2010).

The study of functional network properties can also be conducted from a multilayer perspective (Kivela et al., 2014). In this way, each layer can be defined as network configurations obtained under certain circumstances or properties, constituting what is essentially a network of networks (Kivela et al., 2014). Multilayer approaches applied to EEG involve the analysis of multiple graphs, each usually representing a different frequency band. By comparing the properties of the graphs across different frequency ranges, it is possible to identify changes in the connectivity and interactions between different brain regions as a function of frequency. This can provide insights into how different cognitive processes affect not only network configurations, but also the relationships between multiple networks. Some recent examples of this methodology are shown in Table 1.4.

1.6.3 Correlation analyses between genetics and EEG parameters

A large body of research has shown that EEG parameters are sensitive to genetic variation, meaning that individual differences in EEG measures can be partly explained by differences in genetic makeup (Horvath, 2018; Jeong, 2004; Maestú et al., 2019). For example, previous studies have identified genetic variants that are associated with differences in the amplitude, frequency, and synchronization of EEG signals (Horvath, 2018; Jeong, 2004; Maestú et al., 2019).

To investigate the relationship between genetics and EEG parameters, researchers typically use correlational analysis. This involves examining the

Table 1.4: Summary of the main results obtained in previous multilayer network analysis in MCI and AD.

Study	Data set	Methods	Results
Guillon et al. (2017)	25 AD patients and 25 control subjects	MPC	Abnormal connectivity distribution in AD patients across frequency bands as compared to controls, causing a decrease of MPC
Yu et al. (2017)	27 AD patients and 26 control subjects	OWD, P	Several hub regions presented increased vulnerability in AD patients compared to control subjects
Cai et al. (2020)	20 AD patients and 20 control subjects	PLV, ClC, P_i	Brain networks of AD patients are disrupted with reduced segregation for both cross-frequency and time-varying networks. Combining integration and segregation, classification performance reached an accuracy of 92.5%
Ruiz-Gómez et al. (2021)	51 control subjects, 51 MCI patients, 51 mild AD patients, 50 moderate AD patients, and 50 severe AD patients	CCA, S, L, ClC	AD patients showed a significant increase in average connectivity and a loss of integration and segregation

MPC: Multi-participation coefficient; OWD: Overlapping weighted degree; P: Participation coefficient; PLV: Phase locking values; ClC: Clustering coefficient; P_i: Functional integration; CCA: Canonical correlation analysis; S: Multiplex strength; L: Multiplex characteristic path length

association between genetic variations and EEG measures using statistical techniques, such as regression analysis and correlation analysis. In addition, machine learning algorithms can be applied to analyze the data, such as principal component analysis and support vector machines (García-Pretelt et al., 2022). By using these techniques, researchers can identify patterns in the data and establish the strength of the relationship between genetic variations and EEG parameters.

One of the most widely studied genetic variations are single-nucleotide polymorphisms (SNPs). SNPs are the most frequent form of genetic alterations that entail single-base substitutions at specific genetic loci. Multiple genome-wide association studies have been conducted to evaluate the impact of SNPs on various diseases (Harold et al., 2009; Lambert et al., 2013). Prior investigations have found statistical correlations between specific genotypes and neurodegeneration. These findings highlight the importance of studying the genetic basis of brain function in

order to better understand disease pathogenesis and potential therapeutic targets.

Overall, the correlational analyses between genetics and EEG parameters have provided important insights into the complex interplay between genetics and brain function. Some findings regarding associations between EEG parameters and genetic expression are shown in Table 1.5. However, it is important to note that correlational studies cannot establish causality. Further research is needed to determine the precise nature of the relationship between genetics and EEG parameters and to identify potential interventions to improve brain function and cognitive performance.

The agglutination of the aforementioned research perspectives (*i.e.*, local activation assessment in the form of power shifting, bispectrum, and non-linear analysis; functional connectivity evaluation in both single and multi-layer configurations; and genetics) may be able to provide a multi-faceted and interdisciplinary perspective to elucidate a set of potential associations between biological aspects and alterations in brain electrical activity. This will be detailed in the following chapter 2, which explains the hypothesis driving this work and each study integrated into this Thesis. This section also outlines the specific objectives in detail.

Table 1.5: Summary of the main results obtained in previous association analysis between EEG and genetic parameters in MCI and AD.

Study	Data set	Methods	Results
Ponomareva et al. (2013)	87 non-demented subjects	RP	*CLU* CC carriers at SNP rs11136000 showed an increase of alpha3 absolute power. The influence of the genotype was higher in older subjects
Ponomareva et al. (2017)	137 non-demented subjects	RP	*PICALM* GG carriers at SNP rs3851179 showed increased beta relative power. The influence of the genotype was higher in older subjects
Gutiérrez-de Pablo et al. (2020)	46 control subjects, 49 MCI patients, 46 mild AD patients, 44 moderate AD patients, and 33 severe AD patients	LZC	AD continuum is characterized by a progressive complexity loss. Brain activity from control subjects showed differences between genotypes, being *ApoE* ϵ4 carriers' more complex
Ponomareva et al. (2020)	104 non-demented subjects	LLC	*PICALM* AA and AG carriers showed higher widespread interhemispheric LLC of alpha sources compared to *PICALM* GG carriers
Macedo et al. (2021)	45 control subjects, 45 MCI patients, and 109 AD patients in several stages of severity	RP	Carriers of risk alleles in *IL1RAP* (rs10212109, rs9823517, rs4687150), *UNC5C* (rs17024131), and *NAV2* (rs1425227, rs862785) genes showed a slowing in the EEG
Smailovic et al. (2018)	50 MCI patients and 51 AD patients	GFP, GFS	Amyloid positive carriers of *ApoE* ϵ4 alleles showed higher GFP in beta and lower GFS in theta and beta
Ponomareva et al. (2023)	94 non-demented subjects	ERD	Activation during LFT in *CLU* CC carriers at SNP rs11136000 exhibited more pronounced alpha2 desynchronization than CT and TT carriers

RP: Relative power; *CLU*: Clusterin gene; C: Cytosine; SNP: Single nucleotide polymorphism; *PICALM*: Phosphatidylinositol binding clathrin assembly protein gene; G: Guanine; LZC: Lempel-Ziv complexity; *ApoE*: Apolipoprotein E gene; A: Adenine; LLC: Lagged linear connectivity; *IL1RAP*: Interleukin-1 receptor accessory protein gene; *UNC5C*: Unc-5 netrin receptor C gene; *NAV2*: Neuron navigator 2 gene; GFP: Global field power; GFS: Global field synchronization; ERD: event-related desynchronization; T: Thymine.

Chapter 2

Hypothesis and objectives

AD is a complex disorder featuring multiple structural and biochemical brain alterations. At the same time, the brain is a massively intricate organ composed of millions of neurons activating synchronously to conduct numerous processes. In order to understand AD from a physiological standpoint, it is crucial to investigate the alterations that this disorder causes in these neural dynamics. For this reason, this Doctoral Thesis focuses on collecting diverse and novel parameters calculated from EEG to identify particular mechanisms affected by AD. To this end, EEG was studied from different perspectives in four studies. First, the study of the disruptions in EEG complexity with the severity of the disease was carried out by means of multiscale entropy metrics. Local activation in the AD continuum was further investigated by studying the bispectral properties of EEG, which made it possible to characterize inter-band component interactions in neurodegenerative states. In this Thesis, the correlation between several genetic polymorphisms was studied to ascertain the impact of DNA sequence in the EEG oscillations. In this way, *CLU* and *PICALM* gene variations were inspected to determine differences in spectral power values and their distribution across the brain between carriers of risk and protective alleles in both healthy subjects and AD patients. Finally, the interactions between different frequency bands in the brain functional network were examined in carriers with multiple *MAPT* variations using a novel parameter called "participation coefficient". The hypotheses and objectives that motivated these works are shown below.

2.1 Hypothesis

Due to the poor understanding of the essential causes of neurodegeneration, the diagnosis of MCI and dementia due to AD still presents a great degree of subjectivity. These conditions are generally diagnosed using complex procedures that involve cognitive tests, clinical examinations, and the inspection of clinical history. AD and MCI come with an additional drawback, which is they are often accompanied by other neurological disorders (Alzheimer's Association, 2022). It makes these conditions particularly challenging to identify with precision, especially in the early stages of deterioration. In order to determine definite AD, the accepted hallmark is the presence of Aβ and tau proteins in the brain, along with indicators of neuronal injury (Jack et al., 2016, 2018). The most robust procedure to inspect these molecules is conducted through histological examination of brain tissue, which leads to extreme levels of invasiveness (Yates, 2011). In recent years, medical image techniques have improved technologically enough to be sensitive to these molecules. However, their use is still massively costly and sometimes even impractical (Gauthier et al., 2021). For these reasons, the development of new methods to detect early signs of neurodegeneration due to AD is essential. Therefore, exposing features derived from a wide variety of EEG analyses could be useful in detecting and characterizing AD at a fundamental level. Thus, the main driving hypothesis of this Thesis is that *MCI and AD manifest biochemical-induced alterations in brain electrical activity associated with information processing, in which genetic anomalies may play a fundamental role*. The ascertainment of this premise may enhance our understanding of neurodegenerative conditions attending to the triad of pathology, EEG, and genetics. This approach could potentially allow the characterization of MCI and AD with diagnostic utility.

2.2 Objectives

The main goal of this Doctoral Thesis is to extract novel features from EEG data that are able to characterize the AD continuum and study the relationships between these features and genetic anomalies previously associated with dementia (Harold et al., 2009; Lambert et al., 2009; Tanzi, 2012). This would allow elucidating the disruptions in EEG features as signs of neural dysfunction and the implication of certain genotypes on cortical dynamics under specific neurophysiological conditions. In order to achieve the main objective, the following

specific objectives were established:

1. To identify novel EEG-derived features that are sensitive to the electrophysiological perturbations present along the AD continuum from different perspectives, encompassing non-linear, spectral, and multiplex network methodologies.

2. To study the association between alterations in EEG and genetic anomalies previously determined as AD risk factors, affecting Aβ and tau metabolism, structure and clearance.

3. To examine common patterns among the proposed approaches and suggest interpretations that may reveal physiological originators influencing the obtained results.

Chapter 3

Subjects and signals

This chapter provides information about the database used in the Doctoral Thesis, the first steps of EEG acquisition, and raw data pre-processing. Section 3.1 outlines the socio-demographic features of the subjects who participated in the study. Section 3.2 specifies the setup of the EEG acquisition process, while section 3.3 details the pre-processing protocol applied to EEG signals. Subsequently, the genetic analyses of the biological samples are detailed in Section 3.4. Finally, section 3.5 describes the source-level localization algorithm utilized on those studies centered in brain electrical activity in specific brain regions.

3.1 Subjects

A database composed of 253 subjects was used along the Doctoral Thesis, divided by 51 healthy control (HC) subjects, 51 patients with MCI due to AD, 51 mild AD patients (AD_{MIL}), 50 moderate AD patients (AD_{MOD}), and 50 severe AD patients (AD_{SEV}). EEG and genetic data from each subject were obtained in a research environment as a result of the POCTEP 2014-2020 project called: 'Analysis and correlation between whole genome sequence and brain activity for the diagnosis enhancement of Alzheimer's disease' (AD-EEGWA). All subjects in the study were diagnosed with dementia or MCI due to AD using the criteria established by the National Institute on Aging and Alzheimer's Association (Jack et al., 2018). Cognitive impairment was assessed for each subject using the Mini-Mental State Examination (MMSE) test (Folstein et al., 1975). To qualify for inclusion in the AD and MCI patient cohorts, participants needed to be aged 65 or above and diagnosed from a specialized physician. Exclusion criteria for the study included

atypical signs of cognitive decline, a history of neoplasia under treatment, recent surgery, hypercatabolic states, chronic alcoholism, and indications of vascular pathology. The inclusion criteria for HC subjects include being over the age of 65, having MMSE scores equal to or higher than 27, and having no history of neurological or major psychiatric disorders. All study participants or their caregivers provided written informed consent, in accordance with the World Medical Association's Code of Ethics (Declaration of Helsinki). The study protocol was approved by The Ethics Committee at Porto University (Porto, Portugal. Report No. 38/CEUP/2018). Table 3.1 specifies the number of participants enrolled in the studies that constitute this Doctoral Thesis. Noteworthy, due to genotype requisites and other constraints, certain subjects were excluded in those works involving genetic analyses. Additionally, Table 3.2 presents the demographic information of the participants, which includes age, sex, educational attainment, and other relevant characteristics.

3.2 Acquisition protocol

Each subject underwent an acquisition of brain electrical activity data consisting of 5 minute EEG recording in resting-state conditions. The procedure was conducted in a relaxed and noise-free environment to minimize the presence of artifacts caused by external stimuli. The state of vigilance was controlled to avoid drowsiness of the subjects. EEG was acquired using a 19-channel Nihon Kohden Neurofax JE-921A EEG system with a sampling frequency of 500 Hz and common average. The electrodes were placed on the scalp according to the 10-20 international system at Fp1, Fp2, F3, F4, F7, F8, T3, T4, T5, T6, C3, C4, P3, P4, O1, O2, Fz, Cz, and Pz. The obtained data were stored in ASCII format on a personal computer before subsequent processing analyses.

Study	**HC**	**MCI**	**AD**
Maturana-Candelas et al. (2019)	51	51	151 (along continuum)
Maturana-Candelas et al. (2020)	51	51	150 (along continuum)
Maturana-Candelas et al. (2021)	24	0	53 (along continuum)
Maturana-Candelas et al. (2024)	45	0	110

Table 3.1: Number of subjects in each group for each study from the POCTEP database. HC: Healthy control subjects; MCI: Mild cognitive impairment patients; AD: Alzheimer's disease patients

Group	N	Age ($\overline{x} \pm \sigma$)	Sex (F:M)	MMSE ($\overline{x} \pm \sigma$)	Education (Pr:Sc)	Smoker (Y:Ex:N)	Diet (M:A:H)	Alcohol (Y:N)	Diseases (C:S:H)
HC	51	80.1±7.1	25:26	28.8±1.1	33:18	1:11:39	42:7:2	18:33	30:1:12
MCI	51	85.5±7.3	36:15	23.3±2.8	38:13	2:5:44	45:3:3	9:42	32:12:10
AD_{MIL}	51	80.7±7.1	30:21	22.5±2.3	37:14	3:4:44	45:4:2	7:44	30:10:9
AD_{MOD}	50	81.3±8.0	43:7	13.6±2.8	37:13	1:6:43	44:6:0	5:45	28:4:18
AD_{SEV}	50	80.0±7.8	43:7	2.4±3.7	45:5	0:2:48	42:6:2	0:50	33:5:16

Table 3.2: Demographic data. $\overline{x}$: Mean; σ: Standard deviation; F: Female; M: Male; HC: Healthy controls; MCI: Mild cognitive impairment patients; AD_{MIL}: Mild AD patients; AD_{MOD}: Moderate AD patients; AD_{SEV}: Severe AD patients; MMSE: Mini-mental state examination score; education: (Pr: Primary education or below, Sc: Secondary education or above); smoking habits: (Y: Smoker, Ex: Ex-smoker, N: Non-smoker); dietary habits: (M: Balanced/mediterranean, A: Antidiabetic, H: Hypocaloric); alcohol consumption: (Y: Occasional drinker, N: Non-drinker); clinical story: (C: Cardiovascular, as arterial hypertension, high cholesterol, etc.; S: Sensorimotor as visual impairment, abnormal gait, etc.; H: Hormonal, as diabetes, thyroid dysfunctions, etc.). Clinical story describes the prevalence of clinical issues in the sample. Several diseases can affect the same subject and can only count one of each type.

3.3 Pre-processing

Previous to the processing of EEG data, a pre-processing stage was conducted to remove or minimize presence of artifacts and components not related to brain electrical activity. This procedure is defined in the following steps.

1. **Filtering**. EEG signals were digitally filtered with a band-pass filter between 0.4 and 98 Hz and a notch filter at 50 Hz to reduce power grid interference. Both filters were configured as Hamming window finite impulse response (FIR) filters of order 2000 and applying forward and backward filtering to avoid phase delay. In some studies, additional filtering was applied in order to minimize the effect of higher frequency bands or very slow oscillations. Namely, these band-pass filters were set between 1.5 and 30 Hz (Maturana-Candelas et al., 2020), between 1 and 70 Hz (Maturana-Candelas et al., 2021), and between 1 and 30 Hz (Maturana-Candelas et al., 2024).

2. **Independent component analysis (ICA)**. ICA was used to minimize the impact of artifacts in the EEG caused by factors such as electrode impedance or other biosignals including myographic, cardiographic, and oculographic activity. ICA allows for the identification and isolation of these components, thus making it possible to reconstruct the EEG without their contribution to the main signal. ICA is computed by minimizing mutual information between data projections or maximizing their joint entropy (Delorme and Makeig, 2004). ICA can detect components that are mutually independent, which means that the cross-correlation between components, as well as all the higher-order moments of the signals, are zero (Makeig et al., 1997). ICA operates based on feature extraction methods such as blind signal separation algorithms. It entails statistical decomposition, premised on the assumption that distinct sources of activity, such as ocular signals, are separable from the underlying brain activity (Jutten and Karhunen, 2004). In this Doctoral Thesis, ICA was calculated using the Infomax algorithm (Bell and Sejnowski, 1995) through the runica.m MATLAB® function, which prioritizes the characterization of temporal dynamics (Dien, 2010).

3. **Standardized low resolution brain electromagnetic tomography (sLORETA)**. In some of the studies involved in this Doctoral Thesis (Maturana-Candelas et al., 2021, 2024), the analysis of source-level activity was conducted. To this end, the source localization algorithm sLORETA was

used (Pascual-Marqui, 2002). sLORETA calculates 3D linear solutions to solve the inverse problem of the EEG, providing a noise-normalized estimate of the distribution of electrical activity within a brain model (Pascual-Marqui, 2002). These brain models provide regions of interest (ROIs) depending on different criteria, such as a gyrus-based classification (*e.g.*, Desikan-Killiany atlas) (Desikan et al., 2006) or functional profiles (*e.g.*, Yeo-7 Network atlas) (Yeo et al., 2011). This topic is extended in Section 3.5.

4. **EEG segmentation and artifact-free epoch selection**. The resulting EEG was segmented in non-overlapping 5 seconds-length epochs, consisting on 2500 samples each. Each single epoch was visually inspected to identify artifact presence that were not reduced by previous steps.

Digital pre-processing and analysis of the signals were carried out with MATLAB® (R2018a version, Mathworks, Natick, MA), Brainstorm toolbox, an open-source application dedicated to the analysis of brain recordings (accessible at http://neuroimage.usc.edu/brainstorm and implemented by Tadel et al. (2011)), EEGLab, an environment for human EEG and other related data analysis (accessible at https://eeglab.org and implemented by Delorme and Makeig (2004)), and Brain Connectivity Toolbox, a set of functions for complex brain-network analysis (accessible at https://sites.google.com/site/bctnet and implemented by Rubinov and Sporns (2010)).

3.4 Genetic analyses

Samples of biological material for genetic characterization were obtained from each participant using either a saliva sample or buccal mucosa, with saliva samples preferred and collected using the Oragene DNA 500 collection kit (DNAgenotek). For patients at advanced stages of the disease who were unable to provide saliva samples, buccal mucosa was acquired using three buccal swabs. Prior to analysis with the genome-wide Axiom Spain Biobank Array (Thermo Fisher Scientific) at the Spanish National Center for Genotyping (CEGEN), DNA extraction and quality control assessments were conducted on all samples. Quality control (QC) procedures for variant calling were conducted on both individuals and markers, adhering to the Affymetrix best practices guide (Anderson et al., 2010). This process utilized either Affymetrix Power Tools or PLINK (Purcell et al., 2007). Variants of the probes belonging to the recommended calling categories were annotated based on the Genome Reference Consortium Human Build 37

(GRCh37) SNP assembly. Both individual and per-marker QC analyses considered sex, duplications or relatedness, and divergent ancestry. Afterwards, linkage disequilibrium (LD) for each genetic variant that was studied in this Thesis was assessed by resorting to the informatics tool LDlink (Machiela and Chanock, 2015), hosted by the Division of Cancer Epidemiology and Genetics site (National Institutes of Health, `https://ldlink.nci.nih.gov`). The genetic information relevant for the studies composing this Doctoral Thesis is the following: Risk and protective alleles of *PICALM* at the SNP rs3851179, risk and protective alleles of *CLU* at the SNP rs11136000, and risk and protective alleles of *MAPT* at the SNPs rs2258689, rs242557, rs11656151, rs2435207, rs16940758, rs7521, and rs8070723. More details about these genetic variations are shown in Table 3.3 for *PICALM* and *CLU* genes, and Table 3.4 for the *MAPT* gene.

3.5 EEG source localization

EEG source localization refers to the process of identifying the location of the neural generators that produce the scalp-recorded electrical signals in EEG. This is conducted utilizing source localization algorithms such as sLORETA (see Section 3.2). One approach to define 3-dimensional regions for each EEG source is using an anatomical reference space called "atlas". An atlas allows for guiding the identification of the underlying neural sources, which are called ROIs in this Doctoral Thesis. Several different atlases have been developed for use in EEG source localization. These atlases differ in terms of the underlying anatomical and/or functional data they are based on, the spatial resolution they provide, and the level of detail they offer.

In this Doctoral Thesis, two atlases were used: Desikan-Killiany (Desikan et al., 2006) and Yeo-7 (Yeo et al., 2011). The Desikan-Killiany atlas is a brain atlas that is based on high-resolution structural MRI data from a large sample of healthy adults (Desikan et al., 2006). It was developed to provide a detailed parcellation of the cerebral cortex into 34 gyral-based regions per hemisphere, for a total of 68 regions (Desikan et al., 2006). The Desikan-Killiany atlas has been widely used in neuroimaging research, including studies that involve EEG source localization (Blanco et al., 2023; Chang et al., 2015; Zhou et al., 2023). This atlas provides a high level of spatial resolution and allows for the identification of specific cortical regions that are involved in different cognitive processes.

Genotype	**Group**	**N**	**Age** ($\overline{x} \pm \sigma$) **(years)**	**Sex (M:F)**	**MMSE** ($\overline{x} \pm \sigma$)
Risk alleles	HC	12	80.33 ± 6.64	8:4	29.33 ± 0.65
	AD_{MIL}	6	80.00 ± 4.38	2:4	21.00 ± 1.26
rs3851179: G (Ref)	AD_{MOD}	8	84.25 ± 3.24	2:6	12.50 ± 1.60
rs11136000: C (Ref)	AD_{SEV}	4	76.50 ± 7.94	0:4	2.25 ± 4.50
Protective alleles	HC	12	81.41 ± 7.75	5:7	28.59 ± 1.08
	AD_{MIL}	17	79.29 ± 8.42	9:8	23.06 ± 2.75
rs3851179: A (Alt)	AD_{MOD}	8	83.13 ± 6.94	0:8	14.13 ± 2.30
rs11136000: T (Alt)	AD_{SEV}	10	80.70 ± 5.08	3:7	4.40 ± 4.27

Table 3.3: Demographic and genetic data for the intersection of the populations with *PICALM* and *CLU* variations. $\overline{x}$: Average; σ: Standard deviation; Ref: Reference allele; Alt: Altered allele; M: Male; F: Female; MMSE: Mini-Mental State Examination score; HC: Healthy control subjects; AD_{MIL}: Mild Alzheimer's disease patients; AD_{MOD}: Moderate Alzheimer's disease patients; AD_{SEV}: Severe Alzheimer's disease patients

SNP	Base	Eff	Subjects HC	Subjects AD	Sex (M:F) HC	Sex (M:F) AD	Age ($\overline{x} \pm \sigma$) (yrs.) HC	Age ($\overline{x} \pm \sigma$) (yrs.) AD	MMSE ($\overline{x} \pm \sigma$) HC	MMSE ($\overline{x} \pm \sigma$) AD
rs2258689 (In/Ex)*	T (Ref)	P	27	75	14:13	40:35	80.0±7.4	79.9±7.5	28.9±1.1	16.0±7.6
	C (Alt)	R	18	35	8:10	20:15	79.2±7.2	82.0±6.6	28.8±1.2	13.3±8.2
rs242557 (In)	G (Ref)	P	18	44	8:10	22:22	81.3±8.1	79.1±7.2	28.8±1.2	14.4±8.3
	A (Alt)	R	27	66	14:13	35:31	78.7±6.6	81.6±7.2	28.9±1.1	15.6±7.6
rs11656151 (In)	A (Ref)	P	33	76	17:16	40:36	80.6±8.0	80.8±7.2	28.6±1.1	15.3±7.6
	G (Alt)	R	12	34	6:6	20:14	77.3±4.3	80.1±7.4	29.5±0.7	14.6±8.5
rs2435207 (In)	G (Ref)	P	20	52	9:11	25:27	80.4±7.9	80.4±6.3	29.1±1.1	13.3±8.3
	A (Alt)	R	25	58	14:11	30:28	79.2±6.9	80.7±8.1	28.7±1.1	16.7±7.2
rs16940758 (In)	C (Ref)	P	31	69	16:15	37:32	80.1±6.9	80.6±7.3	29.1±1.0	14.3±8.1
	T (Alt)	R	14	41	8:6	23:18	78.9±8.2	80.6±7.2	28.4±1.2	16.4±7.4
rs7521 (3'UTR)	C (Ref)	P	17	41	8:9	22:19	82.0±8.4	80.0±7.3	28.6±1.2	16.2±8.0
	A (Alt)	R	28	69	15:13	37:32	78.3±6.3	80.9±7.3	29.0±1.1	14.5±7.8
rs8070723 (In)	A (Ref)	R	23	62	12:11	34:28	77.7±6.2	81.1±7.0	28.7±1.2	15.7±7.5
	G (Alt)	P	22	48	11:11	24:24	81.8±7.8	79.8±7.6	29.0±1.0	14.4±8.4

Table 3.4: Demographic and genetic data for *MAPT* genotypes. $\overline{x}$, average; σ, standard deviation; Ref, reference allele; Alt, altered allele; M, male; F, female; MMSE, Mini-Mental State Examination score; Eff, effect of the allele; R, risk allele; P, protective allele; HC, healthy control subjects; AD, Alzheimer's disease patients; In, intronic variant; Ex, exonic variant; 3'UTR, 3' untranslated region. (*) rs2258689 belongs to exon 6 or to an intron depending on the splicing process.

On the other hand, the Yeo-7 atlas is a brain atlas that divides the cerebral cortex into seven distinct large-scale functional networks per hemisphere based on resting-state functional MRI data (Yeo et al., 2011). These functional networks are referred to as visual, somatomotor, dorsal attention, ventral attention, limbic, frontoparietal, and DMN (Yeo et al., 2011). The Yeo-7 atlas has been used in neuroimaging research to investigate the organization of functional connectivity in the brain and to identify brain regions that are involved in different neuropathologies (Pini et al., 2021; Son et al., 2022). One advantage of the Yeo-7 atlas is that it provides a functional rather than an anatomical parcellation of the cerebral cortex (Yeo et al., 2011). This can be useful in EEG source localization studies where the focus is on identifying brain regions that are functionally connected rather than just anatomically neighboring. Figures 3.1 and 3.2 display Desikan-Killiany and Yeo-7 atlases.

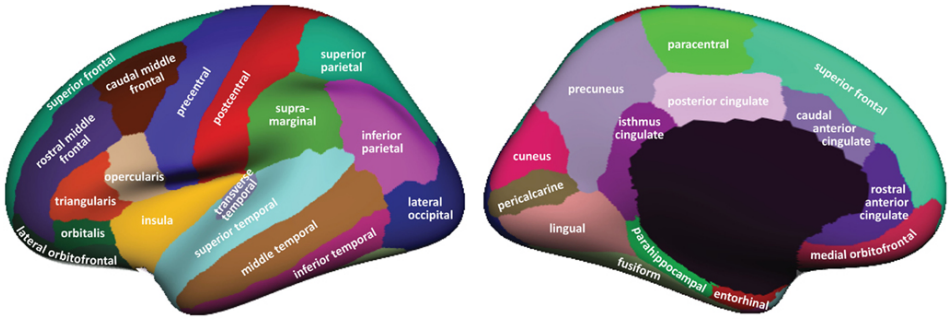

Figure 3.1: Desikan-Killiany atlas FreeSurfer visualization. Figure obtained from iELVis web site: `http://ielvis.pbworks.com`, accessed on May 5, 2023

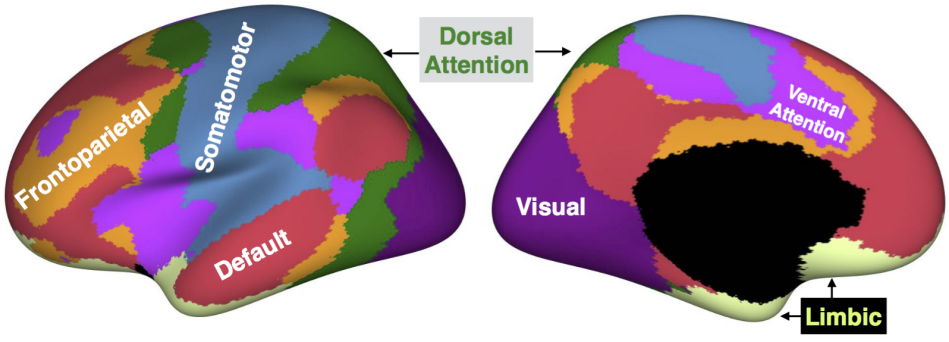

Figure 3.2: Yeo-7 atlas FreeSurfer visualization. Figure obtained from iELVis web site: `http://ielvis.pbworks.com`, accessed on May 5, 2023

Chapter 4

Methods

In this chapter, the methods that were used in the studies comprising the compendium of publications are briefly described. These computational processes are strictly applied to the data once the pre-processing stage is complete. Section 4.1 is devoted to local activation parameters, including metrics calculated in both the time and spectral domains. Section 4.2 illustrates the multilayer network analysis and the connectivity measures on which it is based. Finally, Section 4.3 outlines the statistical methods used to ascertain significant differences between study groups and correlations between EEG-derived parameters and genetic variants.

4.1 Local activation analysis

Local activation metrics are designed to extract features from brain electrical patterns originating at individual neural populations in isolation. These measures are vastly varied and can be conducted in spectral and time domains (Engels et al., 2017). Although local activation studies disregard neurodynamic associations between different brain subsystems, the resulting metrics have been useful to characterize AD (Engels et al., 2017; Jeong, 2004; Vecchio et al., 2013). In this Doctoral Thesis, "local activation" is referred to the analysis of brain activity in the vicinity of each electrode. This approach was applied in Maturana-Candelas et al. (2019), Maturana-Candelas et al. (2020), and Maturana-Candelas et al. (2021).

4.1.1 Multiscale entropies

In Maturana-Candelas et al. (2019), an entropy analysis was proposed from a multiscale perspective. This procedure allows the assessment of EEG-derived entropy values across multiple temporal scales. Originally, entropy was a thermodynamic concept. This magnitude reflects the possible number of molecular "microstates" in a thermodynamic system, which has been commonly associated with "disorder" (Natal et al., 2021). This perspective was later applied in the field of information theory, aiming to quantify the irregularity or uncertainty of a sequence (Natal et al., 2021). The first mention of entropy in this regard was proposed by Claude E. Shannon in 1948, aiming to address the "fundamental problem of communication" (Shannon, 1948). This matter exposed the question of being able to identify the data generated by a specific source, based on the signal a receiver detects through the channel (Shannon, 1948). Shannon's entropy is calculated based on the probability distribution of the values in the signal. For a discrete random variable X, it is computed as follows:

$$H(X) = -\sum_{x \in X} p(x) \log p(x), \tag{4.1}$$

where x is each value in the X series and is distributed according to $p : X \to [0, 1]$. The choice of logarithm varies between applications, being base 2 commonly used in binary series. If the values in the signal are evenly distributed, the entropy will be high, indicating a high level of uncertainty and randomness. Conversely, low entropy values denote signal values concentrated within narrower ranges. Entropy is often used in signal processing and compression applications to optimize the amount of information that can be transmitted or stored.

In the past, entropy has been employed in EEG data analysis to reveal indications of neurodegeneration, and it has been found that an entropy decrease is strongly linked to AD (Sun et al., 2020). This means that brain electrical patterns become more regular and predictable during neurodegeneration, suggesting a loss of information processing due to deficits in synaptic efficiency, lack of connectivity, and neuronal death (Sun et al., 2020). Multiple additional approaches to estimate signal irregularity have been designed to overcome diverse limitations of Shannon's entropy, such as approximate entropy (Pincus, 1995), SampEn (Richman and Moorman, 2000), and fuzzy entropy (Kosko, 1986), among others (Sun et al., 2020). Besides, these methods were proven useful to also characterize the brain activity in AD (Abásolo et al., 2005, 2006a,b; Cao et al., 2015). Furthermore, this approach

can be extended to the frequency domain by means of spectral entropy (SpecEn) (Powell and Percival, 1979). Analogous to the previously mentioned metrics, SpecEn assesses the level of irregularity derived from the PSD, demonstrating utility in delineating the dynamics of the AD brain (Abásolo et al., 2006b). In this Doctoral Thesis, entropy calculations in the time domain were carried out using SampEn, since it can be applied to short and relatively noisy time series such as the EEG (Costa et al., 2002; Ruiz-Gómez et al., 2018a,b). Both SampEn and SpecEn were used in Maturana-Candelas et al. (2019).

Sample entropy

The SampEn algorithm is explained in detail in the work of Richman and Moorman (2000). It is a non-linear metric used to assess the irregularity of a signal, which was developed as an improvement of approximate entropy (Richman and Moorman, 2000). SampEn is a type of embedding entropy that measures the similarity between a time series and its delayed version. To calculate SampEn, a positive integer m (dimension) and a positive real number r (tolerance) are used, and it is defined as the negative logarithm of the conditional probability that two sequences of length m from the time series are similar within an r threshold (normalized by the standard deviation of the original time series) at the next point, while excluding self-matches (Richman and Moorman, 2000). Given a time series of N points, $X(n) = x(1), x(2), ..., x(N)$, the $k = 1, ..., N - m + 1$ vectors of length m can be expressed as $X_m(k) = x(k + i), i = 0, ..., m - 1$. The calculation of the distances between vectors involves finding the maximum absolute difference between their corresponding scalar components. The value of B_i represents the count of vectors that meet the criterion of having a distance less than r. The normalized number of vectors that satisfies this criterion is defined as (Ruiz-Gómez et al., 2018a):

$$B^m(r) = \frac{1}{N-m} \sum_{i=1}^{N-m} \frac{B_i}{N-m-1}. \tag{4.2}$$

The process is repeated for vectors of length $m + 1$, which gives $B^{m+1}(r)$ as a result. Finally, SampEn is calculated as follows:

$$SampEn(m, r) = -\ln \left[\frac{B^{m+1}(r)}{B^m(r)} \right]. \tag{4.3}$$

SampEn returns a positive number, being the larger values indicators of greater signal irregularity. The values of r and m are crucial for the performance of SampEn, but there are no specific guidelines for optimizing these variables

(Escudero et al., 2006). However, previous studies have found that a low r value may cause the calculation to fail, while a high value may introduce bias (Escudero et al., 2006). It has been reported that setting $m = 1$ and $r = 0.25$ times the standard deviation of the original time series for sequences longer than 100 samples provided good statistical reproducibility (Escudero et al., 2006).

Spectral entropy

Shannon's definition of entropy can also be applied to assess the irregularity of a PSD. In this way, the homogeneity of the contribution of each frequency component can be estimated. Powell and Percival (1979) defined the term SpecEn to assess the frequency spread of a signal. Indeed, this approach has previously been used to evaluate disruptions in the EEG caused by AD, suggesting complementarity with non-linear methodologies for AD categorization (Abásolo et al., 2006b). SpecEn is calculated as follows:

$$H(f) = -\frac{1}{\ln(F)} \sum_{i=1}^{N} p_i \ln(p_i), \tag{4.4}$$

where p_i are the spectral amplitudes in bin i, F is the number of frequency bins (bin width is one spectral unit), and the sum of p_i is equal to 1. The p_i values correspond to the normalized value of the PSD in each frequency bin (Abásolo et al., 2006b). The results given by the formula are comprised between 0 and 1, being higher values corresponding to a flatter and more uniform spectrum with diverse spectral content (*e.g.*, white noise), and lower values indicating most of the power being condensed in fewer frequency bins (*e.g.*, sinusoidal signal) (Abásolo et al., 2006b).

The multiscale paradigm

Physiological systems are modulated by interactions between a vast number of mechanisms in different scales across space and time, which account for "chaotic". Chaotic systems, although deterministic in essence, are highly non-linear, and initial conditions may result in huge outcome differences (Eberhart, 1989), resulting in being presented as "apparently random" (Grassberger, 1991). One of the properties of chaotic systems is that they are "complex", in the sense that they are capable to store "meaningful information" or present "meaningful structural richness" (Grassberger, 1991). To fulfill this requirement, a complex system (such as time series generated by biological organisms) most likely contains

deterministic and stochastic components (Costa et al., 2005). For this reason, aligning complexity necessarily with the degree of variability of an object (which can be calculated using entropy metrics) can be misleading, since the relation between irregularity and physiologic complexity is not evident. This claim becomes apparent when realizing that white noise, although expressing maximal entropy, does not present a "complex structure" (Costa et al., 2005). This is the reason why some entropy-based metrics, such as Kolmogorov complexity (which grows monotonically with the degree of randomness), are not good estimations of complexity (Costa et al., 2005).

In the present Doctoral Thesis, we proposed the use of MSE to evaluate EEG complexity from HC subjects and patients with MCI and AD. MSE is a technique that allows to reveal entropy values from a time series at different temporal scales. Previously, the assessment of biosignal complexity was conducted by applying this metric (Costa et al., 2002, 2005). MSE is based on the computation of SampEn in coarse-grained time series derived from the original signal (Costa et al., 2002, 2005). The coarse-grained procedure is calculated as follows:

1. Given a one-dimensional discrete time series, $X(n) = x(1), x(2), ..., x(N)$, the resulting coarse-grained series Y^τ are built according to the scale factor τ. This process is carried out by calculating the mean value of the data points from non-overlapping windows of length τ (Costa et al., 2005; Escudero et al., 2006). As τ increases, the number of samples for each subsequent coarse-grained series is reduced by a factor of τ, being the Y^1 sequence equivalent to the original time series. The coarse-grained process is illustrated below:

$$Y^\tau(j) = \frac{1}{\tau} \sum_{i=(j-1)\tau+1}^{j\tau} x(i), \qquad 1 \leq j \leq \frac{N}{\tau} = N^\tau, \tag{4.5}$$

2. For each $Y^\tau(j)$ sequence, SampEn is calculated. As aforementioned, SampEn is reliable when evaluating sequences of 100 samples or more (Escudero et al., 2006). Since EEG epochs contain 2500 samples (see Section 3.3), the maximum τ value was set to 25.

Refined multiscale spectral entropy

Multiscale approaches can also be applied to SpecEn calculations. In this case, a refined version of multiscale SpecEn (rMSSE) was considered based on the work of Humeau-Heurtier et al. (2016) to assess the complexity of the PSD of

cardiovascular signals. This enhanced variant provides greater robustness against aliasing due to downsampling, which reduces spurious oscillations between 0 Hz and the cutoff frequency of the filter (Humeau-Heurtier et al., 2016). Analogously with MSE, rMSSE is the result of sequential entropy calculations applied to the PSD of coarse-grained versions of the original signal. The rMSSE is computed as follows (Humeau-Heurtier et al., 2016):

1. Given a one-dimensional discrete time series, $X(n) = x(1), x(2), ..., x(N)$, the coarse-grained sequence is obtained with the process described in equation 4.5.

2. The PSD of the time series Y^τ is calculated. Prior to the rMSSE application, the normalized PSD ($nPSD$) of the coarse-grained sequence is determined for each scale factor τ as $nPSD_\tau(f_j)$ for each frequency f_j, where $1 \leq j \leq \frac{N}{2\tau}$, being $\frac{N}{2\tau}$ the length of the PSD of Y^τ. Then, the $nPSD$ is computed as follows:

$$nPSD_\tau(f_j) = \frac{PSD_\tau(f_j)}{\sum_{j=1}^{N/(2\tau)} PSD_\tau(f_j)}, \tag{4.6}$$

3. Finally, the normalized rMSSE is calculated applying the Shannon's definition of entropy to the $nPSD$:

$$rMSSE_\tau = -\frac{1}{\ln(\frac{N}{2\tau})} \sum_{j=1}^{N/(2\tau)} nPSD_\tau(f_j) \ln[nPSD_\tau(f_j)]. \tag{4.7}$$

The obtained MSE and rMSSE profiles can be used to quantify complexity by measuring slope values (Escudero et al., 2006) and areas under the curve (AUC) (Mcintosh et al., 2010; Weng et al., 2015). In this Doctoral Thesis, scale factors were divided into two groups for both MSE and rMSSE parameters. MSE lower scales were considered from scale factors 1 to 10, and higher scale factors from 11 to 25. Regarding rMSSE, lower scales were considered from scale factors 1 to 3, and higher scale factors from 4 to 25. This decision was considered *post hoc* to ease the evaluation of MSE and rMSSE profiles as high and low scales manifested patterns notoriously different.

4.1.2 Bispectrum

In Maturana-Candelas et al. (2020), a bispectral analysis was conducted. This perspective permits ascertaining the non-linear interactions between different

frequency components. In general, spectral analysis is a valuable tool for comprehending the characteristics of a signal in the frequency domain, revealing information that may be obscured, or not immediately apparent, in the time domain. The most common method to examine the features of the frequency spectrum is through the PS, a function based on the signal autocorrelation in the time domain. PS is defined as the second-order spectrum (Rosenblatt and Ness, 1965). Nonetheless, although PS provides useful insights to study problems of a "linear nature" (*e.g.*, Gaussian signals), it is not sufficient to analyze non-linearity (Rosenblatt and Ness, 1965). For this reason, non-linear elements, such as phase relations between frequency components, are neglected in PS (Nikias and Mendel, 1993). In order to inspect these interactions, spectra defined in terms of higher order statistics or "cumulants" are needed, which comprises HOS (Nikias and Mendel, 1993). In signal theory, the Fourier transform of the third-order statistics of a stationary signal constitutes what is called "bispectrum". The use of bispectrum has previously been applied in the clinical field, revealing features for facilitating Parkinson's disease diagnosis (Yuvaraj et al., 2018), prediction of epileptic seizures (Chua et al., 2010), and monitoring depth of anesthesia (Kissin, 2000). In this Doctoral Thesis, bispectrum has been used to study the interactions between different frequency bands (Maturana-Candelas et al., 2020). The bispectrum of a signal $x(t)$ is defined as:

$$Bisp(f_1, f_2) = E[X(f_1)X(f_2)X^*(f_1 + f_2)], \tag{4.8}$$

where $X(f)$ is the Fourier transform of the signal $x(t)$, $X^*(f)$ its complex conjugate and $E[\cdot]$ represents the expectation operation (Chua et al., 2010). This set of factors is known as a triplet (f_1, f_2, and $f_1 + f_2$), which incorporates both power and phase information (Rampil, 1998). Strong phase coupling results in higher values of the third factor of the triplet ($X^*(f_1 + f_2)$), as it implies that f_1 and f_2 may have a common generator or that the neural circuitry synthesizes new dependent components at the modulation frequency $f_1 + f_2$ (Rampil, 1998). This means that Bisp returns nonzero values as long as phase angles are aligned, regardless of the power at each frequency component, being this the reason why bispectrum is sensible to phase coupling interactions. The outcome of the Bisp computation is a bispectral matrix that shows the interactions between every pair of frequency components in the signal spectrum.

Bispectral features

In order to inspect the bispectrum, several parameters calculated from bispectral matrices have been proposed, such as the mean of bispectral magnitude, the sum of logarithmic amplitudes, or bispectral entropies, among many others (Nasrolahzadeh et al., 2018; Vaquerizo-Villar et al., 2018). However, these metrics are applied to the whole bispectral matrices, being unable to reveal interactions between specific frequency bands. In this Doctoral Thesis, three novel metrics are proposed to study these interconnections: bispectral relative power (BispRP), bispectral cubic entropy (BispEn), and bispectral median frequency (BispMF), which were applied in the bispectrum regions that represent interactions between each band and strictly the rest of the spectrum. For the sake of clarity, an example of an inter-band bispectral region is depicted in Figure 4.1.

The aforementioned metrics are described below:

- BispRP is defined as the quantity of bispectral power accumulated within a particular bispectral region. In our case, BispRP was used to calculate bispectral power in regions that describe the interaction between a frequency band and the remaining spectrum. Elevated levels of BispRP suggest stronger inter-band correlations. BispRP is computed as:

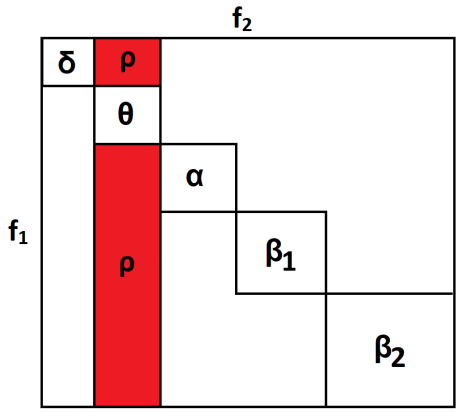

Figure 4.1: Illustration of the bispectral inter-band region (ρ) for theta band (θ), which corresponds to the region of the bispectrum matrix that reflects interactions between a specific frequency band and the global spectrum, excluding the interactions among frequencies within that frequency band.

$$BispRP = \sum_{(f_1,f_2)\in\rho} |Bisp(f_1, f_2)|, \tag{4.9}$$

where ρ refers to the subset of the bispectrum matrix that represents the correlations between a particular frequency band and the overall spectrum, while disregarding intra-band correlations (see Figure 4.1).

- BispEn quantifies the homogeneity of the distribution of bispectral values within a bispectral region. BispEn is calculated based on Shannon's definition of entropy. High values of BispEn are the result of homogeneously distributed values, while low BispEn values indicate more inter-band interactions condensed in fewer frequency components. BispEn is defined as the cubic version proposed by Nasrolahzadeh et al. (2018):

$$BispEn = -\frac{1}{N}\sum_i p_i \ln(p_i), \tag{4.10}$$

where

$$p_i(f_1, f_2) = \frac{|Bisp(f_1, f_2)|^3}{\sum_{(f_1,f_2)\in\rho} |Bisp(f_1, f_2)|^3}, \tag{4.11}$$

being i each point in region ρ and N the total number of points in ρ.

- BispMF is defined as the frequency at which the bispectral overall power in ρ is divided by two. BispMF is a measure of the tendency of certain frequency bands to interact with either the higher or lower frequency components of the global spectrum. This is the application of the traditional median frequency defined in Poza et al. (2007) to the bispectrum. The expression for BispMF is presented below:

$$0.5 \sum_{(f_1,f_2)\in\rho} |Bisp(f_1, f_2)| = \sum_{(minf_2)\in\rho}^{BispMF} \sum_{f_1\in\rho} |Bisp(f_1, f_2)|. \tag{4.12}$$

4.1.3 Relative power

Maturana-Candelas et al. (2021) is the first of the publications in which genetic information was considered. In this study, the relative power (RP) and the

homogeneity of the distribution of these values across the brain were computed. RP is one of the most commonly used parameters to characterize the spectrum of a signal due to its simplicity. RP quantifies the power allocated in a specific frequency range according to the whole spectral power (Bachiller et al., 2014). RP is useful for identifying changes in the spectral content of a signal that may not be immediately evident in the time domain. One of the hallmarks of EEG perturbations caused by AD is the slowing of the signal. This issue can be perceived simply by measuring the RP ratio between slower frequency bands and faster frequency bands (Benwell et al., 2020). Computationally, RP is defined as the sum of the power contribution in a specific frequency range:

$$RP_{band} = \sum_{f \in f_p} PSD(f), \qquad f_p = \{\delta, \theta, \alpha, \beta, \gamma\}, \tag{4.13}$$

being PSD the normalized power spectral density associated with each frequency component f. As seen in equation 4.13, RP was calculated in the classical frequency bands previously described in Section 1.5.1, namely, delta (δ, 1-4 Hz), theta (θ, 4-8 Hz), alpha (α, 8-13 Hz), beta (β, 13-30 Hz), and gamma (γ, $>$ 30 Hz).

Spatial entropy

Shannon's entropy is subject to be used in circumstances not directly related to signals. For instance, when analyzing the distribution of RP values across each ROI in the brain, spatial entropy (SE) is a convenient measure to use. Analogously with other types of entropy metrics, higher values would mean greater value heterogeneity or diversity, and lower entropy signifies homogeneous distributions. In one of the studies included in this Doctoral Thesis (Maturana-Candelas et al., 2021), RP values were obtained in the 68 ROIs designed by the Desikan-Killiany atlas (Desikan et al., 2006) and, for determining the homogeneity of their distribution, SE was used for each frequency band. SE is defined below:

$$SE_{band} = -\frac{1}{\log N} \sum_{n}^{N} PDF_n(f_p) \log(PDF_n(f_p)), \qquad f_p = \{\delta, \theta, \alpha, \beta, \gamma\}, \tag{4.14}$$

where PDF is the probability density function, which was estimated from the normalized histogram of RP values obtained from each frequency band. Also, n is each bin in the PDF, and N is the total number of bins. In order to set the

number of bins of the histogram, the Freedman-Diaconis rule was used (Freedman and Diaconis, 1981).

4.2 Multiplex network analysis

The opposite approach of analyzing the EEG from each channel or ROI individually entails the investigation of the brain functional architecture, which is constructed by the interconnections between each pair of nodes. This is called the brain functional network (see Section 1.6.2), and it permits the exploration of brain activation as a whole. However, these networks are usually built from EEG signals encompassing the entire spectrum and, given that specific frequency bands are involved in particular cognitive processes (Siegel et al., 2012; Wang, 2010), some information may remain hidden. In fact, brain functional networks have been suggested to be frequency-dependent (Bullmore and Sporns, 2009; Hillebrand et al., 2012; Stam, 2014). In order to assess the implications of each frequency band in brain functioning, a multiplex network analysis (MNA) can be useful. MNA establishes a framework to inspect frequency-specific functional networks in isolation and the relations between themselves. Also, multiplex networks differ from other interconnected networks in that interlayer edges can only connect nodes that represent the same node in different layers (Kinsley et al., 2020) (see Figure 4.2). This technique has been proved to be useful in the characterization of the relationships between frequency-specific networks in MEG (Brookes et al., 2016; Tewarie et al., 2016; Yu et al., 2017). In this Doctoral Thesis, MNA was used to study the homogeneity of the contribution of each node in each frequency band to the whole spectrum to elucidate the impact of several variations of the *MAPT* gene in the brain functional network (Maturana-Candelas et al., 2024).

Before constructing the multiplex networks, a connectivity analysis has to be previously conducted. Connectivity accounts for the second hierarchical level of brain activity analysis, reflecting the associations between EEG signals obtained from different generators. These generators can be channels or ROIs depending on whether source localization algorithms were previously applied. Among the numerous connectivity metrics that exist in the literature, PLI has the capability of being relatively insensitive to the effects of volume conduction (Ruiz-Gómez et al., 2019; Stam et al., 2007). This issue is of great importance since primary and secondary leakage can lead to spurious connectivity estimations (Palva and Palva, 2012; Schoffelen and Gross, 2009) being, for this reason, the used connectivity metric in this Doctoral Thesis. PLI quantifies the asymmetry of the distribution

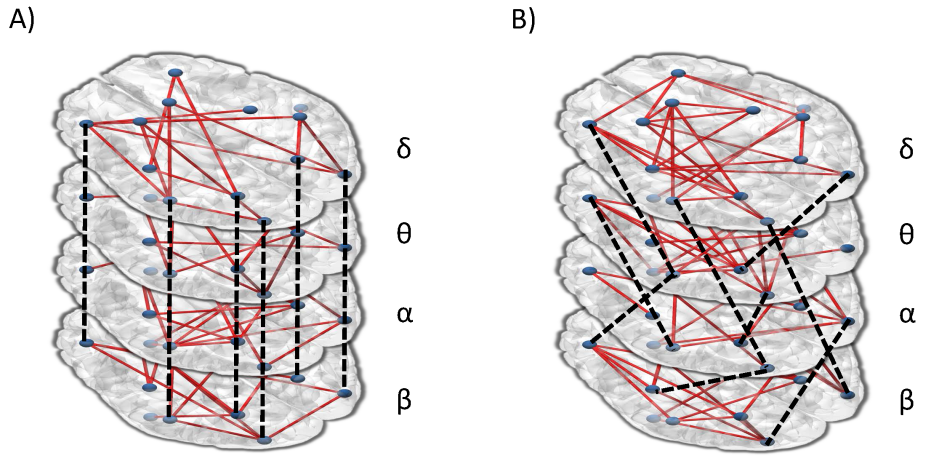

Figure 4.2: Multilayer networks. Dashed lines represent interlayer connections and solid red lines represent intralayer connections. A) Multiplex network formed by brain functional networks in each frequency band from δ to β. Interlayer connections are exclusively linking the same node in different layers. B) Interconnected network with the same configuration. Interlayer edges connect different nodes between layers.

of instantaneous phase differences between two series as follows (Stam et al., 2007):

$$PLI = |\langle sign[sin(\Delta\phi(t_k))]\rangle|, \tag{4.15}$$

where $\Delta\phi(t_k)$ indicates the phase difference for each sample between two time series, and $\langle\cdot\rangle$ designs the mean value (Stam et al., 2007). The resulting PLI values are ranged between 0 and 1, with 0 indicating no coupling or a phase difference centered at zero or π; and 1 indicating perfect, non-zero-centered phase coupling (Stam et al., 2007). In this Doctoral Thesis, MNA was applied to source-level EEG using Yeo-7 atlas. Thus, each PLI calculation resulted in a 14x14 adjacency matrix for each epoch, frequency band, and subject, representing all pair-wise connections between every ROI. The average of all adjacency matrices of all the epochs at each frequency band was calculated, resulting in four matrices (*i.e.*, frequency layers) for each subject. The integration of these layers yielded the multiplex network, which was analyzed to reveal the multiplex features of specific nodes in the brain functional network.

To quantify the heterogeneity of the connectivity contribution of a node to the different layers of a network, the participation coefficient (P) was used. P estimates the extent to which a node allocates its connectivity values to either a single layer or to multiple layers homogeneously. P has previously been used to assess hub

disruption in AD, aiding in characterizing the network alterations caused by the disease (Cai et al., 2020; Yu et al., 2017). In order to calculate P, the degree of the node i on a layer ψ must be previously calculated as follows (Battiston et al., 2014; Yu et al., 2017):

$$s_i^{[\psi]} = \sum_{j=1}^{n} w_{ij}^{[\psi]}, \qquad \psi = \{\delta, \theta, \alpha, \beta\}, \tag{4.16}$$

where w_{ij} is the connectivity value between node i and j which, in our case, corresponds to the value calculated from the PLI algorithm. In addition, n was established to 14, according to the number of nodes (sources of the Yeo-7 atlas). Each ψ layer was obtained from the grand average of PLI values between each node pairwise calculated in each artifact-free epoch from source-level EEG. Then, the node degree $s_i^{[\psi]}$ from each node was summed across layers, which resulted in the overlapped weighted degree:

$$o_i = \sum_{\psi} s_i^{[\psi]}, \qquad \psi = \{\delta, \theta, \alpha, \beta\}, \tag{4.17}$$

which was computed for each of the 14 nodes in each subject. Finally, the P coefficient was calculated for each node i as shown below (Battiston et al., 2014; Yu et al., 2017):

$$P_i = \frac{M}{M-1}\left[1 - \sum_{\psi}\left(\frac{s_i^{[\psi]}}{o_i}\right)^2\right], \qquad \psi = \{\delta, \theta, \alpha, \beta\}, \tag{4.18}$$

where $M = 4$ corresponds to the number of layers. The results obtained from the P calculation can range from 0 to 1. A P value of 1 indicates connectivity values homogeneously distributed across layers, while a value of 0 means all connections with the node are concentrated in a single layer (Battiston et al., 2014). The definite P coefficient for each ROI was obtained by averaging P values for each subject. Previously, greater differences in P values between HC subjects and AD patients have been related to disruption of nodal hub features (Yu et al., 2017).

To ascertain the global hub disruption in the brain functional network, the k index was proposed (Achard et al., 2012). The k parameter displays the gradient of the regression line, which is the least-squares first-order polynomial fit that associates the P values of AD patients minus the average P values of HC subjects (namely, P disruption) to the mean P values of HC subjects (Achard et al., 2012; Yu et al., 2017). Low k values indicate less global hub disruption, as the P values

from AD patients would be more similar to those from HC subjects. Thus, the k parameter enables comparison of hub properties in brain functional networks between different groups.

4.3 Statistical tests

To assess normality and homoscedasticity of the data, Kolmogorov-Smirnov and Shapiro-Wilk tests were utilized. In this Doctoral Thesis, no study showed any data meeting these parametric assumptions. For this reason, in order to determine differences with statistical significance, non-parametric tests were used. Kruskal-Wallis test was calculated for multiple group comparisons and the Mann-Whitney U-test for pairwise group comparisons (for both, $\alpha = 0.05$). To avoid falsely rejected hypotheses in comparisons between multiple classes, a false discovery rate (FDR) correction was applied (Benjamini and Hochberg, 1995). In addition, Chi-squared tests (χ^2) were used to compare qualitative variables, such as sex or presence of genetic variants to identify confounding factors.

Finally, a classification analysis was conducted in Maturana-Candelas et al. (2019). To select the optimal features for classification, a stepwise multilinear regression (SMR) with a conditional forward selection approach was used. The feature selection process was carried out using a leave-one-out cross-validation scheme (Dominguez, 2009), which performed 253 iterations excluding a different subject from the training set in each fold. The predictor was then built using the remaining subjects, and the excluded subject was classified using this predictor. Subsequently, the remaining subjects were classified using the same set of features that were previously selected during the SMR feature selection process. After feature selection, quadratic discriminant analysis (QDA) was used to classify the subjects. QDA has some advantages over linear discriminant analysis (LDA) in that the assumption of data homoscedasticity and normality is not required (Bishop, 2007). In addition, LDA discriminates based on a linear decision threshold, whereas QDA classifies each class based on quadratic decision boundaries between classes, which minimizes misclassification (Bishop, 2007).

Chapter 5

Results

In this chapter, the main results obtained in this Doctoral Thesis are summarized. These findings correspond to the scientific articles that consolidate the compendium of publications (Appendix 8), and are presented sorted by date of publication as follows. First, Section 5.1 exposes the outcomes of an EEG complexity examination along the AD continuum (Maturana-Candelas et al., 2019). This study is based on the calculation of entropy metrics in different temporal scales to estimate the "structural richness" of the EEG. Section 5.2 exhibits the results of the bispectral computation to EEG data from AD patients. Besides, three parameters were obtained in the inter-band regions of the bispectrum to characterize the interactions between frequency components located at different frequency bands (Maturana-Candelas et al., 2020). Then, Section 5.3 describes the EEG alterations in the first out of two studies involving genetic data. In this work, the association between AD-related variants of *PICALM* and *CLU* genes and anomalies in the EEG was investigated (Maturana-Candelas et al., 2021). Finally, Section 5.4 is devoted to analyzing disruptions in the brain functional network linked to several *MAPT* variants. This work was conducted from an MNA approach, which was able to identify greater anomalies in specific brain areas specialized in resting-state activity (Maturana-Candelas et al., 2024).

5.1 Multiscale entropies in the assessment of EEG complexity along the AD continuum

To assess EEG complexity, multiscale entropies in the time domain (MSE) and in the frequency domain (rMSSE) were computed. Initially, the resultant values pertaining to each study cohort were obtained, encompassing HC subjects, MCI patients, and AD patients across varying severity stages. Subsequently, these data were graphically represented by plotting entropy values across different scale factors. The resulting MSE and rMSSE curves are delineated in Figures 5.1 and 5.2 correspondingly. These diagrams also illustrate the differences between consecutive severity groups at each scale factor that accounted as statistically significant, using a FDR-corrected Mann-Whitney U-test. To ascertain statistical differentiation among these cohorts, we applied the Kruskal-Wallis test, consistently revealing p-values below 0.05 for both metrics across all scales.

MSE profiles exhibited an increase of entropy values at lower scales, while rMSSE displayed a contrasting decrement. Moreover, both metrics showed trends toward stabilization or reduction at higher scales. Cohorts associated with healthier cognitive states manifested higher entropy at lower scales but relatively

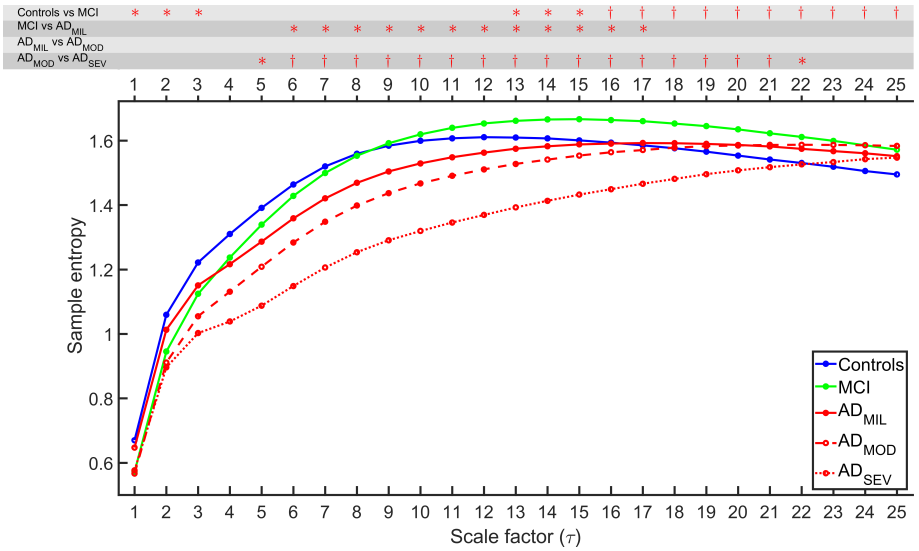

Figure 5.1: Averaged MSE profiles for each study group. Statistically significant differences are displayed on the top of the figure for each comparison between consecutive groups in each scale factor (∗: p-value < 0.05, †: p-value < 0.01, FDR-corrected Mann–Whitney U-test). Figure adapted from Maturana-Candelas et al. (2019).

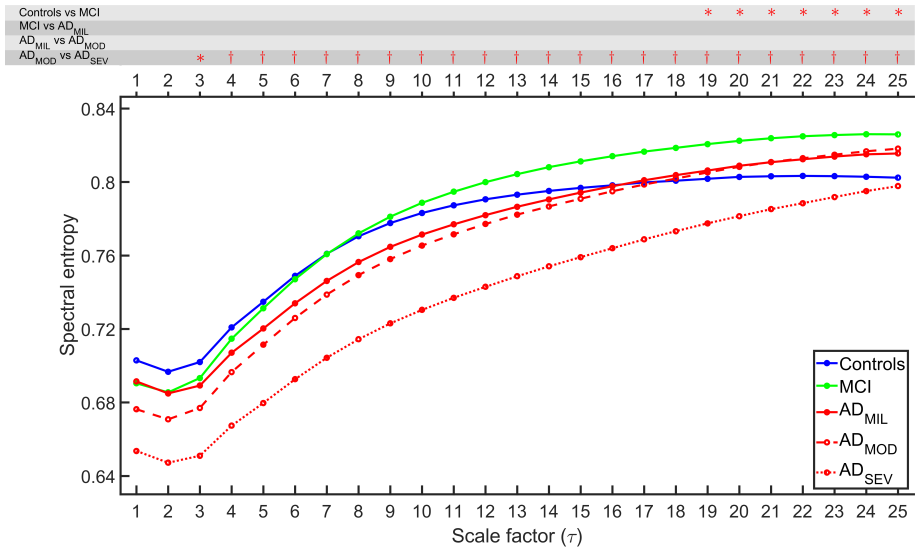

Figure 5.2: Averaged rMSSE profiles for each study group. Statistically significant differences are displayed on the top of the figure for each comparison between consecutive groups in each scale factor (∗: p-value < 0.05, †: p-value < 0.01, FDR-corrected Mann–Whitney U-test). Figure adapted from Maturana-Candelas et al. (2019).

diminished entropy at higher scales. MCI cohorts presented contradictory tendencies, displaying overall higher entropy values compared to other groups at higher scales.

In terms of statistical analysis, MSE unveiled significant differences between HC subjects and MCI across scale factors 1, 2, 3, and from 13 to 25, while rMSSE showed significant differences at scale factors 19 to 25. In addition, MSE indicated significant differences between MCI and AD_{MIL} groups at scale factors from 6 to 17. Finally, comparison between AD_{MOD} and AD_{SEV} groups revealed statistical differentiation at scale factors 5 to 22 for MSE and from 3 to 25 for rMSSE. Noteworthy, no significant differences emerged between AD_{MIL} and AD_{MOD} groups in either metric.

Subsequently, slope and AUC values were computed to estimate complexity, as displayed in Figures 5.3 and 5.4. To maximize group distinction, a differentiation was established between higher and lower scales. Lower scales were defined within the ranges 1-10 and 1-3 for MSE and rMSSE, respectively, while higher scales encompassed the ranges 11-25 and 4-25 for each metric. MSE provided statistically significant differences in slope and AUC values across multiple group comparisons. In contrast, rMSSE profiles primarily exhibited significant differences in slope

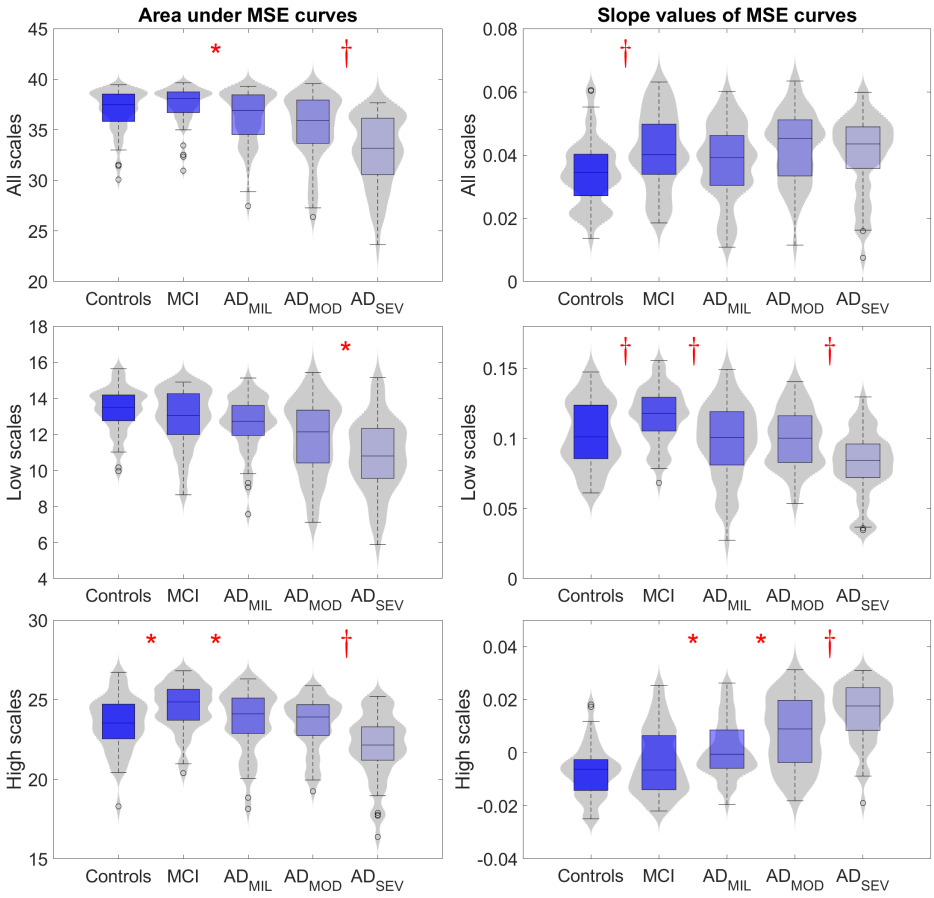

Figure 5.3: Distribution of complexity parameters: (a) area under the whole MSE curve; (b) area under the MSE curve for scale factors from 1 to 10; (c) area under the MSE curve for scale factors from 11 to 25; (d) average slope values of MSE curve; (e) average slope values of MSE curve for scale factors from 1 to 10; and (f) average slope values of MSE curve for scale factors from 11 to 25. Significant differences along AD continuum are indicated (∗: p-value < 0.05, †: p-value < 0.01, FDR-corrected Mann–Whitney U-test). Figure adapted from Maturana-Candelas et al. (2019).

values when comparing HC subjects and MCI patients. Additionally, AUC values displayed statistically significant differences between $\mathrm{AD_{MOD}}$ and $\mathrm{AD_{SEV}}$ groups. Notably, the MCI group showed statistical differentiation from $\mathrm{AD_{MIL}}$ in slope values at lower scales.

Finally, a classification analysis was conducted to determine the capability of MSE and rMSSE metrics to discriminate between study groups. 62 features were proposed: the averaged MSE and rMSSE values at each scale factor, averaged

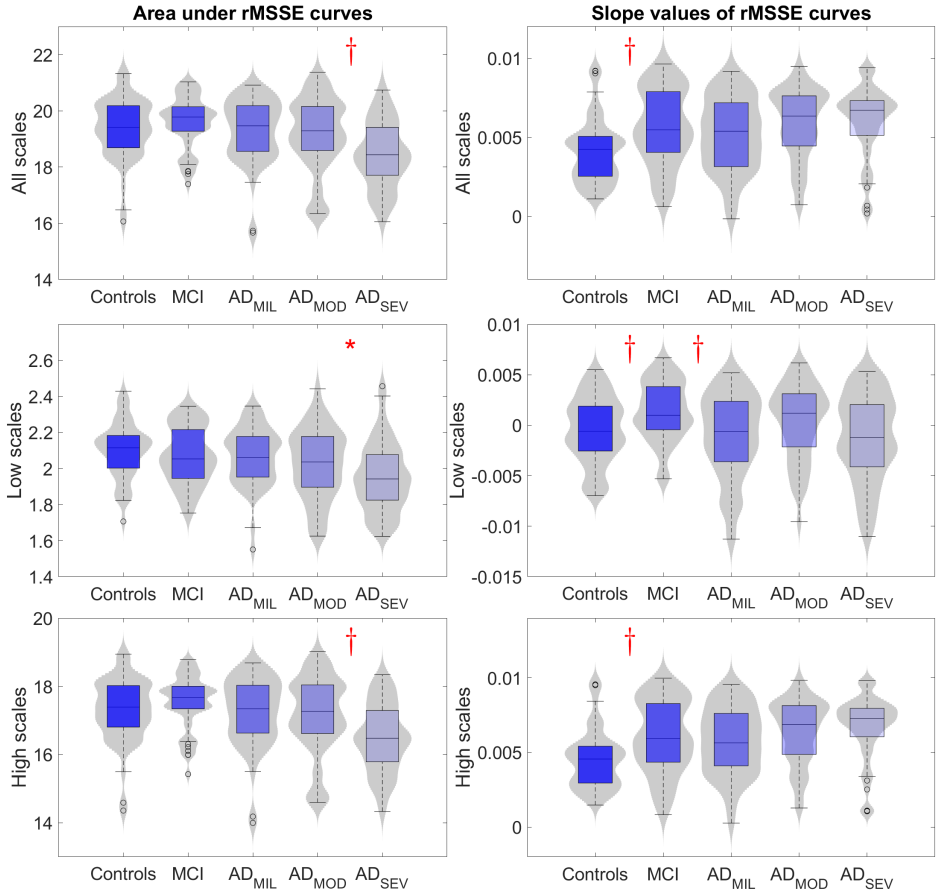

Figure 5.4: Distribution of complexity parameters: (a) area under the whole rMSSE curve; (b) area under the rMSSE curve for scale factors from 1 to 3; (c) area under the rMSSE curve for scale factors from 4 to 25; (d) average slope values of rMSSE curve; (e) average slope values of rMSSE curve for scale factors from 1 to 3; and (f) average slope values of rMSSE curve for scale factors from 4 to 25. Significant differences along AD continuum are indicated ($*$: p-value < 0.05, †: p-value < 0.01, FDR-corrected Mann–Whitney U-test). Figure adapted from Maturana-Candelas et al. (2019).

slope values of MSE and rMSSE (total, high and low temporal scales), and areas under MSE and rMSSE curves (total, high and low temporal scales). The SMR feature selection indicated the best five features to categorize groups throughout the cross-validation process: scale factors 12 and 24 of MSE, averaged MSE slopes at high temporal scales, scale factor 2 of rMSSE, and averaged rMSSE slopes at high temporal scales. Subsequently, a QDA classification was performed using separately MSE and rMSSE features, yielding confusion matrices (Table 5.1) that

Est. Class / True Class	HC	MCI	AD_{MIL}	AD_{MOD}	AD_{SEV}
HC subjects	22	16	6	4	3
MCI patients	14	27	2	7	1
AD_{MIL} patients	12	14	4	10	11
AD_{MOD} patients	4	13	3	15	15
AD_{SEV} patients	4	1	1	10	34

Table 5.1: Confusion matrix obtained from the QDA classification. HC, healthy controls; MCI, mild cognitive impairment; AD_{MIL}, mild Alzheimer's disease; AD_{MOD}, moderate Alzheimer's disease; AD_{SEV}, severe Alzheimer's disease

generated Cohen-Kappa (CK) values of 0.219 and 0.200, respectively. Nonetheless, the combination of both approaches exhibited superior performance, yielding a CK value of 0.254.

The AD groups were classified against non-AD subjects with an accuracy of 69.7% (sensitivity of 81.8% and specificity of 58.5%). Furthermore, a classification was performed between the HC group and AD group (excluding MCI subjects), which yielded an accuracy of 79.1% (sensitivity of 88.8% and specificity of 52.3%). It should be noted that if the classifier predicts a subject to be an AD_{MIL}, AD_{MOD}, or AD_{SEV} patient, the subject has a 90% probability of suffering, at least, from MCI.

5.2 Inter-band bispectral features characterizing the AD continuum

The bispectrum and its derived features were computed across cohorts comprising 51 HC subjects, 51 MCI patients, and 50 AD patients in each severity stage. Figure 5.5 showcases the grand-averaged absolute bispectrum values across channels for each respective group, revealing a discernible decrease in the diversity of inter-frequency coupling associated with pathological severity. The distribution of BispRP, BispEn, and BispMF across various frequency bands is presented in Figure 5.6, using violin plots for visual representation. Statistical comparisons, employing the FDR-corrected Mann-Whitney *U*-test, delineate significant differences between consecutive groups, visually indicated atop each figure. Additionally, these statistical values, accompanied by their corresponding *U*-values, are compiled in Table 5.2.

BispRP exhibits increasing values in the delta and theta bands along the AD

continuum. Conversely, a decrement in BispRP is observed across the alpha, beta-1, and beta-2 bands as the severity of the disease progresses. Notably, statistically significant differences emerged specifically within the alpha and beta-1 bands between the most severe groups (AD_{MOD} and AD_{SEV}). Furthermore, statistically significant differences in the theta and beta-2 frequency bands were observed between HC and MCI subjects.

Regarding BispEn, a consistent reduction aligned with the severity of AD was reported within the delta and theta bands, showing statistically significant differences between the AD_{MOD} and AD_{SEV} groups. BispEn exhibited a decrement corresponding to the severity of AD in the delta and theta frequency bands, highlighting statistically significant differences between the AD_{MOD} and AD_{SEV} groups.

In the case of BispMF, a consistent diminishing trend across all frequency bands was observed as pathological severity increases. Statistical differences emerged in the delta and theta bands between HC subjects and MCI patients. Moreover, additional statistical disparities were noted between MCI and AD_{MIL} groups, as well as between AD_{MOD} and AD_{SEV} patients in the beta-2 band. Lastly, comparisons between AD_{MOD} and AD_{SEV} groups exhibited significant differences across all frequency bands.

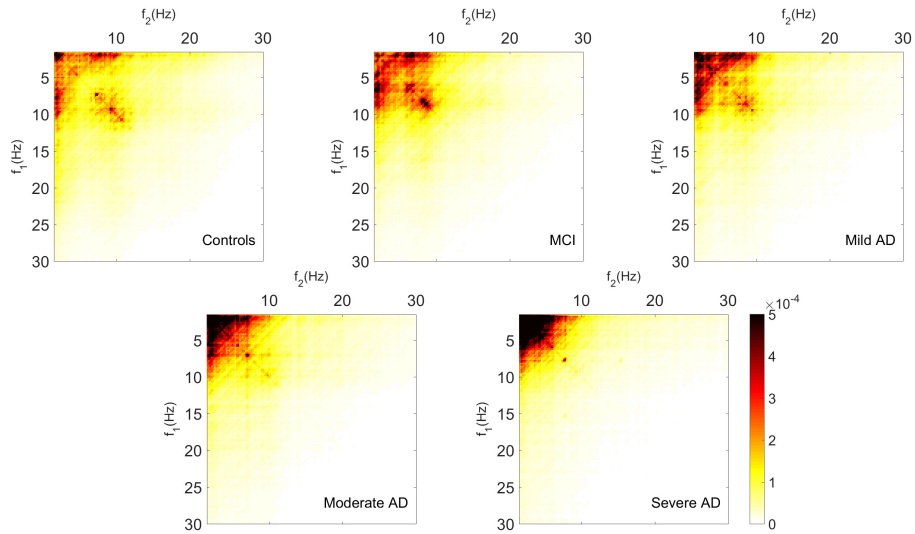

Figure 5.5: Grand average of absolute Bisp values for each group. Figure adapted from Maturana-Candelas et al. (2020).

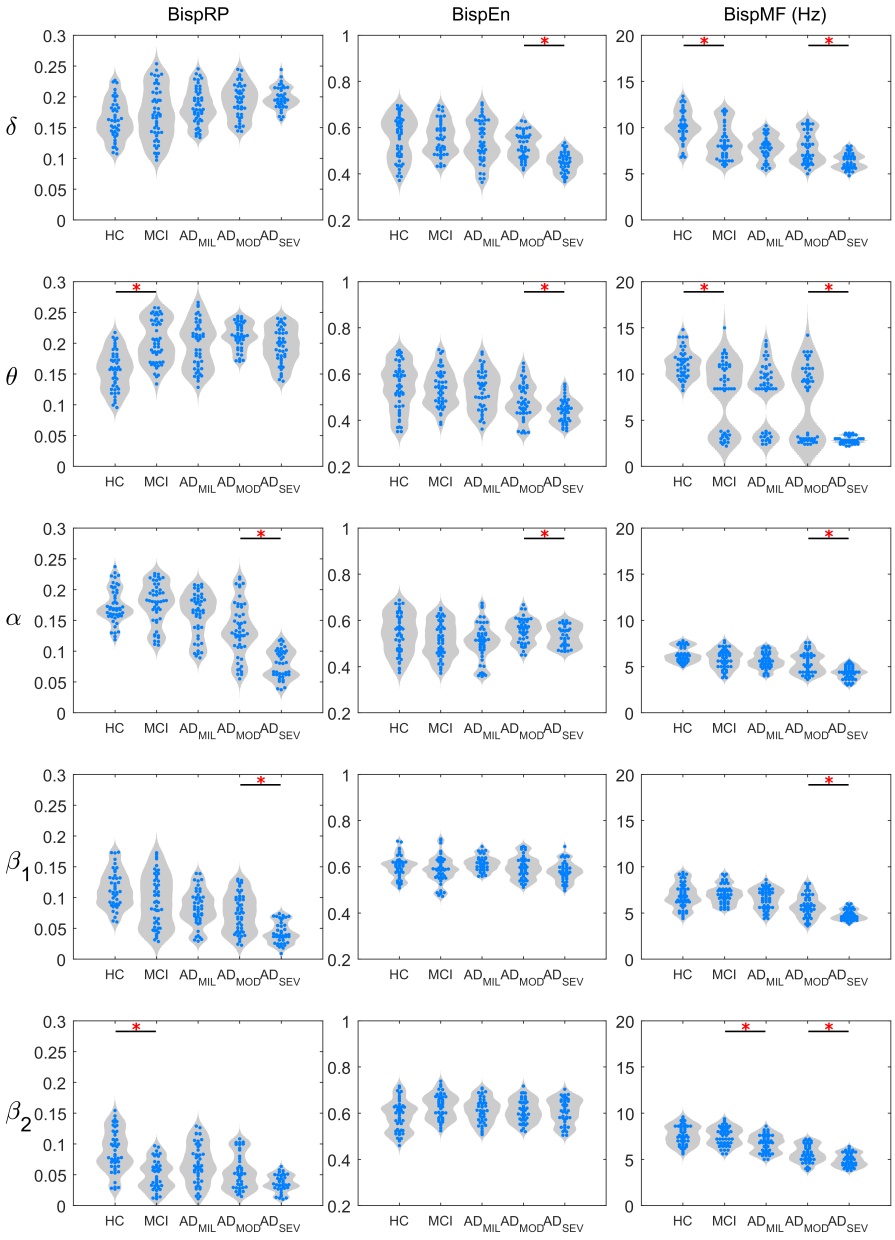

Figure 5.6: Distributions of BispRP, BispEn, and BispMF values for each frequency band. Statistically significant differences between consecutive groups are indicated with a red asterisk (p-value < 0.05, FDR-corrected Mann–Whitney U-test). Figure adapted from Maturana-Candelas et al. (2020).

Band	Comparison (group vs. group)	BispRP		BispEn		BispMF	
		U-value	*p*-value	*U*-value	*p*-value	*U*-value	*p*-value
Delta	HC vs. MCI	2574.0	0.8087	2662.0	0.8429	**3106.5**	**0.0151**
	MCI vs. AD_{MIL}	2402.0	0.3551	2729.0	0.5393	2670.5	0.7518
	AD_{MIL} vs. AD_{MOD}	2452.0	0.7407	2661.0	0.5388	2727.0	0.3410
	AD_{MOD} vs. AD_{SEV}	2506.0	0.9137	**2955.0**	**0.0188**	**2935.5**	**0.0233**
Theta	HC vs. MCI	**2098.0**	**0.0082**	2741.0	0.6047	**3021.0**	**0.0378**
	MCI vs. AD_{MIL}	2701.0	0.6239	2766.0	0.4373	2681.5	0.7175
	AD_{MIL} vs. AD_{MOD}	2347.0	0.4020	2700.5	0.4041	2657.5	0.5393
	AD_{MOD} vs. AD_{SEV}	2791.0	0.1613	**2905.0**	**0.0378**	**2955.0**	**0.0188**
Alpha	HC vs. MCI	2522.0	0.6209	2739.0	0.6047	2803.0	0.4083
	MCI vs. AD_{MIL}	2407.0	0.1085	2748.0	0.5048	2837.5	0.2501
	AD_{MIL} vs. AD_{MOD}	2864.0	0.0712	2196.0	0.0743	2580.0	0.8087
	AD_{MOD} vs. AD_{SEV}	**3171.0**	**0.0005**	**2902.0**	**0.0378**	**2959.0**	**0.0188**
Beta-1	HC vs. MCI	2921.0	0.1281	2735.0	0.6128	2581.0	0.8202
	MCI vs. AD_{MIL}	2815.0	0.3267	2412.0	0.3879	2781.5	0.4020
	AD_{MIL} vs. AD_{MOD}	2653.0	0.5393	2578.0	0.8087	2849.0	0.0767
	AD_{MOD} vs. AD_{SEV}	**3102.0**	**0.0021**	2799.0	0.1484	**2985.0**	**0.0151**
Beta-2	HC vs. MCI	**3126.0**	**0.0126**	2285.0	0.0743	2581.5	0.8202
	MCI vs. AD_{MIL}	2438.0	0.4373	2806.0	0.3410	**3033.0**	**0.0188**
	AD_{MIL} vs. AD_{MOD}	2655.0	0.5393	2524.0	0.9972	2862.0	0.0712
	AD_{MOD} vs. AD_{SEV}	2822.0	0.1117	2562.0	0.8429	**2949.0**	**0.0188**

Table 5.2: *U*-values and *p*-values from Mann-Whitney *U*-test for pairwise comparisons between consecutive groups (FDR-corrected). Comparisons with *p*-values below 0.05 are highlighted.

5.3 Relative power values linked to *PICALM* and *CLU* variants

RP values were calculated from EEG data from each region of interest (ROI) attending to the Desikan-Killiany atlas in each traditional frequency band. Study cohorts consisted of 53 AD patients categorized as 18 carriers of the risk alleles of *PICALM* and *CLU* genes, and 35 with the protective variants, alongside 24 HC subjects (12 with risk alleles and 12 with protective alleles). Figure 5.7 illustrates

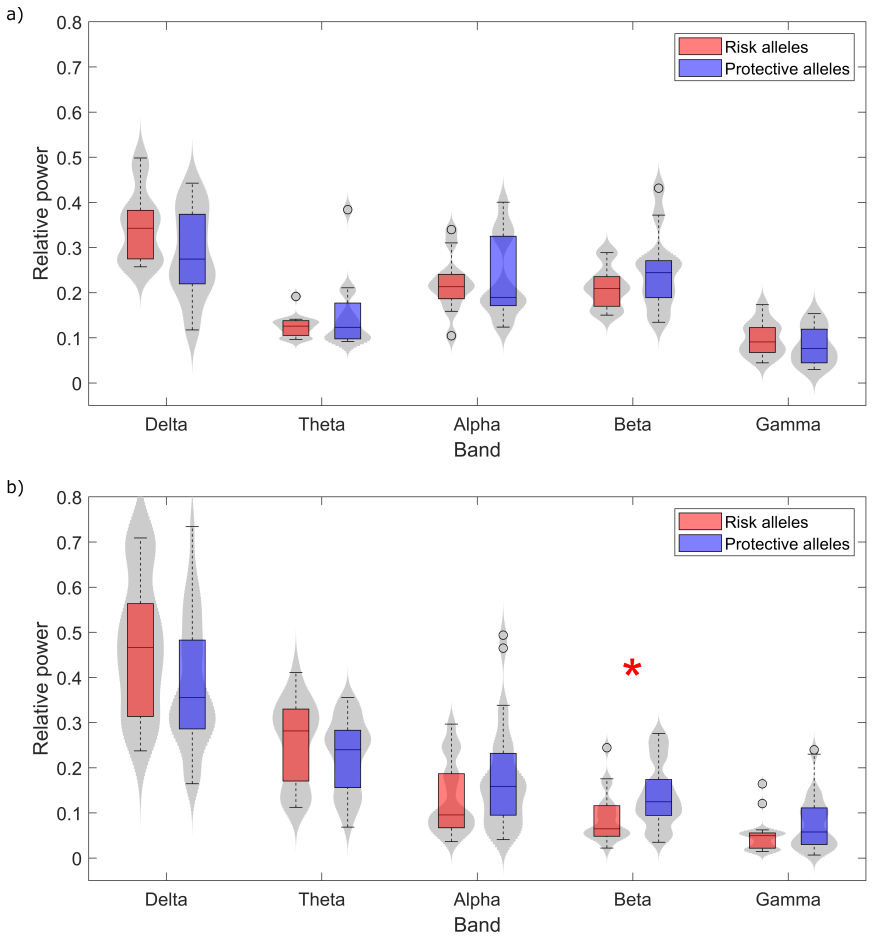

Figure 5.7: Grand-averaged RP values across ROIs for (a) controls and (b) AD patients in each frequency band. Subjects with risk alleles for both *PICALM* and *CLU* are represented in red, whereas subjects with both protective alleles are displayed in blue. Statistically significant differences (p-value < 0.05, Mann–Whitney U-test) are highlighted with a red asterisk. Figure adapted from Maturana-Candelas et al. (2021).

the distribution of grand-average RP values across all ROIs for (a) HC subjects and (b) AD patients. Within the AD cohort, the group with risk alleles exhibited higher RP values in lower frequency bands (delta and theta) and lower RP values in higher frequency bands (alpha, beta, and gamma). Notably, a statistically significant difference between risk and protective genetic variants was obtained in the beta frequency band (U-value = 342, p-value = 0.007, Mann–Whitney U-test). While no other frequency band exhibited statistically significant differences, the delta band approached the threshold of statistical significance (U-value = 584, p-value = 0.067, Mann–Whitney U-test). Conversely, the HC group displayed inconsistent variations between genotypes. Although the beta band presented higher RP values in the protective genotype, no significant differences were observed.

In addition, differences in beta-band RP values between genotype groups in AD were represented for each ROI individually outlined in the Desikan-Killiany atlas (see Section 3.5). A total of 58 out of the 68 ROIs in the AD group expressed significant distinction, as shown in Figure 5.8. In this model, red balls indicate statistically significant differences (p-value < 0.05, Mann–Whitney U-test) between AD carriers of risk and protective alleles of *PICALM* and *CLU*. Noteworthy, regions exhibiting no evidence of significant differences were primarily situated within the left hemisphere, with the exception of a singular ROI located at the right frontopolar lobe.

Furthermore, the distribution uniformity of RP values across the brain was examined by means of SE. SE computations were performed for each frequency band and genotype across HC and AD groups, as depicted in Figure 5.9. Similarly

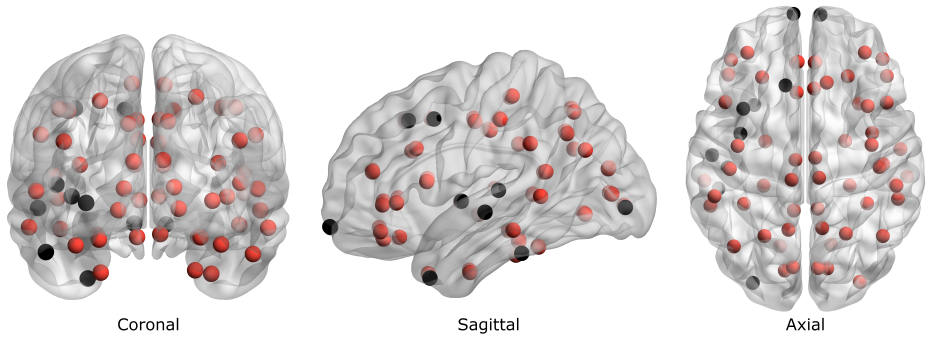

Figure 5.8: ROI localization in 3D brain model (BrainNet Viewer, v1.63 (Xia et al., 2013)) according to the Desikan-Killiany atlas. Red balls represent ROIs that showed statistically significant differences in beta RP values between AD patients with risk and protective *PICALM* and *CLU* alleles (FDR-corrected p-value < 0.05, Mann–Whitney U-test). Figure adapted from Maturana-Candelas et al. (2021).

to the RP analysis, no significant differences between genotypes were observed at any frequency band within the HC group. Conversely, the AD group showed significantly different SE values between genotypes in the beta band (U-value = 321, p-value = 0.002, Mann–Whitney U-test). Notably, AD patients carrying protective alleles showed reduced SE values at delta and theta frequency bands, and increased SE values at alpha, beta, and gamma frequency bands.

Finally, a comparison of the PSDs between genetic populations was conducted in each severity group along the AD continuum. The normalized average PSDs

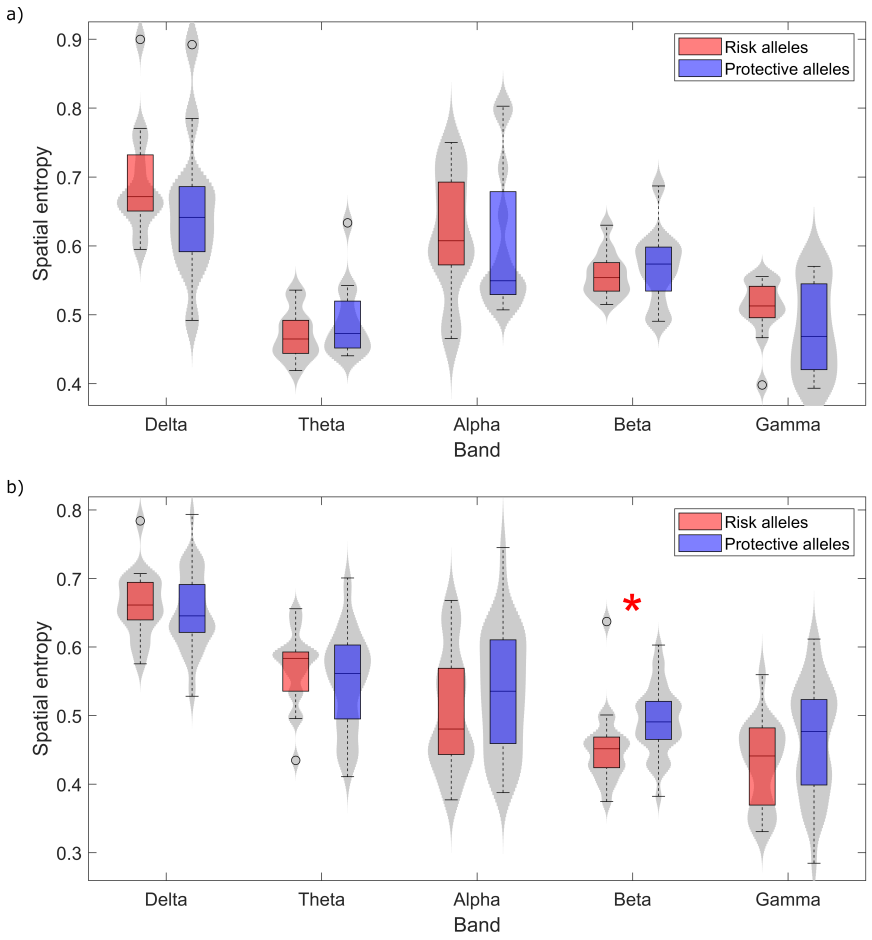

Figure 5.9: Spatial entropy of RP values for (a) controls and (b) AD patients in each frequency band. Subjects with risk alleles for both *PICALM* and *CLU* are represented in red, whereas subjects with both protective alleles are displayed in blue. Statistically significant differences (p-value < 0.05, Mann–Whitney U-test) are highlighted with a red asterisk. Figure adapted from Maturana-Candelas et al. (2021).

obtained from HC subjects, AD_{MIL}, AD_{MOD}, and AD_{SEV} patients for both genotypes were exhibited in Figure 5.10 alongside spider plots depicting RP values at each frequency band. These PSDs suggested a general slowing of the EEG from carriers of the risk variants compared to the carriers of the protective variants. In fact, excluding the HC group, PSDs derived from individuals with risk alleles resembled PSDs from individuals with protective alleles corresponding to the subsequent severity stage.

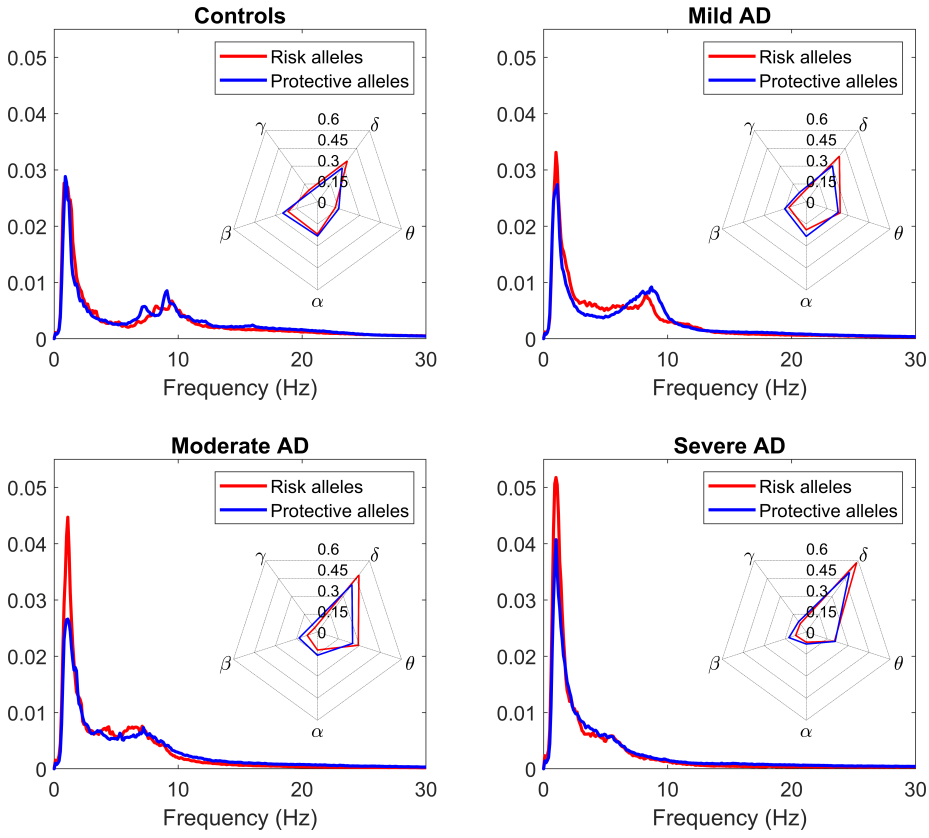

Figure 5.10: Normalized PSDs for controls and AD patients at different stages of the disease are displayed for each genotype (red, carriers of risk alleles; blue, carriers of protective alleles). Spider plots presenting RP values at each frequency band are shown for each group (Controls, Mild AD, Moderate AD, and Severe AD). Figure adapted from Maturana-Candelas et al. (2021).

5.4 Alterations associated with *MAPT* variations on the brain functional network by means of MNA

The assessment of the association between genetic expression and disruptions in the brain functional network was conducted by calculating the P coefficient. This metric served to delineate connectome disparities between subjects carrying risk and protective alleles across seven genetic *MAPT* loci for both HC and AD individuals. Initially, a scatterplot illustrating hub disruption was displayed in Figure 5.11. Each data point represents the P disruption value (*i.e.*, P in AD minus P in HC) expressed against the average P value in HC subjects across various ROIs.

Generally, carriers of protective alleles tended to exhibit lower P disruption values (average of -0.0010 $\pm$ 0.0015) compared to carriers of risk alleles (average of 0.0018 $\pm$ 0.0012). Upon examination of Figure 5.11, the protective variants of

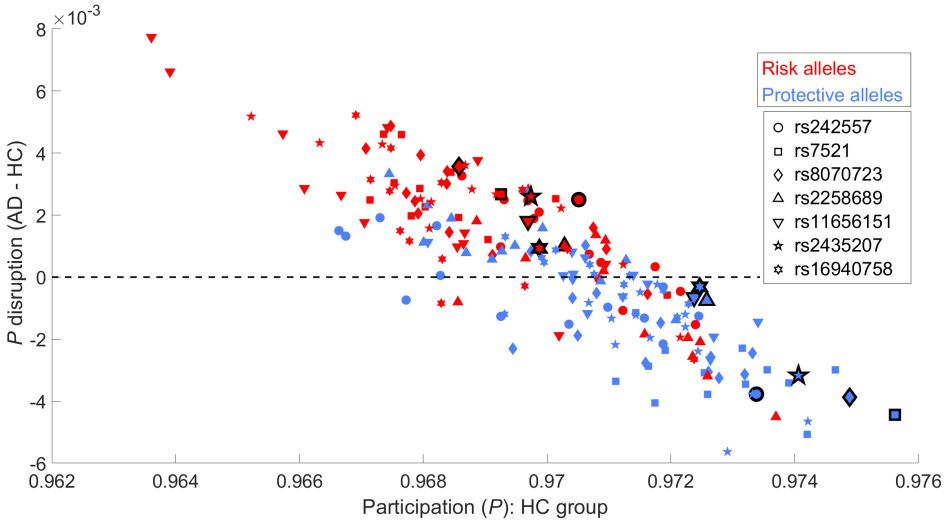

Figure 5.11: Scatterplot visualizing the relationship between P disruption values and P values obtained from the HC group. Each data point corresponds to a specific SNP, represented by different symbols: Circles for rs242557, squares for rs7521, diamonds for rs8070723, upward-pointing triangles for rs2258689, downward-pointing triangles for rs11656151, pentagrams for rs2435207, and hexagrams for rs16940758. Symbols with a black border indicate the left DMN region. Risk and protective alleles are denoted by red and blue colors, respectively. A black dashed line is included to represent the zero crossing. Figure adapted from (Maturana-Candelas et al., 2024).

certain SNPs were associated with the lowest averaged P disruption values across ROIs, specifically rs7521 ($-0.0032 \pm 9.688 \cdot 10^{-4}$), rs8070723 ($-0.0019 \pm 0.0015$), and rs2435207 ($-0.0022 \pm 0.0016$). In addition, these SNPs showed the highest values of the P coefficient averaged by ROIs in HC subjects for these alleles (0.9729 ± 0.0013, 0.9717 ± 0.0016, and 0.9722 ± 0.0011, respectively). Particularly, the SNP rs7521 presented the highest value of P coefficient in the controls' left DMN (0.9756).

Three possible causes may account for the observed differences in P disruption values between genotypes: (i) differing connectivity patterns in the control group, (ii) differing connectivity patterns in AD patients, or (iii) a combination of both factors. To investigate this issue, the distribution of P values was analyzed for each SNP and genotype, as illustrated in Figure 5.12. Within the HC group, five out of the seven SNPs exhibited significantly higher P values in protective alleles compared to risk alleles (rs7521, rs8070723, rs11656151, rs2435207, and rs16940758), one SNP showed the inverse relationship (rs2258689), and one SNP did not manifest statistically significant differences between the subgroups (rs242557). Conversely, in the AD group, significantly higher P values were identified in the risk group across four SNPs (rs242557, rs7521, rs8070723, and rs2435207), while the remaining SNPs did not exhibit statistically significant differences. These findings suggest that distinctive connectivity patterns observed in both HC subjects and AD patients contribute to the observed disparities in P disruption values between genotypes, as depicted in 5.12c.

Furthermore, Figure 5.12 showcased the P and P disruption values specific to the left DMN denoted by black crosses in each boxplot. This region not only exhibited the consistently high P values in HC carriers with protective alleles, but also displayed low values of P disruption, being even the lowest in some SNPs. Remarkably, the absolute mean value of P disruption across SNPs was the highest in the left DMN (4.610^3). Additionally, the left DMN consistently displayed higher P values in HC protective carriers across all SNPs, with the highest mean value (0.974) observed in this allele.

To assess the connectivity implications of each layer in the multiplex network, the analysis focused on individual frequency bands. Theta and beta bands exhibited the most consistent tendencies in node degree between HC and AD patients (see Figure 5.13), while delta and alpha bands displayed more diverse patterns. Findings pertaining to the theta and beta bands are showcased in Figure 5.13. Within HC subjects, the group with protective alleles generally displayed decreased node degree values in the theta band, with exceptions noted in SNPs rs2435207 and rs16940758. Conversely, the opposite case was observed in the beta

band across all SNPs, except for rs11656151. Furthermore, AD patients exhibited generally reduced and less uniform differences in node degree values across all frequency bands.

Finally, the P-derived parameter k was obtained for each SNP and genotype and summarized in Table 5.3. Notably, every SNP exhibited negative k values, indicating an association between regions exhibiting high P values in HC subjects and negative values of P disruption (*i.e.*, higher P values in AD compared to HC). Furthermore, k values derived from risk and protective alleles were statistically significant different (p-value = 0.011, Mann-Whitney U-test). This finding indicates an increased global hub disruption among subjects with risk alleles, given the more pronounced disparity in P values between the AD and HC groups.

SNP	k_{risk}	$k_{protect}$
rs242557	-1.112	-0.595
rs7521	-0.733	-0.352
rs8070723	-0.864	-0.704
rs2258689	-1.135	-0.660
rs11656151	-0.989	-0.628
rs2435207	-0.837	-0.108
rs16940758	-1.001	-0.402
Mean	**-0.953**	**-0.631**
p**-value**	**0.011**	

Table 5.3: Hub disruption index (k) calculated from the gradient coefficient of the regression line derived from the scatterplot of P disruption values for each SNP. The statistical significance of the genotype differences was also shown (Mann-Whitney U-test).

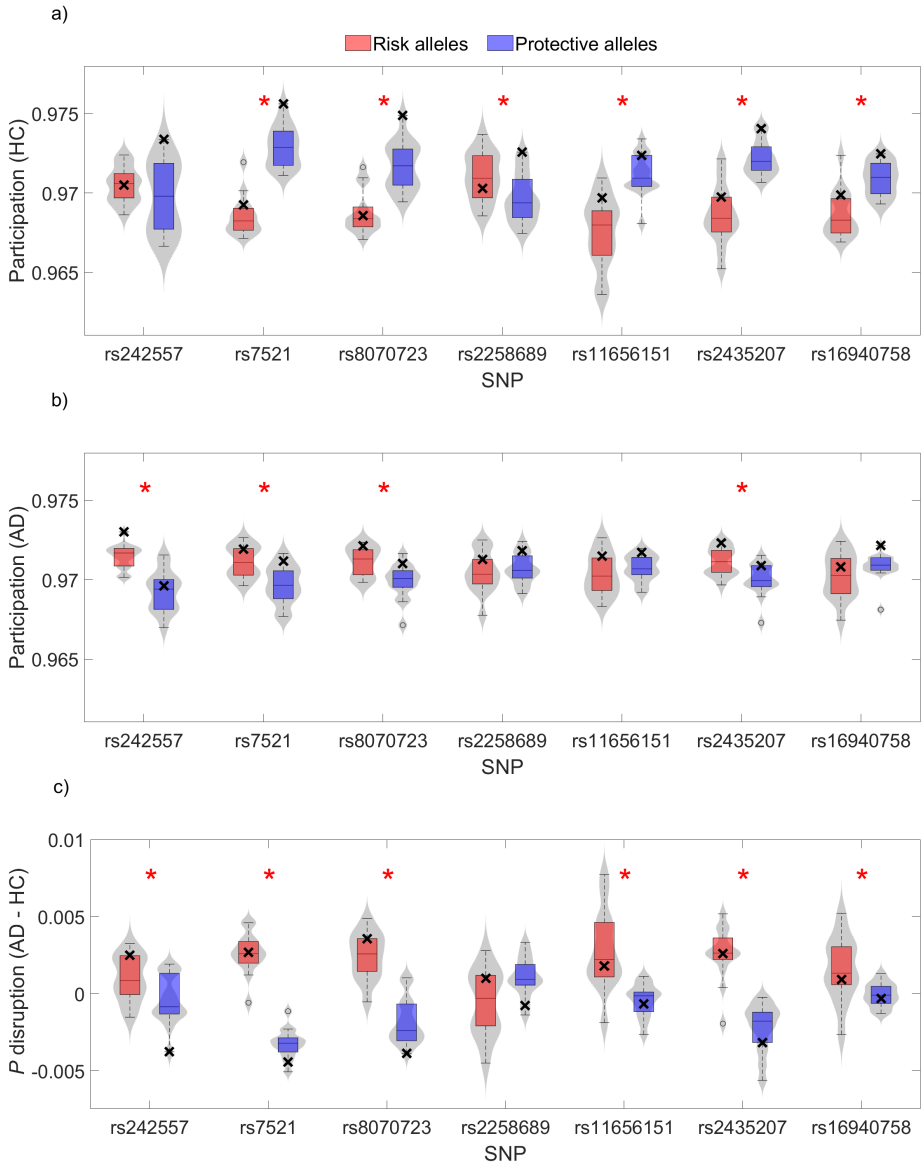

Figure 5.12: Average distribution of P values across all ROIs for each SNP in both the a) HC and b) AD groups. Additionally, the P disruption values were displayed in c). Statistically significant differences between genotypes were marked with a red asterisk (FDR-corrected p-values < 0.05, Mann-Whitney U-test). The black cross in each distribution represents the value corresponding to the left DMN region. Figure adapted from (Maturana-Candelas et al., 2024).

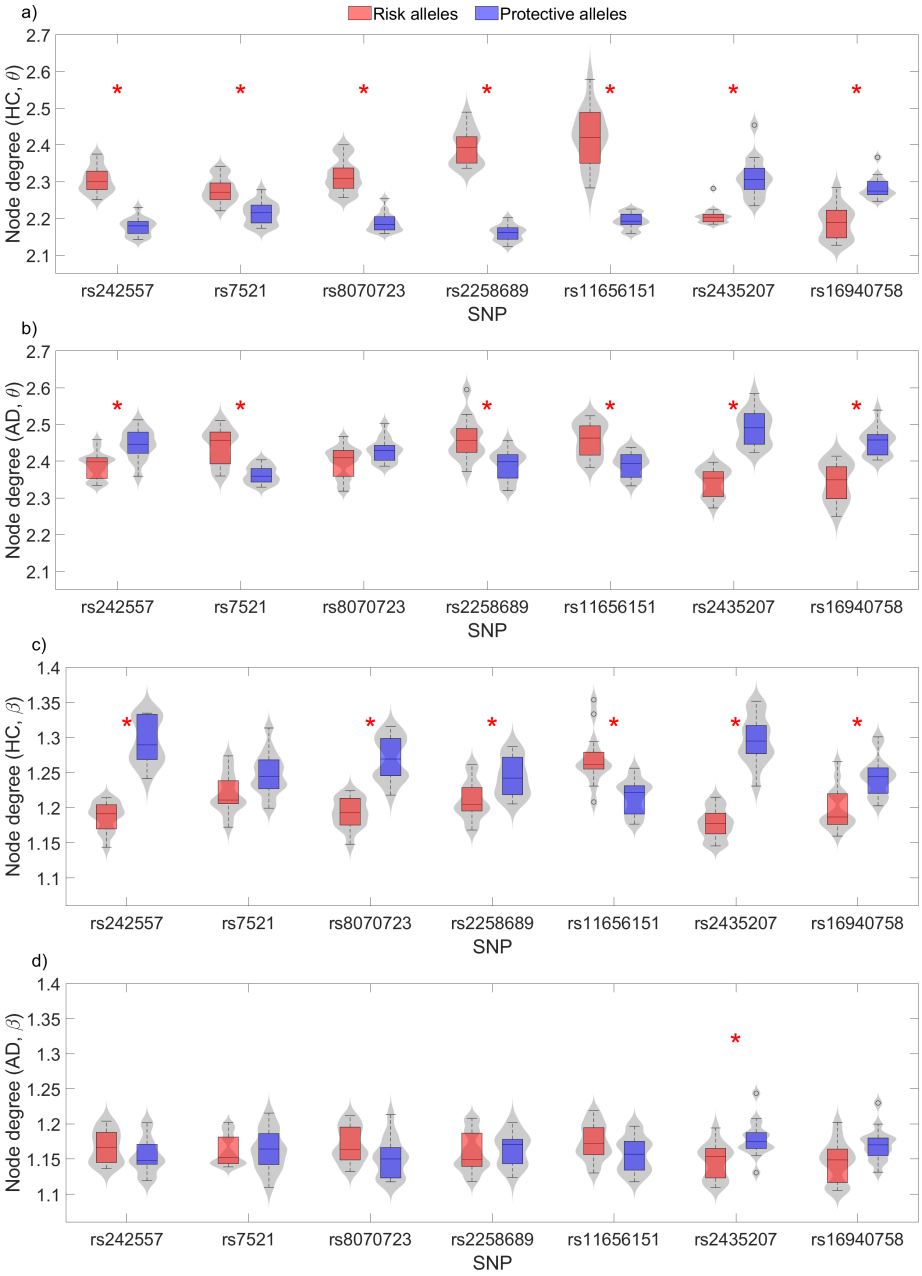

Figure 5.13: Average distribution of node degree across all ROIs in each SNP for a) HC subjects in theta band, b) AD patients in theta band, c) HC subjects in beta band, and d) AD patients in beta band. Statistically significant differences between genotypes were denoted by a red asterisk (FDR-corrected p-values < 0.05, Mann-Whitney U-test). Figure adapted from (Maturana-Candelas et al., 2024).

Chapter 6

Discussion

In this Doctoral Thesis, the brain electrical activity has been explored from multiple perspectives in several stages of neurodegeneration, from healthy conditions to severe dementia. In addition, the associations between *PICALM*, *CLU*, and *MAPT* variants and alterations in neural dynamics were studied. From a clinical standpoint, the results obtained could be useful in detecting signs of neural disruption that could eventually lead to disease, even in healthy states. First, the ability of multiscale entropies to detect differences in the EEG between severity groups was demonstrated (Maturana-Candelas et al., 2019). MSE and rMSSE were useful in distinguishing these groups, even though they provided similar values of traditional entropy measures (*i.e.*, scale factor 1). This point exposes evidence that the EEG, due to its highly complex and non-linear structure, integrates information that can only be unveiled with sophisticated processing approaches. This is also the case of bispectrum, a computational technique that allows to examine the interactions between different frequency components. For the sake of novelty, bispectral regions expressing inter-band coupling were inspected to determine hints of neurodegeneration along the AD continuum (Maturana-Candelas et al., 2020). Differences among severity groups were obtained, which emphasizes the importance of the non-linear nature of the EEG. However, simple parameters can still be useful in the evaluation of the impact caused by biological elements in brain electrical activity. In this way, RP has been proven to reflect neurodegeneration with notorious precision. For this reason, differences in spectral power related to genetic expression can therefore be associated with neural dysfunction. In Maturana-Candelas et al. (2021), different variants *PICALM* and *CLU*, which have been previously linked with Aβ clearance

mechanisms, were associated with RP disruptions in AD patients. This insight can be the result of increasing the impact of Aβ accumulation in circumstances where the brain loses physiological flexibility to ensure homeostasis and it is not able to cope with excessive biochemical anomalies. The impact of *MAPT* variations was assessed from a network organization framework (Maturana-Candelas et al., 2024). In this case, seven SNPs located at the *MAPT* gene and associated with neurodegeneration or abnormalities in tau deposition were selected. This perspective increases the robustness of the associations since consistent results would increase the likelihood that *MAPT* expression is directly implicated in neural dynamics. This was the case, as HC subjects were attributed with genotype-dependent hub disruptions (especially in resting-state brain networks), and also alterations in node degree in theta and beta frequency bands. This point is crucial for understanding that neural alterations can happen when cognition is still not affected. This chapter is dedicated to discussing the aforementioned findings in detail, providing evidence from previous studies in order to elucidate physiological interpretations from the obtained results. Finally, the main limitations encountered throughout the present Doctoral Thesis were explained alongside potential solutions to avoid them in future investigations.

6.1 Characteristic EEG elements that describe the AD continuum

Identifying EEG-derived biomarkers that discretize the presence of AD is challenging since the signs that reflect neurodegeneration are numerous and their manifestation is gradual and continuous. As there are no discrete and evident changes in brain functioning along its process, characterizing the AD continuum itself is greatly useful. This approach permits to infer any neurodegenerative state by studying the tendencies that arise between healthy cognition to the most severe cases of dementia. In this Doctoral Thesis, the exploration of the AD continuum has been conducted from different perspectives: Complexity decrease and loss of inter-band interactions.

6.1.1 Entropy and complexity: Towards the understanding of "structural richness"

In signal theory, entropy reflects irregularity (or unpredictability) of a time series. Entropy is not measured in a single way, as it accounts for a family of metrics, such

as approximate entropy (Pincus, 1995), sample entropy (Richman and Moorman, 2000), and fuzzy entropy (Kosko, 1986), among others (Sun et al., 2020). However, when applied to a stationary time series, all of these metrics return maximal values when applied to random noise compared to any other kind of signal. This is an obvious sign of inability to predict the future samples attending to the pattern observed in the past. However, unpredictability cannot be associated (at least, directly) with complexity, as they reflect different features. According to the definition provided by Kolmogorov, complexity can be assumed by the quantity of "uniqueness" of an object (Kolmogorov, 1968), which can be viewed as the "quantification of absolute information in an object that is invariant up to an additive constant" (Li and Vitányi, 2008). The most relevant indicator for Kolmogorov to detect complexity is to what extent an object is complicated to describe (Kolmogorov, 1968; Li and Vitányi, 2008). Therefore, if an object contains regularities, it can be defined with shorter descriptions and, thus, designated as 'compressible' (Li and Vitányi, 2008). Since a perfectly random object cannot be compressed (it requires a long description), this entity is complex under Kolmogorov's definition (Li and Vitányi, 2008). However, the physical process that generates this object may have a very simple description (Bialek et al., 2001; Grassberger, 1991). This is the case for structures such as Julia and Mandelbrot sets, being these utterly complex, but still generated by a relatively simple model (Grassberger, 1991). For this reason, Kolmogorov algorithmic complexity is actually a manifestation of randomness and not a measure of complexity in the intuitive sense. This is specially relevant for physiological systems, as they are governed by chaotic interactions between multiple interdependent components that operate at different scales (Lau et al., 2022). This ability enables them to dynamically distinguish "relevant" from "not-relevant" inputs (Grassberger, 1991) with the aim to adapt to the environment and increase chances of survival (Costa et al., 2005). For this reason, physiological systems necessarily have to present, not only chaotic behavior (often studied by biosignal processing), but also be generated by convoluted models that manage and regulate those behaviors. This results in systems capable to process and store "meaningful" information, which some authors characterize as "structural richness" (Costa et al., 2002, 2005; Escudero et al., 2006; Grassberger, 1991; Labate et al., 2013; Li et al., 2018). Since time series generated by biological systems contain deterministic and stochastic components (Costa et al., 2005), we can hence conclude that entropy by itself is an unreliable estimator of biosignal complexity.

In this Doctoral Thesis, we aimed to estimate EEG complexity using a

multiscale approach (Maturana-Candelas et al., 2019). This framework was applied to explore entropy quantification in different temporal scales along each epoch. Although, as aforementioned, entropy can be misleading when evaluating complexity, its multiscaled application has been previously used to conduct complexity analyses (Costa et al., 2002, 2005; Escudero et al., 2006; Labate et al., 2013; Li et al., 2018; Weng et al., 2015). Multiscale consists of generating "coarse-grained" sequences derived from the original signal (see Section 4.1.1), allowing the analysis from different temporal scopes. In order to make the comparison possible, conventional entropy values were inspected first in the original series (scale factor 1). Both MSE and rMSSE show a decrease of irregularity in AD patients compared with HC subjects, as seen in Figures 5.1 and 5.2. This finding is consistent with other entropy studies aimed to characterize AD (Abásolo et al., 2006b, 2008; Simons et al., 2015). However, it has been found that the first scale factor is not optimal for distinguishing subjects. For MSE, scale factors between 5 and 17 were more suitable to discriminate AD severity stages. Additionally, higher scale factors, especially in the range of scales 16-25, showed a highly significant distinction between HC subjects and MCI patients. This insight was also true for rMSSE values, as temporal scales from 19 to 25 were able to significantly differentiate between these two classes. These results are evidence that calculating entropy from a variety of temporal scales is able to reflect information that could remain hidden when applying the traditional approach. This could also be perceived as non-linear interactions that are only unveiled when inspected from different dimensions, which is a hint of complex structure and "richness".

Other means to estimate complexity from the MSE and rMSSE curves obtained in Figures 5.1 and 5.2 is the extraction of parameters derived from these curves, such as slopes in different scale ranges (Escudero et al., 2006) and AUCs (Weng et al., 2015). As can be observed in Figure 5.3, MSE average slope values in low temporal scales tended to decrease with the severity of the disease, while the opposite was observed in higher temporal scales. Similar trends were observed in the case of rMSSE, albeit with a less pronounced inclination, as seen in Figure 5.4. Consequently, there was an instance where entropy values of AD groups exceeded those of the HC group at higher temporal scales. These cross-over patterns were also observed in other studies aiming to characterize AD from a multiscale approach. For example, Escudero et al. (2006) observed comparable dynamics across various temporal scales when comparing individuals with AD and HC. This finding suggests a relationship between normal neurophysiology and low entropy values at higher temporal scales. Similarly, Labate et al. (2013)

investigated the connection between multiscale permutation and sample entropy and found consistent trends in entropy as the disease progressed. In line with these findings, Mizuno et al. (2010) proposed that AD may not only exhibit decreased entropy in EEG signals but also an increase in entropy at longer temporal scales. They emphasized the significance of these entropy increases, as they correlated with measures of cognitive impairment. Our own results support this notion by demonstrating a relationship between higher-scale calculations and disease severity based on slope values. Although there is no consensus in the quantitative definition of complexity (Costa et al., 2005), it was proposed that higher entropy values in most of the time scales could be a sign of higher complexity. In addition, white noise (a signal with no complexity) was observed to exhibit very high entropy values in lower scales and very low entropy values in higher scales, decreasing in an exponential way (Costa et al., 2002). Arguably, this trend is completely opposite to the pattern that is shown when analyzing the EEG, which suggests that this signal is, essentially, complex. The decrease in complexity may be due to alterations in long-range neuronal dynamics that arise from disruptions in brain structural pathways, which can be interpreted as abnormal interactions between neuronal systems that could be due to neuronal death, neurotransmission deficits, and connectivity alterations of local neuronal networks (Jelles et al., 1999; Jeong, 2004).

Remarkably, when examining all temporal scales, the MCI group exhibited the highest values in both measures. This finding suggests that EEG signals from MCI subjects demonstrate the highest level of complexity during the resting state compared to other subjects. These alterations observed in MCI patients may be associated with an increased complexity as a compensatory mechanism for functional deficits. Previous studies have reported evidence of brain plasticity in preclinical AD patients, wherein compensatory mechanisms are employed to counter early neurodegeneration even before the onset of symptoms (Becker et al., 1996). However, other studies suggest this hyperactivation as a straightaway pathological marker, as it is associated with greater atrophy and cortical thinning in medial temporal lobe regions (Dickerson et al., 2005; Putcha et al., 2011).

6.1.2 Inter-band alterations unveiling neurodegenerative progression

Bispectrum was used to characterize the AD continuum (Maturana-Candelas et al., 2020). In Figure 5.5, the bispectral matrices are shown for each severity group,

from HC subjects to severe AD patients. A visual inspection reveals greater and more diverse interactions in MCI patients compared to HC subjects. Then, an apparent decrease of diversity in frequency interactions begins to be observed as severity increases, concentrating the highest bispectral values at lower frequency bands. *Bisp* values are calculated throughout the multiplication of three factors based on: Power frequency components f_1 and f_2, and a conjugate built from $f_1 + f_2$ (see Section 4.1.2). This last term expresses non-linear interactions, which are divergences from Gaussianity such as phase coupling. This means that linear dependencies are suppressed in the calculation, resulting in zero *Bisp* values. As presence of chaotic synergies between neural oscillators is a requisite for "structural richness" (see previous Subsection), absence of non-linear interactions could be perceived as a lack of complexity. That being said, the observed broader interactions in MCI patients, as suggested beforehand, could be a sign of neural hyperactivation associated with early signs of neurodegeneration. On the other hand, the reduced variety of frequency interactions in AD patients suggests more predictive, less rich, more linearly-dependent EEG signals, which are the result of levels of atrophy and neuronal damage excessively present for the brain to maintain the compensatory mechanisms of previous stages.

In order to quantify these changes, BispRP, BispEn, and BispMF features were calculated. In addition, only inter-band regions of the bispectrum (which enclose frequency interactions that are not often evaluated) were considered in this Doctoral Thesis. First, BispRP represents the summation of bispectrum values for each frequency band interacting with the global spectrum. Higher BispRP values within a frequency band indicate a greater level of interactions between the frequency components of that band and those in other bands. As illustrated in Figure 5.6, there is an increase in BispRP for the delta and theta frequencies as the severity of the disease progresses. This could indicate an elevation in coupled interactions of the delta and theta bands with the global spectrum, but it could also be interpreted as a decrease in interactions between the higher frequency bands and the global spectrum. Conversely, the alpha, beta-1, and beta-2 bands showed a decrease in BispRP across the continuum of AD, which implies a potential coupling decline among higher frequency components. Next, BispEn was computed to evaluate the homogeneity of interaction distributions. As shown, only the delta and theta bands exhibit a decreasing trend in entropy with AD progression. This insight indicates that delta and theta bands interact with fewer components in the global spectrum. A decrease in spectral irregularity in EEG is a well-known effect of neurodegeneration, which was evaluated through entropy calculations

(Abásolo et al., 2006b; Maturana-Candelas et al., 2019; Ruiz-Gómez et al., 2018b). This is consistent with a previous study, which reported an overall decrease in bispectral entropy in AD patients (Wang et al., 2015). Entropy has the potential to discriminate time series generated by different systems (Costa et al., 2005), and this may be linked to dynamic cooperation between neural populations. From our results, it is worth noting that bispectral entropy alterations occur specifically at low frequencies, and the loss of heterogeneity in inter-band interactions at these frequency bands progresses along the AD continuum. Finally, BispMF quantifies the predominant components of the global spectrum that interact with each frequency band. Remarkably, BispMF consistently decreases in each band as the severity of AD increases. This trend has two underlying factors: A reduction in interactions involving higher frequency bands (alpha and beta) and an increase in interactions between the delta and theta bands. This observation is consistent with our BispRP findings, which display an increasing presence of delta and theta band interactions with the whole spectrum in more advanced AD stages. All in all, it can be concluded that inter-band bispectral interactions are disrupted in neurodegenerative states, being these disruptions proportional to their severity.

There are numerous studies that associate alterations in synchronization between different frequency bands and disruptions in diverse neurophysiological mechanisms. For instance, coupling between theta activity in the frontal cortex and gamma activity in the parieto-occipital cortex was positively correlated with reward evaluation (Riddle et al., 2022). Furthermore, working and retention memory related to visual stimulation involve interactions in theta and alpha frequency ranges (von Stein and Sarnthein, 2000). Anomalies in inter-band frequency coupling have been also associated with AD symptomatology. For instance, a decrease in cross-frequency coupling between the beta band and the rest of the spectrum was reported in AD patients (Engels et al., 2016). Furthermore, a significant decrease in delta modulation of the beta frequency band was reported, being the best discriminant to distinguish HC subjects and AD patients among other modulation alterations (Fraga et al., 2013). Additionally, lower alpha/beta interactions have been observed in AD, which were associated with reduced cognitive ability (Palva and Palva, 2007). When intersecting the aforementioned results, it arises the idea that interactions involving beta rhythms are present in functional processes that are lost during neurodegeneration. However, from a global standpoint, loss of general EEG synchronization obtained with numerous metrics has also been found in MCI and AD (Dauwels et al., 2010). Since synchrony can be viewed as a manifestation of diverse neuronal groups activating

cooperatively (Bressler, 1995), we hence can reach a similar conclusion regarding the previous subsection: The obtained disruption in bispectral features could reflect hindered brain function due to neural pathways disruption by tissue alterations or neurotransmitter deficits (Jelles et al., 1999; Jeong, 2004; Tononi et al., 1998). For this reason, a causal link could be proposed between neuronal activation complexity, bispectral interactions, and neurodegeneration, the former two being a direct reflection in the EEG of the latter. In this way, the AD continuum has been characterized from two different perspectives, which are also complementary to each other.

6.2 Genetic and biochemical elements inducing an indirect impact on the development of AD

AD is a multifactorial disorder in which innumerable biological factors take part along the process of neurodegeneration. Among those, the two main molecular biomarkers that allow definite diagnosis of AD are SPs and NFTs (see Section 1.3.1). Although there is currently a debate about the causal relationship between these molecules and atrophy or synaptic dysfunction, their neurotoxic properties have been widely suggested and their presence could lead eventually to pathological states (Farias et al., 2011; Haass and Selkoe, 2007; Kirkitadze et al., 2002; Klein et al., 2004; Wegmann et al., 2015). Given that genetics are intimately linked to protein expression, the inspection of variants directly or indirectly related to Aβ and tau proteins would facilitate the understanding of their role in neural dynamics.

Tau is encoded by the *MAPT* gene and its mutation has been suggested to induce tauopathy (Takashima, 2013). Hence, the inspection of several risk and protective variants of this gene and their correlations with parameters derived from brain electrical activity is of immediate interest. In the case of Aβ, it is already known that more profuse aggregation can be due to mutations in genes *APP*, *PSEN1*, and *PSEN2*, which lead to EOAD (Tanzi, 2012). However, since this AD variant is quite uncommon (Gauthier et al., 2021), in this Doctoral Thesis we opted for investigating the impact of two genes that are associated with Aβ endocytic removal from the brain tissue, which are *PICALM* and *CLU*.

6.2.1 Effects of *PICALM* and *CLU* genotypes in local brain activation

The study of the spectrum obtained from the EEG in each ROI designated by the Desikan-Killiany atlas was conducted (Maturana-Candelas et al., 2021). AD patients showed a power increase in slow frequency rhythms (delta and theta) and a decrease in fast frequency bands (alpha, beta, and gamma) when studying populations with risk variants in both *PICALM* and *CLU* genes. Furthermore, statistically significant differences were reported in the beta band. This finding is a hint of EEG slowing for the carriers of the risk variants, which is commonly associated with neurodegeneration (Jeong, 2004). In fact, the obtained trends in each frequency band correspond to the typical spectral disruptions during AD (Coben et al., 1983, 1985), among which beta oscillations are included. Beta rhythms have been associated with cognitive processes such as sensory processing (Lalo et al., 2007), visual attention (Wróbel, 2000), reasoning (Basile et al., 2013), and working memory (Hsu et al., 2017). For this reason, our results suggest that beta band perturbations may be related to slightly greater neuronal damage that could lead to higher cognitive impairment. On the other hand, excessive beta amplitude could be associated with stress, anxiety, overthinking, and overstimulation, as beta rhythms have been presumed to maintain the status quo (Spitzer and Haegens, 2017). Therefore, we can propose that specific ranges of beta power in the EEG may be associated with optimal cognitive performance. In light of previous research suggesting that carriers of the *PICALM* GG genotype (*i.e.*, risk alleles) are predisposed to stress reactions (Ponomareva et al., 2017), it is plausible to hypothesize that this specific variant of the *PICALM* gene has a propensity to destabilize neural dynamics under abnormal circumstances. In essence, the presence of the protective allele of *PICALM* may be associated with more stable ranges of beta activity, indicative of healthier brain function.

The previous rationale can also be extended to other frequency bands. For instance, it was observed a shift in the pattern of RP values in the alpha band in the HC group compared to individuals with AD. Even though no statistically significant differences were found, this insight could potentially reflect another instance of the genotype exerting divergent effects on EEG dynamics depending on the stage of neurodegeneration. A prior study reported an association between the *CLU* gene and upper alpha RP among cognitively healthy individuals (Ponomareva et al., 2013), with higher values observed for the risk allele. Alpha oscillations are implicated in neural processes essential for cognitive functions,

such as memory, intelligence, and attention (Cooper et al., 2006; Klimesch, 2012). However, excessive alpha power has been linked to behavioral disinhibition and poor executive functioning in Attention-Deficit Hyperactivity Disorder patients. These associations could potentially arise from brain connectivity dysfunction (Robbie et al., 2016) and cholinergic anomalies (English et al., 2009). Analogously with beta oscillations, these observations suggest an optimal range of alpha activity generally linked with better brain functioning. In this case, the observed shift in tendency within our results may be attributed to significant disturbances in physiological mechanisms involving neurotransmitter populations. Consequently, the protective allele of the *CLU* gene may play a role in promoting cholinergic processes that align more closely with healthy conditions across various cognitive statuses.

Interestingly, the HC group did not exhibit significant differences in any frequency band. In addition to this, although the beta band still showed higher RP values in carriers of the protective variants, trends between genotypes were more erratic. These findings may be attributed to the opposing influence of *PICALM* alleles in healthy individuals, as Ponomareva et al. (2017) previously reported. This observation suggests that the impact of the *PICALM* gene may differ depending on the cognitive status of the subject or, at the very least, the severity of neurodegeneration.

Considering the potential association of *PICALM* and *CLU* genes with Aβ clearance processes (DeMattos et al., 2002; Xu et al., 2015; Zhao et al., 2015; Zlokovic et al., 1994), it is plausible to propose that dysfunction in these mechanisms could contribute to establishing physiological conditions that promote greater Aβ deposition in the brain, thereby amplifying the detrimental effects of dementia. Beta RP values showed statistically significant differences in AD patients across 58 out of the 68 ROIs according to the Desikan-Killiany atlas (FDR-corrected p-values < 0.05, Mann-Whitney U-test). Figure 5.8 visually depicts the differences in beta RP values across each ROI in a three-dimensional brain model (BrainNet Viewer, v1.6356). Histological investigations of AD have revealed that the deposition of neuritic plaques does not exhibit a spatial preference in affected brains, also reporting large between-subject variation in their distribution, which contrasts with the patterns observed for neurofibrillary tangles (Braak and Braak, 1991). Given the premise that *PICALM* and *CLU* variations affect Aβ deposition, the widespread distribution of differences in beta activity across the brain may be an indication of the relationship between the observed outcomes and anomalies in Aβ presence in neural tissue. It is worth noting that regions lacking significant

differences were located primarily in the left hemisphere. This finding may be due to the functional asymmetry of the brain, rather than predilection in Aβ deposition. Indeed, previous research has implicated left hemisphere activity and beta band oscillations in time perception (Ghaderi et al., 2018; Nicholls and Whelan, 1998), a cognitive process that may be particularly engaged during the resting-state period when patients await the completion of EEG acquisition. The absence of significant differences in beta band activity among certain ROIs can be attributed to subtle fluctuations in beta activity, which can be attributed to the functional specialization of the brain.

In order to enrich our perspective about the homogeneity of RP values across the brain, SE was calculated. Figure 5.9 represents the distribution of the ROI-grand-averaged SE values in each frequency band for a) HC subjects and b) AD patients. Curiously, SE values obeyed similar trends to RP values when comparing genotypes: While the HC group showed no significant differences and no clear patterns, AD patients revealed a p-value lower than 0.05 (Mann-Whitney U-test) in beta power. In addition, protective alleles in AD were associated with lower delta and theta SE and higher alpha, beta, and gamma SE. Different brain areas defined by cytoarchitectonic structures with specialized functions were previously identified (Bressler, 1995). Furthermore, previous studies have suggested that local patches of synchrony are primarily associated with higher frequencies, whereas slower rhythms tend to dominate long-distance interactions (Varela et al., 2001; von Stein and Sarnthein, 2000). Hence, we can presume that SE alterations may be reflecting connectivity impairments, as synchronous activation from numerous neural networks could result in alterations in the distribution of RP at different frequency bands. In our case, *PICALM* and *CLU* variations may be implicated in disruptions in brain functioning.

Furthermore, PSDs along the AD continuum for each genotype were represented in Figure 5.10, revealing notorious differences. Carriers of the risk alleles showed a general slowing in all groups, which was noticeable by the shifting of power to slower frequency ranges. In fact, carriers of risk alleles display PSDs more similar to further severity stages. As mentioned beforehand, EEG slowdowns have been associated with disruption of information processing and cognitive dysfunction (Jeong, 2004). These insights may indicate that risk alleles of *PICALM* and *CLU* are prone to induce neurophysiological abnormalities that may lead to worse cognition. Besides, beta power differences sustained as the severity of the disease increased could imply a persistent impact of AD-inducing genotypes on neural dynamics throughout the progression of the disease. This effect may be

attributed to translational alterations of the implicated genes in the later stages of AD. Indeed, previous studies have reported a positive correlation between plasma clusterin levels and deterioration status (Schrijvers, 2011; Thambisetty et al., 2010).

Finally, the inflammatory effect of Aβ in neural tissue is just one of the aspects that can lead to disturbed brain function. Aβ has been also related to synaptic decay in the form of neurotransmitter affections. For instance, a decreased acetylcholine and dopamine release has been observed in Aβ-infused rat brains (Itoh et al., 2002; Trabace et al., 2007). As *PICALM* and *CLU* risk alleles may be associated with impaired Aβ clearance, neurotransmitter deficits may also contribute to the EEG alterations observed in our results. In fact, the more notorious effects of genotypes on PSDs at earlier stages of the disease could be explained by the indirect implications of these genes in neurotransmission. This is supported by the notion that cytopathology in cortical cholinergic pathways arises as an early event in the AD continuum (Mesulam et al., 2004). Additionally, differences in beta activity may be due to neurotransmission deficits. It is known that AD is considered a "disconnection syndrome", which is characterized by disrupted connectivity within and between neural networks that greatly affects brain electrophysiology (Brier et al., 2012). Nonetheless, if AD is solely understood as a disconnection syndrome primarily caused by neuronal loss, it would be challenging to provide an explanation for alterations observed in a single frequency band (Stam et al., 2003). Hence, it is important to consider other factors that contribute to the loss of synchrony, such as disturbances in neurotransmitter pathways. Previous studies have shown that blocking the cholinergic system is associated with reduced coherence of the EEG during rest in specific frequency bands (Kikuchi et al., 2000; Sloan et al., 1992). For this reason, considering the association of *PICALM* and *CLU* with various neurotransmitter metabolisms, individuals carrying AD-inducing alleles may manifest these physiological anomalies as changes in RP within the beta band. In summary, disruptions in multiple neurotransmitter systems may have a significant impact on the EEG alterations observed in individuals with risk genotypes of *PICALM* and *CLU*.

6.2.2 Impact of *MAPT* variants in the brain functional network

The last study in this Doctoral Thesis corresponds to the analysis of inter-band properties of the brain functional network in subjects with different *MAPT* genotypes (Maturana-Candelas et al., 2024). Concretely, seven *MAPT* SNPs related to neuropathologies or alterations in phosphorylated and total tau presence in CSF. MNA was used to evaluate resting-state EEG in HC subjects and AD patients with these genotypes in order to study the homogeneity of the contribution provided by each frequency-specific functional network.

First, P disruption values were obtained from each SNP and ROI, which is displayed in Figure 5.11. As a reminder, P disruption is equal to P values in AD patients minus P values in HC subjects (see Section 4.2). Additionally, Figure 5.12 displays the distribution of the P values across ROIs and SNPs. Carriers of the risk alleles tended to be positive, whereas carriers of the protective alleles showed mostly negative values. This finding indicates that individuals within the AD group who possess risk alleles exhibit higher P values in comparison to individuals with protective alleles. Conversely, subjects in the HC group display the opposite pattern. This difference may be attributed to two possibilities: Firstly, the P coefficient within the AD group significantly increases in subjects with risk alleles compared to those with protective alleles. Alternatively, P coefficient within the HC group significantly increases in subjects with protective alleles as opposed to those with risk alleles. Figure 5.12 reveals that, at least, one of these premises is true for every SNP, except rs2258689. These results indicate that the effect of different *MAPT* variants in the brain electrical activity may be different depending on the clinical status. In addition, it is observed that the impact of risk and protective alleles in the global network is more notorious in HC subjects (Figure 5.12a) than in AD patients (Figure 5.12b), which resulted in, generally, lower values of P disruption in carriers of the protective alleles (Figure 5.12c). This tendency opposes the results obtained from the *PICALM* and *CLU* analysis (previously discussed), which unveiled significant differences only in AD groups. This is evidence that the influence of gene expression on brain dysfunction is sensible and directly contingent on the neurodegenerative condition, which could depend on the specific neurophysiological role assumed by each gene. Indeed, we suggest that the dichotomy between *MAPT* and both *PICALM* and *CLU* may be linked to what extent each gene is implicated earlier or later along the neurodegenerative process. In this way, the impact of *MAPT* variants would

give rise to significant differences in HC subjects because tau alterations (which could manifest in changes in structure, function, and cytotoxic properties) could be visible even in pre-clinical stages, as tau is an ever-present protein along human life. On the other hand, *PICALM* and *CLU* alterations, given that they are implicated in cell debris clearance, may be only significant when a substantial deposition of Aβ has been previously accumulated, which happens in more advanced severity phases of neurodegeneration. In fact, increased CSF levels of CLU protein attached to SPs have been observed in AD patients (Ferrari et al., 2012). This observation suggests greater implication of this protein in amyloid clearance as presence of SPs increases.

Globally, risk and protective alleles exhibited different disruption patterns on their own. In Table 5.3 is showed the k coefficient, which reflects the gradient of the regression line by genotype from Figure 5.11. This parameter is able to reflect a general view of the hub disruption network, enabling the quantification of the diminished global capacity of all nodes to function as hubs. Not only k parameter showed statistically significant differences between risk and protective variants, but also revealed that risk alleles were associated with greater P overall disruption between AD patients and HC subjects. This outcome aligns with the previously mentioned findings, since the P coefficient tends to be higher among AD patients possessing risk alleles and lower among HC subjects carrying these genotypes in most SNPs. This observation implies that the protective alleles of different SNPs might be inducing a mitigating effect on the disruptions within the network, particularly in hub regions.

The inspection of each resting-state network individually was also conducted in this study. It turns out the left DMN displayed an overall greater sensibility to genotype expression, as observed in Figure 5.12. Particularly, in HC carriers of protective alleles, the left DMN region showed the highest P values in most of the SNPs, which were notably higher than those according to carriers of risk alleles. In addition, P disruption associated with the left DMN displayed generally low values, being also negative compared to the risk genotypes (Figure 5.12c). Since low values of P signify more concentrated connectivity contribution in a single layer, it is implied that the left DMN in HC carriers of risk alleles may lack the capacity to integrate information across different layers. Moreover, considering that various frequency bands participate in brain functions across different spatio-temporal scales (Varela et al., 2001; von Stein and Sarnthein, 2000), the association of lower P values with HC carriers of risk alleles may suggest a subtle deficiency in the functional specialization of the left DMN, affecting its hub endeavor. This

may be an indicator of the capability of the protective alleles to maintain the hub properties of the left DMN, even in preclinical states. Furthermore, negative values of P disruption in the left DMN could imply its particular sensitivity to different isoforms of tau in healthy conditions, resulting in more pronounced alterations in neural activity depending on the cytotoxic characteristics of this molecule.

Regarding the AD groups, the greater similarity between genotypes in patients may be attributed to the overshadowing effect of other physiological disruptions on the impact that tau may exert in neurodegenerative states. Furthermore, the observed fluctuations in P between ROIs could be indicative of compensatory mechanisms within specific brain regions involved in the flow and management of neural information. This notion has previously been proposed when observing an increase in the P coefficient in frontal areas during AD (Cai et al., 2020). In this regard, brain regions that do not typically function as hubs may assume this role to maintain the functional integrity of the brain network.

Myelin could play a role in the sensibility of the left DMN to *MAPT* variations. Previous histological explorations have provided evidence of a negative correlation between the dissemination of AD molecular biomarkers and the myelination process during brain development (Braak et al., 1999; Braak and Braak, 1996). It is noteworthy that only in the most advanced stages of dementia, the primary somatosensory, auditory, and visual cortices are affected, which are regions characterized by higher levels of myelination (Braak et al., 1999; Braak and Braak, 1996). This pattern of propagation aligns with the deposition of NFTs along the AD continuum, indicating that these specific neuronal populations may exhibit enhanced resilience against the cytotoxic effects induced by hyperphosphorylated tau. In fact, the relationship between myelin and resistance against the cytotoxic effects of tau was discovered (Rubinski et al., 2022), a finding which is compatible with the close association between low levels of myelin and increased tau concentrations (Dean et al., 2017). As the DMN accounts as a late-myelinated region during brain development (Kernbach et al., 2018), it may lead to increased sensitivity to changes in tau properties that may be driven by *MAPT* variants.

Another reason that could explain the increased sensibility of the DMN to tau cytotoxic properties is its predisposition to accumulate greater amounts of this molecule. The spread of NFTs and other tau-related byproducts among neuronal populations is known to occur through prion-like transfer mechanisms (Mudher et al., 2017), which are more likely to activate in regions characterized by high synaptic density (Calafate et al., 2015). Given that the DMN is considered a hub (Raichle, 2015), it is expected that the constituent brain regions are structurally

more interconnected than others, thereby increasing the likelihood of accumulating higher concentrations of tau. Conversely, brain regions with lower synaptic density may experience less impact not due to resistance to cytotoxicity, but simply due to a lower presence of the protein.

Regarding to changes in specific frequency bands, the contribution of each layer in the functional network was assessed individually. To accomplish this, the grand-average node degree across subjects for each frequency band was calculated, enabling the identification of layers most affected by genotype variations. The results, predominantly consistent in the theta and beta bands, are presented in Figure 5.13. Extensive research has been conducted on the theta band within the context of neurodegenerative processes, yielding multiple evidential findings that establish a correlation between modifications in theta activity and cognitive impairment (Jeong, 2004). Prior research investigating disruptions in brain activity has also revealed a robust correlation between tau/amyloid ratios and an increase in theta activity in healthy individuals (Stomrud et al., 2010). Furthermore, evidence derived from mouse models has proven the relationship between distinct tau species and the theta frequency band (Das et al., 2018). This finding suggests that the precise sequence of tau has the potential to influence the strength of specific brain oscillations. These insights offer a potential explanation for the observed alterations in node degree values within the theta band among different genotypes in the HC group. On the other hand, the slowing of the EEG along neurodegeneration substantially affects beta activity (Jeong, 2004). Inspecting the relationships between alterations in fast frequencies and abnormal tau levels has reported differences in functional connectivity (Canuet et al., 2015) and global power (Smailovic et al., 2018). Considering that different variants of the *MAPT* gene could be related to elevated tau presence (Cheng et al., 2007), it is plausible that genetic variations can impact beta activity as well. It is suggested that these mechanisms might contribute, to some extent, to the consistent patterns observed in the beta and theta bands across various genotypes.

Finally, multiple potential explanations exist regarding the disruptive impact of different *MAPT* alleles on brain functional connectivity. Firstly, variations in the quantity of tau produced by different *MAPT* alleles may contribute to these disruptions. Certain alleles have been associated with different concentrations of CSF tau in amyloid-positive individuals (Kauwe et al., 2008). Abnormal folding of tau is another potential explanation, as alterations in tau folding can lead to increased protein aggregations and potentially higher concentrations of tau (Rudenko et al., 2019). Additionally, different variants of tau may affect

its spreading pathways through the brain, with evidence of heterogeneous tau pathology propagation resulting from different tau species (Dujardin et al., 2018). The structure of tau, including distinct structural configurations, can influence its propagation patterns and physiological properties (Hallinan et al., 2019). To end with, different tau species may cause various physiological disruptions, such as reduced binding to microtubules and impaired functionality (Hasegawa et al., 1998). This can be manifested even by small changes in the peptide chain of tau, as they can have significant impacts on tau cytotoxicity, highlighting the sensitivity of cell function to protein alterations (Fath et al., 2002).

Both the study of the impact of *PICALM* and *CLU* on brain electrical activity and the study of *MAPT* involvement in the functional brain network reported significant alterations in the beta frequency band. It is known that along neurodegenerative processes, numerous neural populations oscillating in diverse frequency bands are disrupted. However, the fact that beta oscillations are specially affected in both studies may lead to interpretation beyond neural damage, such as neurotransmission anomalies. One of the biological factors that are most known to be associated with beta activity is γ-aminobutyric acid (GABA). Beta activity was found to be suppressed by several GABA receptor-mediated inhibitory paradigms, which suggest that beta rhythms are closely related to response inhibition (Cash et al., 2017). Another study reported a beta power increase in the prefrontal cortex as a compensatory activation to pain-related GABAergic dysfunction (Makowka et al., 2023). Further evidence has been reported demonstrating the correlation between GABA deficits and perturbations in beta band activity (Porjesz et al., 2002; Rangaswamy et al., 2002). In the light of these findings, we suggest that differences in Aβ and hyperphosphorylated tau depositions, at least those genetic-mediated ones, may be associated with an imbalance in the excitation–inhibition homeostasis of the brain cortex.

6.3 Limitations of the study

Several considerations and limitations should be acknowledged to improve the performance and enhance the validity of the studies discussed throughout this Doctoral Thesis.

First, this study lacks information about the severity progression of the patients. A longitudinal perspective focusing on individuals progressing to more severe neurodegenerative states would provide valuable insights into the mechanisms underlying the process of neurodegeneration. Furthermore, it is

noticeable the sex imbalance in all the studies, with a higher proportion of females. This issue might be attributed to the longer lifespan and genetic features associated with women, potentially impacting the likelihood of developing dementia. However, this issue may contribute to generating bias in the results, as brain functioning may be sensitive to sex-specific characteristics in neurophysiology. This is an additional reason to consider increasing the database.

In addition, leakage due to volume conduction effects was diminished using PLI when computing connectivity values, as this metric is notoriously resistant to these effects (Stam et al., 2007). However, part of such spurious connections may arise from other stochastic events during acquisition, such as electrode impedance or external noise. These aspects may exert bias in the obtained connectivity results. While randomly generated connectivity values may be diminished when assessing multiple subjects, implementing connectivity thresholds will be considered in future research as a good practice.

Regarding EEG acquisition, although resting state is a widely common standard to obtain data from brain electrical activity, acquiring EEG data during cognitive tasks could reveal more evident differences in aspects such as inter-band interactions or multiscale entropy tendencies. This would allow to elucidate the role of different frequency bands and interpret deviations from basal EEG complexity in specific brain activation. Nonetheless, the challenge that this perspective imposes to the EEG acquisition is evident, as cognitively impaired individuals are usually unable to conduct these tasks. Therefore, this approach would only be possible at the very early stages of neurodegeneration. Moreover, the limited spatial resolution of the EEG acquisition system, comprising 19 channels, can introduce ambiguity in the interpretation of results, particularly in the third study that conducted source reconstruction of 68 ROIs. Since the number of ROIs in the atlas exceeds the number of channels, careful consideration is required when discussing the findings.

In addition, expanding the local activation studies applying connectivity approaches would provide a more comprehensive understanding of the functional role of different brain areas. This aspect can be extended encompassing additional means of network analysis, which can be studied throughout graph theory methods. This perspective would allow the assessment of connectome disruptions with increased precision, aiding in the identification of brain regions susceptible to genetic anomalies. Another consideration regarding genetic aspects is that only SNPs have been taken into account, without considering other relevant polymorphisms. Although less frequent, these other polymorphisms may be

relevant in perturbing neural dynamics.

Furthermore, the limitation derived from the unavailability of medical image data is twofold. First, MRI data is decisive to build realistic head models for each subject. This practice enhances the precision of source localization algorithms in a customized manner. Since the availability of anatomical information per subject is beyond our reach, this Doctoral Thesis have assumed source activity my means of prebuilt templates or atlases. Although it has been previously suggested that there is no inconsistency generated by the selection of head model template (Douw et al., 2018), we look forward to building realistic head modeling in future research related to source activation analyses. Second, the lack of access to medical imaging data greatly limits the ability to establish causal relationships between the results and neurochemical alterations. As quantitative evidence of the presence of Aβ and NFTs in brain tissue, as well as signs of neurodegeneration, are the current hallmarks of definite AD, there is no evidence to suggest that the patients in our database are not afflicted with other neurodegenerative disorders or mixed dementias.

With respect to both genetic studies in this Doctoral Thesis, while the associations between alleles and EEG alterations are summarized based on extensive literature investigation, these studies primarily aim to highlight possible physiological causes associated with the analyzed alleles that may contribute to neurodynamic disturbances. Future research projects with medical imaging availability are planned to determine causality and verify the reported results.

Finally, the algorithm sLORETA is an approach that estimates source localization based on current density assuming that neighboring neurons are simultaneously and synchronously activated (Pascual-Marqui, 2002). Although sLORETA has been extensively used in EEG analysis due to its low dipole localization error and depth bias (Lucka et al., 2012), this algorithm has been suggested to overestimate the spatial extent of the reference source scenario considerably, resulting in mislocalizing the sources (Lucka et al., 2012). This issue could be solved by adjusting the weights in the correct localizations (Lucka et al., 2012). However, alternative methods of source localization have been proposed that could replace sLORETA to avoid this issue (Lucka et al., 2012). Our intent is updating our pre-processing protocols to new standards in order to increase precision of source localization in future research.

6.4 Future research lines

During the course of this Doctoral Thesis, several questions emerged from the obtained results that may potentially increase the robustness or amplify the scope of our findings. These ideas, that were conceived after the completion of each study, were compiled and will be taken into account in future research to the extent possible.

The more straightforward proposal is the replication of the obtained results in each study composing this Thesis. For this reason, the application of the methodologies described throughout this document in different EEG databases would be decisive in ascertaining replicability, which would substantially increase the significance of our findings.

Furthermore, although EEG is a convenient technique to study the electrical activity of the brain, EEG signals by themselves are not enough to determine definite physiological alterations. This issue resulted in being unable to demonstrate causal associations between EEG changes and particular features of brain dysfunction. Analogously, genetic information regarding SNP variations is not necessarily connected to modifications in proteomic features. Both of these concerns could be overcome by the incorporation of medical image data into the analyses, especially those that could confirm atrophic signs and presence of AD molecular biomarkers. For this reason, it is imperative that we engage in research projects that integrate EEG signals with MRI imaging in order to validate prior studies and expand our insights to a level where we can confirm genuine causality.

The importance of MRI imaging is apparent for a second reason. That is, to detect definite signs of AD or any other neurological condition. Even though the diagnosis of the participants in this Doctoral Thesis was conducted by means of MMSE and other subjective evaluations according to the criteria of the NIA-AA (Jack et al., 2018), there is no evidence that dementia patients suffer from exclusively AD. Therefore, we aim in future research to request access to MRI data or to databases composed by patients that were previously diagnosed based on quantitative traits, such as biomarker presence in brain tissue.

Regarding disease identification, future studies aim to increase the reliance of MCI and AD diagnostics and classification of the subjects according to strict biomarker presence through MRI or PET analysis and alignment to the most recent edition of the International Classification of Diseases (ICD-11). In this way, the characterization of the EEG alterations caused by exclusively specific neurodegenerative disorders will be greatly enhanced. Moreover, we intend to

further investigate AD attending to other elements, such as behavior and cognition. Incorporating these kinds of data would allow multiple and interesting research proposals, such as examining the correlations between observable manifestations of AD and EEG alterations in specific brain regions, or assessing the influence of genetics on cognitive task performance. This perspective will help to elucidate the connections between changes in higher brain functions, disruptions in EEG patterns, and dementia across its continuum. Efforts will certainly be dedicated to expanding the framework of our research in this direction, aiming to obtain databases that include such information.

In addition, the enhancement of the quality of the data is of paramount importance. EEG database is composed of 19-channel recordings, which are generally enough to study cortical alterations of brain electrical activity. However, a low number of channels, together with the lack of individual MRI data, may be detrimental when analyzing source-level signals. As these data are built from the original EEG, a larger number of channels and MRI images to establish realistic head models would help in estimating inner brain activity with greater precision, which would enhance its inspection in particularly small brain areas. Additionally, MRI will be useful to determine skull conductivity in relation to its thickness. This aspect has been previously demonstrated to influence EEG acquisition, and may vary substantially between subjects (Antonakakis et al., 2020). For the aforementioned reasons, the acquisition of more sophisticated EEG devices and ensuring the availability of anatomical information has the highest priority in the future.

Besides, the application of methodologies related to machine learning and deep learning has been of great interest in the last few years. These powerful algorithms can analyze and identify complex patterns and relationships within medical data, leading to valuable insights and improved decision-making in healthcare. Machine learning algorithms can learn to detect anomalies and identify specific patterns in biosignals as complex as the EEG. These aspects may be extremely valuable in finding pathological features in the EEG (or in other kinds of data) that remain hidden with traditional approaches. Furthermore, machine learning also shows promise in genomic studies, being able to analyze large genomic datasets to identify genetic variations associated with AD or physiological disruptions that could exacerbate its symptoms. Hence, we are willing to apply this new perspective to our analyses, especially if new data is obtained for upcoming research.

Regarding to the potential spurious connectivity values that may emerge from leakage or other sources, we minimized their effect using PLI. This metric has been

proved to be greatly resistant to volume conduction effects (Stam et al., 2007). In addition, in this Doctoral Thesis we have assumed that the spurious connections derived from other sources are randomly generated and would be diminished when calculating averages or displaying value distributions. However, this matter will be approached in future investigations establishing thresholds in order to take into account only the most relevant connectivity values.

Last, the fulfillment of the ultimate goal, not only regarding this Doctoral Thesis but encompassing AD research itself, is to contribute to detecting AD during prodromal stages so the alleviation of its symptoms can be handled as soon as possible. The development of a bio-computational tool for early AD diagnosis will integrate the findings from the studies provided in this Doctoral Thesis. In this way, and in tandem with the aforementioned proposals, the essential understanding of the AD and a reliable procedure to prevent it may become a little less unattainable.

Chapter 7

Conclusions

The present Doctoral Thesis is devoted to proposing novel and diverse parameters to characterize the brain electrical activity in neurodegenerative states attributed to AD. The tendencies observed from the proposed metrics were studied throughout the AD continuum and in the presence of specific genetic variants. The main objective of this Doctoral Thesis is to enhance the understanding of the neurophysiological alterations caused by the biochemical and functional changes induced by AD. In addition, this document also offers a potential aid to the scientific and clinical community in the diagnostic process, especially aimed at early detection.

During the course of this Doctoral Thesis, the brain electrical activity in the form of EEG was analyzed from different perspectives. Namely, a multiscale entropy approach to assess the disruptions of the EEG complexity; an exploration of the interactions of inter-band frequency components; a study inspecting the disturbances of the power spectral density in relation to specific genetic variants; and an analysis addressing the contribution of each frequency band in the functional brain network depending on tau-related genotypes.

This chapter is dedicated to remarking on the primary contributions that constitute the compendium of publications. Subsequently, the key conclusions derived from the aforementioned studies are enumerated. Finally, suggestions are presented regarding the potential future research that can validate the obtained results or further enhance the understanding of AD neurophysiology.

7.1 Contributions

The main contributions provided in this Doctoral Thesis are the following:

1. Investigation of the multiscale entropy patterns in a wide variety of temporal scales along each phase of the AD continuum, from healthy states to severe dementia (Maturana-Candelas et al., 2019). Also, a five-way classification model (HC, MCI, and each severity stage of AD) was evaluated, which could be used in further strategies of clinical screening to detect AD. No study has previously performed a five-way classification model before using multiscale entropy features.

2. Exploration of the inter-band regions of the EEG bispectrum obtained from preclinical and neurodegenerative states (Maturana-Candelas et al., 2020). Also, the application of bispectral parameters to characterize these bispectral regions is not often employed. These aspects have not been previously considered for AD characterization along its progression.

3. Comparison of features extracted from the brain electrical activity in populations carrying allelic configurations in genes associated with a specific physiological function (Maturana-Candelas et al., 2021). To the best of our knowledge, no EEG study has focused on extracting brain activity parameters from populations carrying risk alleles in *PICALM* and *CLU* simultaneously.

4. Application of an MNA methodology to EEG signals to evaluate the impact of several genotype variations implicated with the tau protein in brain functional connectivity (Maturana-Candelas et al., 2024). Further inspection of each single layer of the multiplex network was also conducted, revealing particular intricacies in each frequency band. The integration of MNA methodologies in conjunction with genetic variations to characterize EEG anomalies in neurodegenerative states has not been previously performed, therefore representing a notable innovation.

7.2 Main conclusions

The results obtained in each study belonging to this Doctoral Thesis were discussed and the main conclusions are listed below.

1. The reliability of multiscale entropy metrics to estimate the complexity of the EEG was demonstrated. The usefulness of both MSE and rMSSE metrics to estimate complex patterns was also determined, resulting in valuable identifiers of neurodegenerative states (Maturana-Candelas et al., 2019). Hence, analytic approaches that include multiscale entropy metrics could be advantageous in characterizing the underlying effects of neurodegeneration along the AD continuum.

2. New evidence of disruptions in inter-band coupling was obtained, which demonstrated greater alterations as AD severity increased (Maturana-Candelas et al., 2020). These findings indicate a general reduction in the interactions among spectral components involving all frequency bands. This observation establishes a connection between brain functionality and inter-band synchronization that could become a reliable indicator of neuronal damage, even in the early stages of neurodegeneration.

3. The interactions between inter-band frequency components were associated with complexity. This insight indicates that structures expressing complex, chaotic, and non-linear behavior might be rooted in interactions between frequency components belonging to diverse frequency bands. For this reason, the inspection of reductions in non-linear, inter-band coupling could be useful for ascertaining brain dysfunction.

4. *PICALM* and *CLU* genes, which are associated with Aβ clearance, may play a decisive role in brain electrical activity. EEG alterations were obtained in AD patients when carrying the risk alleles in specific AD-inducing SNPs of both genes (Maturana-Candelas et al., 2021). In addition, beta power exhibited greater sensibility to genetic variations connected to Aβ metabolism (Maturana-Candelas et al., 2021).

5. The brain functional network showed differences when comparing populations carrying multiple variants of the *MAPT* gene (Maturana-Candelas et al., 2024). These alterations were exposed as changes in the connectivity contribution attributed to each frequency band in the whole network. Additionally, the left DMN in HC subjects expressed higher sensibility to genotype variations, suggesting that genetic factors may have a more prominent impact during preclinical stages in this brain region. This association may be induced by the influence of diverse tau structural properties on the configuration of the brain functional network.

6. The implications of genotype variations on the brain electrical activity are different depending on the stage of AD progression. Genes implicated in mechanisms related to Aβ metabolism may have a greater impact on pathological states, while the effects of those related to tau may be more evident in preclinical states.

7. Genetic factors influencing the accumulation of Aβ and hyperphosphorylated tau could potentially be linked to homeostatic perturbations of cortical excitation and inhibition throughout neurotransmitter imbalance.

Chapter 8

Papers included in the compendium of publications

EEG characterization of the Alzheimer's disease continuum by means of multiscale entropies (Maturana-Candelas et al., 2019)

DOI: 10.3390/e21060544

Aarón Maturana-Candelas, Carlos Gómez, Jesús Poza, Nadia Pinto, and Roberto Hornero. *Entropy*, vol. 21(6), p. 544, 2019. Impact factor in 2019: 2.494, Q2 in "PHYSICS, MULTIDISCIPLINARY" (Journal Citation Reports - Clarivate Analytics).

Alzheimer's disease (AD) is a neurodegenerative disorder with high prevalence, known for its highly disabling symptoms. The aim of this study is to characterize the alterations in the irregularity and the complexity of the brain activity along the AD continuum. Both irregularity and complexity can be studied applying entropy-based measures throughout multiple temporal scales. In this regard, multiscale sample entropy (MSE) and refined multiscale spectral entropy (rMSSE) were calculated from electroencephalographic (EEG) data. Five minutes of resting-state EEG activity were recorded from 51 healthy controls, 51 mild cognitive impaired (MCI) subjects, 51 mild AD patients (AD_{MIL}), 50 moderate AD patients (AD_{MOD}), and 50 severe AD patients (AD_{SEV}). Our results showed statistically significant differences (p-values < 0.05, FDR-corrected Kruskal-Wallis test) between the five groups in every temporal scale. Additionally, average slope values and areas under MSE and rMSSE curves revealed significant changes in complexity for controls vs. MCI, MCI vs. AD_{MIL} and AD_{MOD} vs. AD_{SEV} comparisons (p-values < 0.05, FDR-corrected Mann-Whitney U-test). These findings indicate that MSE and rMSSE reflect the neuronal disturbances associated with the development of dementia, and may contribute to the development of new tools to track the AD progression.

Inter-band bispectral analysis of EEG background activity to characterize Alzheimer's disease continuum (Maturana-Candelas et al., 2020)

DOI: 10.3389/fncom.2020.00070

Aarón Maturana-Candelas, Carlos Gómez, Jesús Poza, Saúl J. Ruiz-Gómez, and Roberto Hornero. *Frontiers in Computational Neuroscience*, vol. 14, p. 70, 2020. Impact factor in 2020: 2.380, Q2 in "MATHEMATICAL & COMPUTATIONAL BIOLOGY" (Journal Citation Reports - Clarivate Analytics).

The aim of this study was to characterize the EEG alterations in inter-band interactions along the Alzheimer's disease (AD) continuum. For this purpose, EEG background activity from 51 healthy control subjects, 51 mild cognitive impairment patients, 50 mild AD patients, 50 moderate AD patients, and 50 severe AD patients was analyzed by means of bispectrum. Three inter-band features were extracted from bispectrum matrices: bispectral relative power (BispRP), cubic bispectral entropy (BispEn), and bispectral median frequency (BispMF). BispRP results showed an increase of delta- and theta-interactions with other frequency bands, and the opposite behavior for alpha, beta-1 and beta-2. Delta- and theta-interactions with the rest of the spectrum also experimented a decrease of BispEn with the disease progression, suggesting these bands interact with a reduced variety of components in advanced stages of dementia. Finally, BispMF showed a consistent reduction along the AD continuum in all bands, which reflects an interaction of the global spectrum with lower frequency bands as the disease develops. Our results indicate a progressive decrease of inter-band interactions with the severity of the disease, especially those involving high frequency components. Since inter-band coupling oscillations are related with complex and multi-scaled brain processes, these alterations likely reflect the neurodegeneration associated with AD continuum.

Influence of *PICALM* and *CLU* risk variants on beta EEG activity in Alzheimer's disease patients (Maturana-Candelas et al., 2021)

DOI: 10.1038/s41598-021-99589-y

Aarón Maturana-Candelas, Carlos Gómez, Jesús Poza, Víctor Rodríguez-González, Víctor Gutiérrez-de Pablo, Alexandra M. Lopes, Nadia Pinto, and Roberto Hornero. *Scientific Reports*, vol. 11(1), p. 1-11, 2021. Impact factor in 2021: 4.996, Q2 in "MULTIDISCIPLINARY SCIENCES" (Journal Citation Reports - Clarivate Analytics).

PICALM and *CLU* genes have been linked to alterations in brain biochemical processes that may have an impact on Alzheimer's disease (AD) development and neurophysiological dynamics. The aim of this study is to analyze the relationship between the electroencephalographic (EEG) activity and the *PICALM* and *CLU* alleles described as conferring risk or protective effects on AD patients and healthy controls. For this purpose, EEG activity was acquired from: 18 AD patients and 12 controls carrying risk alleles of both *PICALM* and *CLU* genes, and 35 AD patients and 12 controls carrying both protective alleles. Relative power (RP) in the conventional EEG frequency bands (delta, theta, alpha, beta, and gamma) was computed to quantify the brain activity at source level. In addition, spatial entropy (SE) was calculated in each band to characterize the regional distribution of the RP values throughout the brain. Statistically significant differences in global RP and SE at beta band (p-values < 0.05, Mann-Whitney U-test) were found between genotypes in the AD group. Furthermore, RP showed statistically significant differences in 58 cortical regions out of the 68 analyzed in AD. No statistically significant differences were found in the control group at any frequency band. Our results suggest that *PICALM* and *CLU* AD-inducing genotypes are involved in physiological processes related to disruption in beta power, which may be associated with physiological disturbances such as alterations in beta-amyloid and neurotransmitter metabolism.

Effect of MAPT gene variations on the brain electrical activity: a multiplex network study (Maturana-Candelas et al., 2024)

Aarón Maturana-Candelas, Roberto Hornero, Jesús Poza, Víctor Rodríguez-González, Víctor Gutiérrez-de Pablo, Nadia Pinto, Miguel A. Rebelo, Carlos Gómez. (UNDER REVIEW in *Computer Methods and Programs in Biomedicine*).

Background and Objective: Tauopathies are usually related to anomalies in brain connectivity patterns. These signs of neurophysiological alterations are associated with disturbances in information flow and processing. However, the implications of genetic variations associated with the tau protein in the brain functional network are not clearly understood. Hence, the aim of this study is to examine how variations in the microtubule-associated protein tau (*MAPT*) gene affect neural dynamics. Methods: Resting-state electroencephalogram (EEG) data from 155 participants were acquired, including healthy controls and Alzheimer's disease patients carrying *MAPT* alleles associated with risk or protective effects against the development of neuropathologies or abnormal tau presence in cerebrospinal fluid. Particularly, seven single nucleotide polymorphisms (SNPs) associated with *MAPT* were analyzed. In order to identify the effects of each genotype on neural activity, we performed a multiplex network analysis on the EEG data. Specifically, the connectivity contribution of each node in the frequency-dependent multiplex network was quantified using the participation coefficient (P). This parameter was obtained calculating the phase lag index (PLI) from the EEG previously filtered in the conventional frequency bands: delta, theta, alpha, and beta. The PLI adjacency matrices in each frequency band corresponded to the layers conforming the multiplex network. Subsequently, P was computed from the PLI distributions across layers in every brain region corresponding to the Yeo-7 atlas, reflecting node degree diversification among frequency bands. Results: Carriers of risk and protective alleles exhibited distinct values of P, especially in healthy controls at the left default mode network. In general, carriers of the risk alleles also presented higher network disruptions. In addition, significant differences in node degree values were observed across SNPs in the theta and beta frequency bands. Conclusions: Different *MAPT* variants may lead to diverse tau species that influence brain function, specifically in the brain regions involved in information flow management in preclinical states. These insights may help understanding network disturbances caused by molecular factors.

Appendix A

Scientific achievements

A.1 Publications

A.1.1 Papers indexed in the JCR

1. **Aarón Maturana-Candelas**, Carlos Gómez, Jesús Poza, Nádia Pinto, Roberto Hornero, "EEG Characterization of the Alzheimer's Disease Continuum by Means of Multiscale Entropies", *Entropy*, vol. 21(6), pp. 554, May, 2019, DOI:10.3390/e21060544

2. **Aarón Maturana-Candelas**, Carlos Gómez, Jesús Poza, Saúl J. Ruiz-Gómez, Roberto Hornero, "Inter-band Bispectral Analysis of EEG Background Activity to Characterize Alzheimer's Disease Continuum", *Frontiers in Computational Neuroscience*, vol. 14, pp. 70, September, 2020, DOI: 10.3389/fncom.2020.00070

3. **Aarón Maturana-Candelas**, Carlos Gómez, Jesús Poza, Víctor Rodríguez-González, Víctor Gutiérrez-de Pablo, Alexandra M. Lopes, Nádia Pinto, Roberto Hornero, "Influence of *PICALM* and *CLU* risk variants on beta EEG activity in Alzheimer's disease patients", *Scientific Reports*, vol. 11, pp. 20465, October, 2021, DOI: 10.1038/s41598-021-99589-y

4. Saúl J. Ruiz-Gómez, Roberto Hornero, Jesús Poza, **Aarón Maturana-Candelas**, Nádia Pinto, Carlos Gómez, "Computational modeling of the effects of EEG volume conduction on functional connectivity metrics. Application to Alzheimer's disease continuum", *Journal of Neural*

Engineering, vol. 16, pp. 066019, October, 2019, DOI: 10.1088/1741-2552/ab4024

5. Pablo Núñez, Jesús Poza, Carlos Gómez, Verónica Barroso-García, **Aarón Maturana-Candelas**, Miguel A. Tola-Arribas, Mónica Cano, Roberto Hornero, "Characterization of the dynamic behavior of neural activity in Alzheimer's disease: exploring the non-stationarity and recurrence structure of EEG resting-state activity", *Journal of Neural Engineering*, vol. 17(1), pp. 016071, January, 2020, DOI: 10.1088/1741-2552/ab71e9

6. Víctor Gutiérrez-de Pablo, Carlos Gómez, Jesús Poza, **Aarón Maturana-Candelas**, Sandra Martins, Iva Gomes, Alexandra M. Lopes, Nádia Pinto, Roberto Hornero, "Relationship between the Presence of the ApoE $\epsilon 4$ Allele and EEG Complexity along the Alzheimer's Disease Continuum", *Sensors*, vol. 20(14), pp. 3849, July, 2020, DOI: 10.3390/s20143849

7. Miguel Rebelo, Carlos Gómez, Iva Gomes, Jesús Poza, Sandra Martins, **Aarón Maturana-Candelas**, Saúl J. Ruiz-Gómez, Luís Durães, Patricia Sousa, Manuel Figueruelo, María Rodríguez, Carmen Pita, Miguel Arenas, Luis Álvarez, Roberto Hornero, Nádia Pinto, "Genome-wide scan for five brain oscillatory phenotypes identifies a new QTL associated with theta EEG band", *Brain Sciences*, vol. 10(11), pp. 870, November, 2020, DOI: 10.3390/brainsci10110870

8. Saúl J. Ruiz-Gómez, Roberto Hornero, Jesús Poza, Eduardo Santamaría-Vázquez, Víctor Rodríguez-González, **Aarón Maturana-Candelas**, Carlos Gómez, "A new method to build multiplex networks using Canonical Correlation Analysis for the characterization of the Alzheimer's disease continuum", *Journal of Neural Engineering*, vol. 18(2), pp. 026002, February, 2021, DOI: 10.1088/1741-2552/abd82c

9. Ana M. Macedo, Carlos Gómez, Miguel Rebelo, Jesús Poza, Iva Gomes, Sandra Martins, **Aarón Maturana-Candelas**, Víctor Gutiérrez-de Pablo, Luís Durães, Patricia Sousa, Manuel Figueruelo, María Rodríguez, Carmen Pita, Miguel Arenas, Luis Álvarez, Roberto Hornero, Alexandra M. Lopes, Nádia Pinto, "Risk variants in three Alzheimer's disease genes show association with EEG endophenotypes", *Journal of Alzheimers Disease*, vol. 80(1), pp. 209-223, March, 2021, DOI: 10.3233/JAD-200963

A.1.2 International conferences

1. **Aarón Maturana-Candelas**, Carlos Gómez, Jesús Poza, Saúl J. Ruiz-Gómez, María Rodríguez, Miguel Figueruelo, Nádia Pinto, Sandra Martins, Alexandra M. Lopes, Iva Gomes, Roberto Hornero, "Analysis of Spontaneous EEG Activity in Alzheimer's Disease Patients by Means of Multiscale Spectral Entropy", *International Conference on NeuroRehabilitation (ICNR 2018)*, ISBN: 978-3-030-01844-3, pp. 579-583, Pisa (Italy), 16 October - 20 October, 2018

2. Sandra Martins, Luis Álvarez, Alexandra M. Lopes, Iva Gomes, Vania Oliveira, Patricia Sousa, María Rodríguez, Carmen Pita, María García, Jesús Poza, **Aarón Maturana-Candelas**, Roberto Hornero, Ana Taborda, Manuel Figueruelo, Miguel Arenas, Carlos Gómez, Nádia Pinto, "Identification of genetic variants contributing to late-onset Alzheimer's disease risk and correlation with cerebral activity of patients", *18th Meeting Portugaliae Genetica*, Porto (Portugal), 22 March - 23 March, 2018

3. Carlos Gómez, Saúl J. Ruiz-Gómez, Jesús Poza, **Aarón Maturana-Candelas**, Nádia Pinto, Miguel A. Tola-Arribas, Mónica Cano, Roberto Hornero, "Assessment of EEG Connectivity Patterns in Mild Cognitive Impairment Using Phase Slope Index", *40th Annual International Conference of the IEEE Engineering in Medicine and Biology Society*, ISBN: 978-1-5386-3646-6, pp. 263-266, Honolulu (United States), 17 July - 21 July, 2018

4. Pablo Núñez, Jesús Poza, Carlos Gómez, Víctor Rodríguez-González, Saúl J. Ruiz-Gómez, **Aarón Maturana-Candelas**, Roberto Hornero, "Characterizing Non-stationarity in Alzheimer's Disease and Mild Cognitive Impairment by Means of Kullback-Leibler Divergence", *International Conference on NeuroRehabilitation (ICNR 2018)*, ISBN: 978-3-030-01844-3, pp. 574-578, Pisa (Italy), 16 October - 20 October, 2018

5. Saúl J. Ruiz-Gómez, Carlos Gómez, Jesús Poza, Pablo Núñez, Víctor Rodríguez-González, **Aarón Maturana-Candelas**, Roberto Hornero, "Analysis of Information Flux in Alzheimer's Disease and Mild Cognitive Impairment by Means of Graph-Theory Parameters", *International Conference on NeuroRehabilitation (ICNR 2018)*, ISBN: 978-3-030-01844-3, pp. 569-573, Pisa (Italy), 16 October - 20 October, 2018

6. Saúl J. Ruiz-Gómez, Carlos Gómez, Jesús Poza, **Aarón Maturana-Candelas**, Víctor Rodríguez-González, María García, Miguel A. Tola-Arribas, Mónica Cano, Roberto Hornero, "Analysis of Volume Conduction Effects on Different Functional Connectivity Metrics: Application to Alzheimer's Disease EEG Signals", *41st Annual International Conference of the IEEE Engineering in Medicine and Biology Society*, ISBN: 978-1-5386-1311-5, pp. 6434-6437, Berlin (Germany), 23 July - 27 July, 2019

7. Pablo Núñez, Jesús Poza, Carlos Gómez, Verónica Barroso-García, Saúl J. Ruiz-Gómez, **Aarón Maturana-Candelas**, Miguel A. Tola-Arribas, Mónica Cano, Roberto Hornero, "Characterization of EEG Resting-state Activity in Alzheimer's Disease by Means of Recurrence Plot Analyses", *41st Annual International Conference of the IEEE Engineering in Medicine and Biology Society*, ISBN: 978-1-5386-1311-5, pp. 5786-5789, Berlin (Germany), 23 July - 27 July, 2019, DOI: 10.1109/EMBC.2019.8856600

8. Saúl J. Ruiz-Gómez, Carlos Gómez, Jesús Poza, Marcos Revilla-Vallejo, Víctor Gutiérrez-de Pablo, Víctor Rodríguez-González, **Aarón Maturana-Candelas**, Roberto Hornero, "Volume Conduction Effects on Connectivity Metrics: Application of Network Parameters to Characterize Alzheimer's Disease Continuum", *42nd Annual International Conference of the IEEE Engineering in Medicine and Biology Society*, ISBN: 978-1-7281-1990-8, Montreal (Canada), 20 July - 24 July, 2020

A.1.3 National conferences

1. **Aarón Maturana-Candelas**, Jesús Poza, Roberto Hornero, Pablo Núñez, Saúl J. Ruiz-Gómez, Víctor Gutiérrez-de Pablo, Marcos Revilla-Vallejo, Carlos Gómez, "Estudio de la relación entre el gen *MAPT* y la conectividad cerebral en la demencia por enfermedad de Alzheimer", *XXXVIII Congreso Anual de la Sociedad Española de Ingeniería Biomédica (CASEIB 2020)*, ISBN: 978-84-09-25491-0, pp. 331-334, Valladolid (Spain), 25 November - 27 November, 2020

2. **Aarón Maturana-Candelas**, Jesús Poza, Roberto Hornero, Víctor Gutiérrez-de Pablo, Carlos Gómez, "La importancia dinámica como indicador de comportamiento de hub en la región parietal de la red neuronal por defecto", *XXXIX Congreso Anual de la Sociedad Española de Ingeniería*

Biomédica (CASEIB 2021), ISBN: 978-84-09-36054-3, pp. 71-74, Madrid (Spain), 25 November - 26 November, 2021

3. **Aarón Maturana-Candelas**, Jesús Poza, Roberto Hornero, Víctor Gutiérrez-de Pablo, Carlos Gómez, "Impacto de la expresión del gen MAPT en las relaciones inter-banda de la actividad eléctrica cerebral", *XL Congreso Anual de la Sociedad Española de Ingeniería Biomédica (CASEIB 2022)*, ISBN: 978-84-09-45972-8, pp. 47-50, Valladolid (Spain), 23 November - 25 November, 2022

4. **Aarón Maturana-Candelas**, Roberto Hornero, Jesús Poza, Vesna Jelic, Una Smailovic, Carlos Gómez, "Análisis múltiplex de la red funcional cerebral en sujetos con hiperintensidades de la sustancia blanca", *XLI Congreso Anual de la Sociedad Española de Ingeniería Biomédica (CASEIB 2023)*, ISBN: 978-84-17853-76-1, pp. 597-600, Cartagena (España), 22 November - 24 November, 2023

5. Víctor Rodríguez-González, Jesús Poza, Carlos Gómez, Pablo Núñez, Saúl J. Ruiz-Gómez, **Aarón Maturana-Candelas**, Roberto Hornero, "Localización de fuentes cerebrales para la caracterización de la demencia debida a enfermedad de Alzheimer", *XXXVI Congreso Anual de la Sociedad Española de Ingeniería Biomédica (CASEIB 2018)*, ISBN: 978-84-09-06253-9, pp. 195-198, Ciudad Real (Spain), 21 November - 23 November, 2018

6. Saúl J. Ruiz-Gómez, Carlos Gómez, Jesús Poza, Pablo Núñez, Víctor Rodríguez-González, Adrián Martín-Montero, **Aarón Maturana-Candelas**, Roberto Hornero, "Estudio del efecto de la conducción de volumen en medidas de conectividad funcional derivadas de la coherencia", *XXXVI Congreso Anual de la Sociedad Española de Ingeniería Biomédica (CASEIB 2018)*, ISBN: 978-84-09-06253-9, pp. 241-244, Ciudad Real (Spain), 21 November - 23 November, 2018

7. Carmen Pita, Manuel Figueruelo, María Rodríguez, Lucía Martín, Elena Ramos, **Aarón Maturana-Candelas**, Roberto Hornero, Jesús Poza, Saúl J. Ruiz-Gómez, María García, Luís Durães, Ricardo González, Ana M. Macedo, Rita Rocha, Luis Álvarez, Sandra Martins, Alexandra M. Lopes, Iva Gomes, Miguel Arenas, Carlos Gómez, Patricia Sousa, Nádia Pinto, "Avances en el diagnóstico temprano de la enfermedad de Alzheimer mediante la correlación entre el genoma y la actividad cerebral", *VIII*

Congreso Nacional de Alzheimer, Huesca (Spain), 14 November - 16 November, 2019

8. Saúl J. Ruiz-Gómez, Carlos Gómez, Jesús Poza, **Aarón Maturana-Candelas**, Miguel A. Tola-Arribas, Mónica Cano, Roberto Hornero, "Modelado computacional de la conducción de volumen en el EEG. Caracterización del deterioro cognitivo leve y su progresión a la enfermedad de Alzheimer", *XXXVII Congreso Anual de la Sociedad Española de Ingeniería Biomédica (CASEIB 2019)*, ISBN: 978-84-09-16707-4, pp. 199-202, Santander (Spain), 27 November - 29 November, 2019

9. Víctor Gutiérrez-de Pablo, Carlos Gómez, Jesús Poza, **Aarón Maturana-Candelas**, Javier Gomez-Pilar, Marcos Revilla-Vallejo, Roberto Hornero, "Redes de asociación: una nueva forma de explorar la huella fisiopatológica de la enfermedad de Alzheimer", *XXXVIII Congreso Anual de la Sociedad Española de Ingeniería Biomédica (CASEIB 2020)*, ISBN: 978-84-09-25491-0, pp. 405-408, Valladolid (Spain), 25 November - 27 November, 2020

10. Álvaro Basterra-García, Jorge Gijón-Ortego, Víctor Gutiérrez-de Pablo, **Aarón Maturana-Candelas**, Roberto Hornero, Jesús Poza, Carlos Gómez, "Evaluación del paradigma de adquisición de la actividad electroencefalográfica en estado de reposo", *XLI Congreso Anual de la Sociedad Española de Ingeniería Biomédica (CASEIB 2023)*, ISBN: 978-84-17853-76-1, pp. 585-588, Cartagena (España), 22 November - 24 November, 2023

A.2 International internship

A three-month stay at the NVS department in Karolinska Institutet, Stockholm, Sweden.

- **Purpose of the internship** The main goal of the stay was to analyze EEG data acquired from AD patients and healthy controls to determine differences in brain activity as a function of clinical parameters, such as atrophy levels and the presence of several biomarkers. Typical AD biomarkers are Aβ and tau proteins in the CSF, which are closely linked to inflammation and degeneration processes in brain tissue. On the other hand, atrophy indices obtained from magnetic resonance imaging were also analyzed. These parameters reflected more or less severe degrees of posterior cortical atrophy

(lateral parietal cortex) and medial temporal atrophy (hippocampus and entorhinal area). More specifically, the tasks that were carried out are defined below:

1. Analysis of the EEG (pre-filtered). PLI and amplitude envelope correlation were calculated as a previous step to obtain the network-derived features. This calculation resulted in an adjacency matrix per subject whose parameters reflect the connectivity of each channel with the others. During this step, other measures, such as SampEn and RP in each classical frequency band, were also calculated for further exploration.
2. The clustering coefficient (ClC) parameter was calculated from the adjacency matrices obtained with the aforementioned metrics. This parameter allows estimating to what extent a node in a network is part of a group of nodes.
3. Different cohorts were established according to levels and types of atrophy, and presence of amyloid/tau in cerebrospinal fluid in different combinations. For example, AD patients with posterior cortical atrophy with and without the presence of tau in CSF. ClC values were compared between these cohorts.
4. Significant differences in ClC values were obtained between various study cohorts expressing different levels of atrophy and presence of biomarkers. These results were presented to the research team on two occasions.

Moreover, this stay is expected to promote a research collaboration between the Biomedical Engineering Group of the University of Valladolid and the NVS department of Karolinska Institutet. By establishing this new bond between both institutions, the quality of the research is meant to increase by including new clinical data in subsequent studies that may enhance the robustness of the results. This could lead to joint publications in the field of AD characterization using novel perspectives.

- **Quality indicators of the institution** The Division of Clinical Geriatrics of the NVS department at Karolinska Institutet has demonstrated extensive expertise in the study of EEG alterations in patients with neurodegenerative diseases. In addition, they are familiar with the analysis of molecular biomarkers and other clinical data using medical imaging. Dr. Vesna

Jelic, researcher and senior advisor in the department, has conducted a vast research career underneath this scope, achieving an h-index of 33 by contributing to 106 articles.

NVS is one of the largest departments within Karolinska Institutet with over 500 employees, several hundred affiliated researchers, and 1600 full-year students. The NVS comprises a specialized AD center known as the Center of Alzheimer Research (CAR), which focuses on conducting research about AD and other forms of dementia. Its main objective is to understand the mechanisms underlying neurodegenerative diseases involving cognitive impairment in order to prevent, diagnose, and treat such disorders. Research at CAR spans across preclinical and clinical domains, and integrates investigation from the molecular level to population studies.

Finally, Karolinska Institutet enjoys high prestige, as the Nobel Assembly of Karolinska Institutet awards the Nobel Prizes in Physiology and Medicine. This organization consists of fifty professors from various medical disciplines at the university. Founded in 1810, Karolinska Insitutet is consistently mentioned among the best medical schools in the world today, reaching sixth place worldwide in 2021 and obtaining the 41st position in the Shanghai Ranking in 2023.

A.3 Awards and honors

- **Award for the second best poster in the I Jornada de Investigación en Bioingeniería y Medicina**, organized by Escuela de Doctorado de la Universidad de Valladolid, Programas de Doctorado en Ciencias de la Visión, Investigación Biomédica, Investigación en Ciencias de la Salud y Tecnología de la Información y las Telecomunicaciones. 12 April, 2018

- **Finalist of the José María Ferrero Corral award of the 39th Annual Conference of the Spanish Society on Biomedical Engineering (CASEIB 2021)**, for the study entitled "La importancia dinámica como indicador de comportamiento de hub en la región parietal de la red neuronal por defecto", conducted by **Aarón Maturana-Candelas**, Jesús Poza, Roberto Hornero, Víctor Gutiérrez-de Pablo, and Carlos Gómez. 25 November - 26 November, 2021.

Apéndice B

Resumen en español

B.1 Introducción

El sistema nervioso es una de las estructuras más complejas que los seres vivos han desarrollado a lo largo de la evolución. Esta intrincada red de células llamadas neuronas permite transmitir información de forma precisa y a gran velocidad por el organismo. La activación sincrónica de las neuronas se produce a través de mecanismos dependientes del voltaje, desencadenando reacciones secuenciales de flujos iónicos, lo cual se manifiesta a nivel macroscópico mediante fluctuaciones en los potenciales eléctricos. El cerebro humano está compuesto por más de 86 mil millones de neuronas distribuidas en diferentes lóbulos especializados que cumplen una amplia diversidad de funciones. Las capacidades cognitivas más destacadas del cerebro humano, conocidas como *funciones cerebrales superiores*, implican procesos tan sofisticados como la cognición, que abarca el lenguaje, la percepción compleja, el juicio y la toma de decisiones, así como el comportamiento, que constituye la manifestación de estas funciones cognitivas (Tranel et al., 2003). Sin embargo, al igual que cualquier sistema biológico, existe la posibilidad de disfunción o deterioro debido a enfermedades o traumatismos.

En la actualidad, uno de los desafíos a los que se enfrenta la humanidad consiste en hacer frente las neuropatologías. Con el inevitable proceso de envejecimiento de la población, la degeneración del sistema nervioso central se ha convertido en una de las principales preocupaciones en el ámbito de la salud pública. El diagnóstico preciso y el tratamiento efectivo de las afecciones cerebrales requieren una comprensión profunda de los fundamentos de la neurodegeneración, especialmente en sus etapas iniciales. Se trata de una tarea complicada debido a la naturaleza

del cerebro y a su comportamiento altamente no lineal. Dado que aún estamos lejos de comprender completamente los matices del funcionamiento cerebral, toda investigación orientada a esta causa representa un valor incalculable.

Las causas que conducen al deterioro de las funciones cognitivas son diversas, siendo la más relevante actualmente la demencia, específicamente la causada por la enfermedad de Alzheimer (EA). Esta afección neurológica se caracteriza por cambios bioquímicos y estructurales en el cerebro que culminan en daño neuronal y, en última instancia, en deterioro cognitivo. La EA constituye la causa más frecuente de demencia, representando entre el 60 % y el 80 % de los casos (Alzheimer's Association, 2022). La edad es el factor de riesgo principal asociado a la EA, incrementándose de forma exponencial conforme el individuo envejece (Carr et al., 1997). No obstante, otros factores como la genética y los hábitos de vida también influyen de manera significativa en el desarrollo de esta enfermedad. Dada la profunda afectación física y mental que conlleva la EA, los familiares y cuidadores se ven obligados a participar en actividades cotidianas para asegurar el bienestar del paciente. Por consiguiente, la EA no solo afecta al paciente, sino que también perturba significativamente la vida de los familiares involucrados.

En las últimas décadas, la EA ha adquirido un destacado nivel de preocupación debido a su impacto significativo en la salud y a la cantidad de personas afectadas. En la actualidad, aproximadamente 55 millones de personas están diagnosticadas con algún tipo de demencia (Gauthier et al., 2021). Debido al gradual envejecimiento demográfico a nivel mundial, se estima un aumento de esta cifra a aproximadamente 78 millones para el año 2030 (Gauthier et al., 2021). Por tanto, resulta de gran interés el desarrollo de nuevas herramientas biocomputacionales para obtener diagnósticos más precisos de la EA en las primeras etapas de la neurodegeneración. A pesar de que la cura de la EA podría ser inalcanzable en un futuro próximo, este enfoque podría ser decisivo para mejorar la efectividad de las terapias.

Existe controversia en torno a la etiología de la EA, y las causas subyacentes siguen siendo difíciles de precisar. No obstante, se han identificado ciertos biomarcadores que muestran una clara asociación con esta enfermedad, los cuales pueden ser útiles para indicar su progresión. De acuerdo con el *National Institute of Aging and Alzheimer's Association* (NIA-AA) (Jack et al., 2018), la presencia histológica de placas seniles y ovillos neurofibrilares en el tejido neuronal se consideran biomarcadores definitivos para identificar la EA. Las placas seniles consisten en agregados insolubles de fibrillas oligomerizadas de beta-amiloide ($A\beta$), resultado de una escisión alterada de la proteína transmembrana APP.

La participación de la β-secretasa en la proteólisis, seguida por la γ-secretasa, genera un residuo peptídico de hasta 42 aminoácidos de longitud. Esta secuencia patogénica constituye el proceso conocido como amiloidogénesis (Kisilevsky, 2000). Posteriormente, debido a su elevada hidrofobicidad, estas moléculas tienden a agregarse, dando lugar a la formación de las placas seniles. Por otro lado, los ovillos neurofibrilares se componen de fibrillas tau hiperfosforiladas (p-tau) que se han desprendido del citoesqueleto neuronal (Chi et al., 2019). La proteína tau, codificada por el gen de la proteína tau asociada a microtúbulos (*microtubule associated protein tau*, *MAPT*), consta de una secuencia de entre 352 a 441 aminoácidos (Drubin and Kirschner, 1986). Tau desempeña un papel crucial en la estabilidad y motilidad neuronal, contribuyendo a la integridad de los microtúbulos (Drubin and Kirschner, 1986). Asimismo, está implicada en el transporte axonal, un proceso fundamental para el funcionamiento sináptico (Terwel et al., 2002). En su estado normal, tau se mantiene en un equilibrio entre procesos de fosforilación y desfosforilación. Sin embargo, cuando este equilibrio se altera, tau experimenta hiperfosforilación y modifica su estructura conformacional. Esta modificación conlleva su separación de los microtúbulos, lo que no solo provoca la acumulación de los ovillos neurofibrilares, sino que también compromete la integridad del axón, contribuyendo a su eventual degradación.

La EA se manifiesta gradual y progresivamente, con síntomas que empeoran con el tiempo (Reisberg, 1986). Este proceso se conoce comúnmente como el "continuo de la EA". Esta progresión comienza con la fase denominada EA leve, en la que los pacientes muestran claras alteraciones cognitivas, como una menor capacidad de recordar acontecimientos recientes o información personal, gestionar finanzas o viajar, entre otros aspectos. A esta etapa le sigue la EA moderada, que se asocia con la incapacidad para recordar eventos significativos de la vida y desorientación tanto temporal como espacial. Finalmente, la EA alcanza su fase más avanzada en la EA severa, caracterizada por una demencia profunda y la pérdida total de las funciones motoras y verbales (Reisberg, 1986). Previamente al desarrollo de la enfermedad, en algunos casos surge un estado conocido como deterioro cognitivo leve (DCL), donde los pacientes presentan déficits cognitivos no lo suficientemente graves para ser diagnosticados como demencia (Petersen, 2004). Aunque no todos los pacientes con DCL avanzan hacia formas más severas de alteraciones cognitivas, la detección temprana de esta condición puede ser de gran importancia para tratamientos preventivos.

La EA es conocida como un "síndrome de desconexión", caracterizada por una conectividad alterada (Brier et al., 2012). Estas disrupciones afectan

considerablemente a la electrofisiología cerebral, lo que enfatiza la importancia del análisis de la actividad eléctrica cerebral en el estudio de enfermedades neurodegenerativas. Una de las técnicas más populares para adquirir datos de la actividad eléctrica espontánea del córtex es el electroencefalograma (EEG). El EEG goza de múltiples ventajas con respecto a otras técnicas de imagen médica, como su no invasividad, su bajo coste y su portabilidad. Además, gracias a su alta resolución temporal, los dispositivos de EEG pueden registrar cambios rápidos y transitorios inherentes a las señales bioeléctricas cerebrales. A lo largo de las últimas décadas, los análisis del EEG han contribuido a la comprensión de las alteraciones fisiológicas asociadas con diversas condiciones, entre ellas, enfermedades neurodegenerativas como la EA (Babiloni et al., 2021; Jeong, 2004; Vecchio et al., 2013). No obstante, los mecanismos causales que provocan la EA aún no han sido completamente dilucidados. Para una mejor comprensión sobre las disrupciones de la funcionalidad cerebral durante la EA, es fundamental ampliar el análisis del EEG considerando diversas perspectivas, abarcando distintas escalas temporales, interacciones no lineales entre componentes frecuenciales y aspectos genéticos.

La presente Tesis Doctoral pretende contribuir al estado del arte existente sobre la caracterización de la EA. Con este fin, se analizó el EEG en diferentes estadios de severidad de la enfermedad, para poder comparar y discutir los parámetros derivados de estos datos, así como su relación con características genéticas. Los resultados obtenidos se presentan en cuatro artículos congruentes con la caracterización de la EA a nivel electrofisiológico y genético. Las propuestas presentadas en estos documentos podrían potencialmente ser relevantes para establecer nuevos marcadores distintivos de la EA, con el propósito de mejorar los métodos de diagnóstico en el futuro.

Las publicaciones incluidas en este compendio se han organizado en orden cronológico. Los dos primeros manuscritos se enfocaron exclusivamente en análisis del EEG, mientras que los dos últimos incorporaron información genética a estos datos. El primer trabajo (Maturana-Candelas et al., 2019) se centró en los efectos de la neurodegeneración sobre la entropía de las señales EEG utilizando un enfoque multiescala para estimar la complejidad de la señal. El segundo trabajo (Maturana-Candelas et al., 2020) se enfocó en el análisis biespectral para caracterizar las interacciones no lineales entre componentes frecuenciales inter-banda. Ambos estudios caracterizaron el continuo de la EA, permitiendo visualizar las alteraciones del EEG a lo largo de su progresión, incluso en sus formas prodrómicas. El tercer trabajo (Maturana-Candelas et al., 2021) fue el primero en estudiar determinados

genotipos. En él, se calculó la potencia relativa (*relative power*, RP) en cada banda de frecuencia clásica en 68 regiones cerebrales de interés (*regions of interest*, ROIs) a partir del EEG de sujetos control y pacientes con EA. Los individuos de cada grupo fueron, a su vez, clasificados como portadores de alelos de riesgo y protectores de los genes *phosphatidylinositol binding clathrin assembly protein* (*PICALM*) y clusterina (*CLU*). Por último, el cuarto trabajo (Maturana-Candelas et al., 2024) examinó las diferencias en la red funcional cerebral entre portadores de alelos de riesgo y protectores de múltiples variaciones del gen *MAPT*. Este estudio incorporó un parámetro derivado del análisis múltiplex para evaluar la homogeneidad de las interacciones de conectividad entre bandas.

B.2 Hipótesis y objetivos

Debido al escaso conocimiento de las causas esenciales de la neurodegeneración, el diagnóstico del DCL y de la demencia debida a la EA sigue adoleciendo de un elevado grado de subjetividad. Por lo general, estas afecciones se diagnostican mediante procedimientos complejos que implican pruebas cognitivas, exámenes clínicos y la inspección de la historia clínica. La EA y el DCL presentan un inconveniente adicional, y es que suelen ir acompañados de otros trastornos neurológicos (Alzheimer's Association, 2022). Esto hace que estas afecciones sean difíciles de identificar con precisión, especialmente en las primeras fases de deterioro. Para determinar la EA de manera definitiva, el *gold standard* aceptado es la presencia de proteínas Aβ y tau en el cerebro, junto con indicadores de lesión neuronal (Jack et al., 2016, 2018). El único procedimiento que permite determinar la presencia de estas moléculas es el examen histológico del tejido cerebral, lo cual conlleva niveles extremos de invasividad (Yates, 2011). En los últimos años, los avances tecnológicos en las técnicas de imagen médica han permitido la detección de moléculas asociadas a la neurodegeneración. Sin embargo, su uso sigue siendo costoso y poco práctico a gran escala. Por ende, el desarrollo de nuevos métodos para detectar precozmente indicios de la neurodegeneración relacionada con la EA resulta fundamental. En este contexto, la hipótesis principal que impulsa esta Tesis es que *el DCL y la EA provocan alteraciones de la actividad eléctrica cerebral asociadas al procesamiento de la información en las que las anomalías genéticas pueden jugar un papel fundamental*. Esto podría contribuir a una mejor comprensión de patologías desde un nivel esencial y, potencialmente, permitir la caracterización diagnóstica del DCL y la EA.

El objetivo principal de esta Tesis Doctoral es extraer del EEG características

novedosas capaces de identificar la EA y su progresión. Esto permitiría asociar alteraciones en estos parámetros como signos de disfunción cerebral y neuronal. Además, dado que la expresión genética se ha asociado con la EA en el pasado (Harold et al., 2009; Lambert et al., 2009; Tanzi, 2012), la implicación de ciertos genotipos en la dinámica cortical puede ser útil para explicar alteraciones neurofisiológicas específicas. Con el fin de alcanzar el objetivo principal, se propusieron los siguientes objetivos específicos:

1. Identificar nuevas características derivadas del EEG que sean sensibles a las perturbaciones electrofisiológicas presentes a lo largo del continuo de la EA desde diferentes perspectivas, abarcando metodologías no lineales, espectrales y de redes múltiplex.

2. Estudiar la asociación entre alteraciones en el EEG y anomalías genéticas previamente determinadas como factores de riesgo de EA, que afectan al metabolismo, estructura y eliminación de Aβ y tau.

3. Examinar patrones comunes entre los enfoques propuestos y sugerir interpretaciones que puedan revelar mecanismos fisiológicos que influyan en los resultados obtenidos.

B.3 Sujetos

En la presente Tesis Doctoral se utilizó una base de datos compuesta por 253 sujetos, dividida en 51 sujetos control sanos (CS), 51 pacientes con DCL debido a EA, 51 pacientes con EA leve (EA_{LEV}), 50 pacientes con EA moderada (EA_{MOD}), y 50 pacientes con EA severa (EA_{SEV}). Los datos EEG y genéticos de cada sujeto se obtuvieron en un entorno de investigación como resultado del proyecto POCTEP 2014-2020 denominado: 'Análisis y correlación entre el genoma completo y la actividad cerebral para la ayuda en el diagnóstico de la enfermedad de Alzheimer' (AD-EEGWA). Todos los sujetos del estudio fueron diagnosticados de demencia o DCL por EA según los criterios establecidos por la NIA-AA (Jack et al., 2018). El deterioro cognitivo se evaluó para cada sujeto mediante el test *Mini-Mental State Examination* (MMSE) (Folstein et al., 1975). Todos los participantes en el estudio y sus cuidadores dieron su consentimiento informado por escrito, de acuerdo con el Código Ético de la Asociación Médica Mundial (Declaración de Helsinki). El protocolo del estudio fue aprobado por el Comité de Ética de la Universidad de Oporto (Oporto, Portugal). La tabla B.1 presenta la información demográfica de los participantes.

B.4 Métodos

Se registraron 5 minutos de señal de EEG en estado de reposo de cada participante en un entorno libre de ruido. El sistema de adquisición de EEG se compone de 19 canales conforme al sistema internacional 10-20 y la frecuencia de muestreo fue establecida a 500 Hz. La metodología empleada en los estudios que componen este compendio de publicaciones consta de dos fases. La primera consiste en el pre-procesado de la señal de EEG, cuyo proceso fue compartido entre estudios. Durante la misma se aplican los siguientes pasos: (i) eliminación de la media; (ii) filtrado pasa-banda que incluya todas las bandas de frecuencia de interés; (iii) eliminación de componentes con presencia de ruido electromagnético externo y otras bioseñales; (iv) segmentación de la señal en épocas de 5 segundos y (v) eliminación visual de artefactos. Los dos últimos estudios (Maturana-Candelas et al., 2021, 2024) incluyeron un paso adicional de localización de fuentes. La segunda fase consiste en el procesado de la señal de EEG mediante el uso de diversas técnicas de computación. Los enfoques propuestos abarcan tanto análisis de activación local (análisis espectral, biespectral y de entropía), como análisis de la red funcional cerebral, que se llevó a cabo mediante un análisis de redes múltiplex. Estas metodologías se describen a continuación.

B.4.1 Entropías multiescala

El primer estudio (Maturana-Candelas et al., 2019) se centra en el análisis de la entropía del EEG a distintas escalas temporales, abarcando tanto el dominio temporal como el frecuencial. El concepto de entropía se basa en la estimación de la impredecibilidad (o irregularidad) de una secuencia o conjunto de datos. De este

Grupo	**N**	**Edad** ($\overline{x} \pm \sigma$)	**Sexo (M:H)**	**MMSE** ($\overline{x} \pm \sigma$)
CS	51	80.1±7.1	25:26	28.8±1.1
DCL	51	85.5±7.3	36:15	23.3±2.8
EA_{LEV}	51	80.7±7.1	30:21	22.5±2.3
EA_{MOD}	50	81.3±8.0	43:7	13.6±2.8
EA_{SEV}	50	80.0±7.8	43:7	2.4±3.7

Tabla B.1: Datos demográficos. $\overline{x}$: media; σ: desviación típica; M: mujeres; H: hombres; CS: controles sanos; DCL: pacientes con deterioro cognitivo leve; EA_{LEV}: pacientes con EA leve; EA_{MOD}: pacientes con EA moderada; EA_{SEV}: pacientes con EA severa; MMSE: puntuación de *Mini-Mental State Examination*.

modo, valores elevados de cualquier métrica de entropía sugieren una distribución uniforme en las muestras de la serie temporal, lo que refleja un alto grado de incertidumbre y aleatoriedad. Por el contrario, resultados de entropía bajos denotan valores de señal concentrados en rangos más estrechos y, por lo tanto, más predecibles. En el primer estudio llevado a cabo en el marco de esta Tesis Doctoral (Maturana-Candelas et al., 2019), se emplearon algoritmos derivados de esta perspectiva con un enfoque multiescala tanto en el dominio temporal como en el espectral. Se calculó la entropía muestral (*sample entropy*, SampEn), una métrica desarrollada como mejora de la entropía aproximada (Richman and Moorman, 2000). Este cálculo se fundamenta en la similitud entre una serie temporal y su versión retardada (Richman and Moorman, 2000). Con el fin de comprobar los efectos de diversas escalas temporales en el cálculo de entropía, SampEn se calculó en diferentes versiones de "grano grueso" del EEG. Estas secuencias son series compuestas de "bloques" de muestras promediados con tamaños variables a partir del EEG original. Ello resulta en versiones "diezmadas" del EEG en un factor de escala determinado. A la aplicación del algoritmo de SampEn a las diferentes versiones de "grano grueso" resultantes de la señal EEG original se le denomina entropía muestral multiescala (*multiscale sample entropy*, MSE).

Por otro lado, el cálculo de entropía se aplicó a la función de densidad espectral de potencia (*power spectral density*, PSD), proporcionando información sobre la diversidad de componentes espectrales del EEG. Para ello, se usó la definición de entropía de Shannon (Shannon, 1948), obteniéndose así la entropía espectral (*spectral entropy*, SpecEn). SpecEn también puede ser analizada aplicando un enfoque multiescala. En este caso, se consideró una versión refinada de SpecEn multiescala (*refined multiscale spectral entropy*, rMSSE) basada en el trabajo de Humeau-Heurtier et al. (2016). Esta variante mejorada proporciona una mayor robustez frente al *aliasing* debido al submuestreo, que reduce las oscilaciones espurias entre 0 Hz y la frecuencia de corte del filtro (Humeau-Heurtier et al., 2016). De forma análoga al MSE, el rMSSE es el resultado de cálculos secuenciales de entropía aplicados a la PSD de versiones de "grano grueso" de la señal original.

B.4.2 Biespectro

En el segundo de los artículos que componen esta Tesis Doctoral se analizó el biespectro de la señal de EEG a lo largo del continuo de la EA (Maturana-Candelas et al., 2020). El biespectro es la representación de las interacciones no lineales entre pares de componentes frecuenciales. Técnicamente, el biespectro

es la transformada de Fourier de los estadísticos de tercer orden de una señal estacionaria. El biespectro cuenta con la ventaja sobre el estadístico de segundo orden, o espectro de potencia, en que esta última únicamente puede ser empleada para abordar problemas de "naturaleza lineal" (Rosenblatt and Ness, 1965). Por esta razón, los elementos no lineales, como las relaciones de fase entre componentes de frecuencia, se desprecian en el espectro de potencia (Nikias and Mendel, 1993). El resultado de un cálculo biespectral consiste en una matriz cuadrada de tamaño equivalente al número de componentes espectrales considerados. En cada punto de la matriz, se muestra la intensidad de la interacción no lineal entre cada uno de los posibles pares frecuenciales. En esta Tesis Doctoral se ha utilizado el biespectro para estudiar las interacciones entre diferentes bandas de frecuencia, o también llamadas "regiones inter-banda". Con el fin de inspeccionar el biespectro en estas regiones, se propusieron tres métricas novedosas: potencia relativa biespectral (*bispectral relative power*, BispRP), entropía cúbica biespectral (*bispectral cubic entropy*, BispEn), y frecuencia mediana biespectral (*bispectral median frequency*, BispMF), que se aplicaron en las regiones del biespectro que representan interacciones entre cada banda y el resto del espectro.

B.4.3 Potencia Relativa

En el siguiente estudio (Maturana-Candelas et al., 2021) se calculó la RP y la homogeneidad de la distribución de estos valores en diferentes regiones cerebrales. La RP es uno de los parámetros más utilizados para caracterizar el espectro de una señal debido a su simplicidad. La RP cuantifica la potencia asignada en una banda de frecuencia específica en relación a la potencia espectral total (Bachiller et al., 2014). La RP es útil para identificar cambios en el contenido espectral de una señal. Uno de los rasgos distintivos de las perturbaciones del EEG causadas por la EA es la ralentización de la señal. Estas alteraciones pueden percibirse midiendo la relación entre la RP en las bandas de frecuencia más lentas y la RP en las bandas de frecuencia más rápidas (Benwell et al., 2020). En el tercer artículo del compendio de publicaciones, se empleó la RP para analizar las alteraciones de la potencia en cada banda de frecuencia en función del genotipo de *PICALM* y *CLU* a lo largo del continuo de la EA (Maturana-Candelas et al., 2021).

Adicionalmente, se aplicó la entropía de Shannon para analizar la distribución de los valores de RP en cada ROI del cerebro. Esta aplicación de la entropía se denominó entropía espacial (*spatial entropy*, SE). De forma análoga a otros tipos de métricas de entropía, valores más altos significarían una mayor heterogeneidad

o diversidad de valores y una entropía más baja significaría distribuciones homogéneas.

B.4.4 Análisis de redes múltiplex

El último estudio que compone el compendio de publicaciones de esta Tesis Doctoral se centra en el análisis de redes múltiplex (*multiplex network analysis*, MNA) (Maturana-Candelas et al., 2024). El MNA es útil para evaluar las implicaciones de cada banda de frecuencia en el funcionamiento del cerebro. El MNA establece un marco para inspeccionar las relaciones entre redes funcionales de frecuencias específicas. Además, las redes múltiplex difieren de otras redes interconectadas en que los enlaces entre capas sólo pueden conectar nodos que representen al mismo nodo en diferentes capas (Kinsley et al., 2020). En este trabajo, cada nodo de la red se corresponde con cada una de las ROIs cerebrales.

Además, se ha utilizado el coeficiente de participación (P) para estudiar la homogeneidad de la contribución de cada nodo en cada banda de frecuencia al conjunto del espectro. El valor de este parámetro pueden oscilar entre 0 y 1. Un valor de P de 1 indica valores de conectividad distribuidos homogéneamente entre capas, mientras que un valor de 0 significa que todas las conexiones con el nodo se concentran en una sola capa (Battiston et al., 2014). Finalmente, con el objetivo de determinar la alteración global de los nodos en la red funcional cerebral, se propuso el índice k (Achard et al., 2012). El parámetro k muestra el gradiente de la línea de regresión, que es el ajuste polinómico de primer orden por mínimos cuadrados que asocia los valores de P de los pacientes con EA menos los valores medios de P de los sujetos CS (es decir, la disrupción de P) con los valores medios de P de los sujetos CS (Achard et al., 2012; Yu et al., 2017). Los valores bajos de k indican una menor alteración de "hub" global, ya que los valores de P de los pacientes con EA serían más similares a los de los sujetos CS. Por lo tanto, el parámetro k permite comparar las propiedades de los nodos en las redes funcionales cerebrales entre diferentes grupos.

B.4.5 Análisis genético

En el tercer y cuarto artículo que componen el compendio de publicaciones de esta Tesis Doctoral se emplearon datos genéticos con el fin de establecer relaciones entre genotipos y cambios en los ritmos oscilatorios cerebrales (Maturana-Candelas et al., 2021, 2024). Las variaciones genéticas de interés corresponden a un polimorfismo de nucleótido simple (*single nucleotide polymorphism*, SNP) en

PICALM, otro SNP en *CLU* y 7 en *MAPT*. Para obtener los datos genéticos, se recolectaron muestras de material biológico de cada participante a través de muestras de saliva o mucosa bucal. Previamente al análisis del genoma completo con Axiom Spain Biobank Array (Thermo Fisher Scientific) en el Centro Nacional de Genotipado (CEGEN), se llevó a cabo la extracción de ADN y un control de calidad en todas las muestras recolectadas. La información genética relevante para los estudios que componen esta Tesis Doctoral es la siguiente: alelos de riesgo y protectores de *PICALM* en el SNP rs3851179, alelos de riesgo y protectores de *CLU* en el SNP rs11136000, y alelos de riesgo y protectores de *MAPT* en los SNPs rs2258689, rs242557, rs11656151, rs2435207, rs16940758, rs7521 y rs8070723.

B.4.6 Análisis estadístico

Para evaluar la normalidad y la homocedasticidad de los datos, se utilizaron las pruebas de Kolmogorov-Smirnov y Shapiro-Wilk. En esta Tesis Doctoral, ningún estudio mostró datos que cumplieran estos supuestos paramétricos. Por esta razón, para determinar diferencias con significación estadística, se utilizaron pruebas no paramétricas. Se calculó la prueba de Kruskal-Wallis para las comparaciones de grupos múltiples y la prueba U de Mann-Whitney para las comparaciones de grupos por pares (para ambas, $\alpha = 0{,}05$). Para evitar falsos rechazos de la hipótesis nula en las comparaciones entre clases múltiples, se aplicó una corrección de tasa de descubrimiento falso (Benjamini and Hochberg, 1995). Además, se utilizaron pruebas de Chi-cuadrado (χ^2) para comparar variables cualitativas, como el sexo o la presencia de variantes genéticas, con el fin de identificar factores de confusión.

Finalmente, en el primer estudio (Maturana-Candelas et al., 2019) se llevó a cabo un procedimiento de clasificación para determinar la capacidad discriminante de MSE y rMSSE utilizando 62 características: los valores promediados de MSE y rMSSE en cada factor de escala, los valores promediados de pendiente de MSE y rMSSE (para todas las escalas temporales, para escalas altas y para escalas bajas) y las áreas bajo las curvas de MSE y rMSSE (para todas las escalas temporales, para escalas altas y para escalas bajas). Para seleccionar las características óptimas para la clasificación, se utilizó una regresión multilineal paso a paso. El proceso de selección de características se llevó a cabo utilizando un esquema de validación cruzada dejando uno fuera para reducir el sesgo en los resultados (Dominguez, 2009). Tras la selección de características, se utilizó un análisis discriminante cuadrático para clasificar a los sujetos.

B.5 Resultados y discusión

El EEG de sujetos sanos y enfermos de EA fue analizado empleando las métricas descritas para caracterizar su progresión, desde estadios preclínicos hasta las fases más severas. Además, se identificaron las alteraciones de la actividad eléctrica asociadas con la presencia de variantes genéticas estrechamente implicadas con las proteínas Aβ y tau.

B.5.1 Entropías multiescala en la evaluación de la complejidad del EEG a lo largo del continuo de la EA

En el transcurso de esta Tesis Doctoral, se procedió a evaluar la complejidad inherente de la señal del EEG mediante la implementación de un enfoque de entropía multiescala. Este método se centró en calcular la entropía en distintas escalas temporales (Maturana-Candelas et al., 2019). Los resultados de MSE y rMSSE obtenidos, calculados en un factor de escala de 1 (es decir, la señal original), revelaron una disminución en la irregularidad observada en los pacientes con EA en comparación con los sujetos CS. Esta conclusión coincide con investigaciones previas que han empleado medidas de entropía para caracterizar la EA (Abásolo et al., 2006b, 2008; Simons et al., 2015). No obstante, se destacó que el primer factor de escala no resulta idóneo para diferenciar grupos de severidad. En el caso del MSE, los factores de escala entre 5 y 17 demostraron ser más eficaces para tal fin. Asimismo, los factores de escala más elevados, especialmente en el rango de 16 a 25, mostraron diferencias estadísticamente significativas entre los sujetos CS y los individuos afectados por el DCL. Esta misma observación se apreció de manera consistente en los valores de rMSSE obtenidos, los cuales mostraron diferencias estadísticamente significativas entre sujetos CS y pacientes con DCL en las escalas temporales entre 19 y 25.

Por otro lado, la estimación de la complejidad puede llevarse a cabo mediante la extracción de parámetros derivados de las curvas de MSE y rMSSE. Estudios previos sugirieron las pendientes en distintos rangos de escala (Escudero et al., 2006) y las áreas bajo la curva (Weng et al., 2015) como medidas relevantes para este propósito. Se observó que los valores promedio de pendiente del MSE en escalas temporales más bajas tienden a decrecer conforme se agrava la severidad de la enfermedad. En contraste, en escalas temporales más altas, se identificó la tendencia opuesta. Este mismo patrón se reflejó en el rMSSE, aunque de forma

menos evidente. En ambas métricas se observó un cruce de las curvas de entropía de los grupos de EA y del grupo CS en escalas temporales más elevadas. Este fenómeno ha sido observado en otros estudios que también buscaban caracterizar la EA utilizando un enfoque multiescala (Escudero et al., 2006; Labate et al., 2013; Mizuno et al., 2010). Aunque no existe un consenso definido en la cuantificación de la complejidad (Costa et al., 2005), se ha planteado que valores más altos de entropía en la mayoría de las escalas temporales podrían indicar una mayor complejidad. Asimismo, se observó que el ruido blanco, una señal sin complejidad, presenta valores de entropía extremadamente altos en las escalas más bajas y valores muy bajos en las escalas más altas, mostrando una disminución exponencial (Costa et al., 2005). Esta tendencia contrasta notablemente con el patrón mostrado por el análisis del EEG, sugiriendo la complejidad inherente de esta señal. La reducción de la complejidad podría atribuirse a modificaciones en la dinámica neuronal generadas por cambios estructurales cerebrales, dando como resultado interacciones anómalas entre sistemas neuronales. Estas alteraciones podrían estar asociadas a muerte neuronal, déficits en la neurotransmisión y perturbaciones en la conectividad funcional cerebral (Jelles et al., 1999; Jeong, 2004).

B.5.2 Parámetros biespectrales inter-banda para caracterizar el continuo de la EA

En el segundo estudio de esta Tesis Doctoral, se empleó el biespectro para caracterizar el continuo de la EA (Maturana-Candelas et al., 2020). Particularmente, se exploraron las alteraciones manifestadas en las regiones inter-banda de las matrices biespectrales. Estas regiones reflejan las interacciones no lineales entre componentes frecuenciales de una banda y el resto del espectro. Con este fin, se usaron tres métricas: BispRP, BispEn y BispMF. BispRP representa la potencia acumulada en relación con el biespectro total. Valores más elevados de BispRP se asociaron con una mayor severidad de la EA en bandas de frecuencia más bajas (delta y zeta), mientras que se observó lo opuesto en las bandas de frecuencia más altas (alfa, beta-1 y beta-2). Además, se identificaron diferencias estadísticamente significativas en las bandas de frecuencia alfa y beta-1 en el último estadio de la progresión de la enfermedad (EA_{MOD} *vs.* EA_{SEV}), y en las bandas zeta y beta-2 en los estadios iniciales (sujetos CS *vs.* pacientes con DCL).

Por otro lado, BispEn cuantifica la homogeneidad en la distribución de los valores del biespectro. Se observó una disminución de los valores de BispEn con respecto a la severidad de la EA en las frecuencias más bajas, mientras que las

bandas más altas no mostraron ninguna tendencia. Se identificaron diferencias estadísticamente significativas entre los grupos de EA_{MOD} y EA_{SEV} en las bandas de frecuencia delta, zeta y alfa. La disminución de la irregularidad espectral en el EEG es un efecto conocido de la neurodegeneración, que se ha evaluado en estudios previos con diferentes medidas de entropía (Abásolo et al., 2006b; Maturana-Candelas et al., 2019; Ruiz-Gómez et al., 2018b). Esto concuerda con investigaciones previas que reportaron una disminución general de la entropía biespectral en pacientes con EA (Wang et al., 2015).

Finalmente, BispMF indica la frecuencia en la cual la potencia biespectral se divide por la mitad. Esta métrica indica si una banda de frecuencia es más proclive a interactuar con frecuencias más altas o bajas. Se observó una tendencia decreciente consistente en todas las bandas de frecuencia, revelándose diferencias estadísticamente significativas entre los grupos EA_{MOD} y EA_{SEV}. A su vez, las bandas de frecuencia más lentas mostraron diferencias estadísticamente significativas entre sujetos CS y pacientes con DCL, mientras que la banda más rápida (beta-2) exhibió diferencias entre pacientes con DCL y EA_{LEV}. Estos resultados podrían estar relacionados con dos factores subyacentes: una disminución de las interacciones que involucran bandas de frecuencia más altas (alfa y beta) y un aumento de las interacciones entre las bandas delta y zeta. Este hallazgo es coherente con los valores obtenidos de BispRP, que muestran un incremento en las interacciones entre las bandas delta y zeta con el resto del espectro a medida que la severidad de la EA aumenta.

Los resultados obtenidos se pueden resumir en varios puntos. En primer lugar, se observa una mayor cantidad y diversidad de interacciones en pacientes con DCL en comparación con los sujetos CS. Sin embargo, a medida que la EA progresa, se puede apreciar una reducción aparente en la diversidad de las interacciones de frecuencia. Se observa una concentración de valores biespectrales más altos en las bandas de frecuencia más bajas, lo que sugiere una disminución de las interacciones no lineales. Dado que la presencia de sinergias caóticas entre osciladores neuronales es requisito para la existencia de "riqueza estructural", la falta de interacciones no lineales podría interpretarse como una disminución en la complejidad. Las interacciones más dispersas observadas a lo largo del espectro en pacientes con DCL podrían ser un signo de hiperactivación neuronal asociada a los primeros signos de neurodegeneración. En segundo lugar, la menor diversidad de interacciones entre componentes frecuenciales en pacientes con EA sugiere señales de EEG más predecibles, menos complejas y con una menor no linealidad. Investigaciones previas han demostrado que múltiples tareas cognitivas de alto

nivel están asociadas a interacciones de actividad cortical inter-banda (Riddle et al., 2022; von Stein and Sarnthein, 2000). Asimismo, anomalías en acoplamientos inter-banda han sido previamente asociadas con la EA (Engels et al., 2016; Fraga et al., 2013; Stam et al., 2003, 2005). Por lo tanto, se puede inferir que las alteraciones apreciadas en el biespectro podrían ser el resultado de la atrofia y daño neuronal presentes en la EA.

B.5.3 Potencia relativa vinculada a las variantes genéticas de *PICALM* y *CLU*

El tercer estudio de la presente Tesis Doctoral abordó el análisis del espectro de frecuencia del EEG en pacientes diagnosticados con EA y sujetos sanos (Maturana-Candelas et al., 2021). En este trabajo, los participantes fueron categorizados como portadores de alelos de riesgo y protectores para desarrollar EA en los genes *PICALM* y *CLU*. Estudios previos han evidenciado la vinculación de estos genes con los procesos de eliminación de Aβ (DeMattos et al., 2002; Xu et al., 2015; Zhao et al., 2015; Zlokovic et al., 1994), lo cual podría tener consecuencias en diversas funciones de neurotransmisión (Itoh et al., 2002; Trabace et al., 2007). Los análisis mostraron un aumento en la potencia de las bandas de frecuencia delta y zeta, junto con una disminución en las bandas de frecuencia alfa, beta y gamma en las poblaciones que presentaban variantes de riesgo y padecían de EA. Además, se identificaron diferencias estadísticamente significativas en la banda beta. Estos resultados sugieren una ralentización del EEG en los portadores de las variantes de riesgo, un patrón comúnmente asociado con la neurodegeneración (Jeong, 2004). De hecho, las tendencias observadas en cada banda de frecuencia concuerdan con las alteraciones espectrales típicas durante la EA (Coben et al., 1983, 1985), entre las que se encuentran la disminución de potencia en la banda beta. Los ritmos beta se han asociado a procesos cognitivos como el procesamiento sensorial (Lalo et al., 2007), la atención visual (Wróbel, 2000), el razonamiento (Basile et al., 2013) y la memoria de trabajo (Hsu et al., 2017). Por consiguiente, la reducción de potencia en la banda beta podrían estar relacionada con un mayor deterioro neuronal en los individuos portadores de alelos de riesgo, lo que podría conducir a un declive cognitivo más acentuado. Por otro lado, una potencia excesiva en la banda beta podría estar asociada a situaciones de estrés, ansiedad, rumiación excesiva y sobreestimulación, dado que se ha planteado que los ritmos beta mantienen el *statu quo* (Spitzer and Haegens, 2017). Por consiguiente, es factible proponer que rangos específicos de potencia beta en el EEG podrían

asociarse con un desempeño cognitivo óptimo. Investigaciones previas sugieren que los portadores del genotipo *PICALM* GG (es decir, alelos de riesgo) están predispuestos a reacciones de estrés (Ponomareva et al., 2017) Por ello, es plausible la hipótesis de que esta variante específica del gen *PICALM* es propensa a desestabilizar la dinámica neuronal en circunstancias anormales. En esencia, la presencia del alelo protector de *PICALM* podría correlacionarse con rangos de actividad beta asociada a un funcionamiento cerebral más saludable. En cuanto al grupo CS, no presentó diferencias significativas en ninguna banda de frecuencia a pesar de que la banda beta mostrara valores de RP más elevados en portadores de las variantes protectoras. Estos hallazgos podrían ser atribuidos a la influencia opuesta de los alelos *PICALM* en individuos sanos, tal como se ha documentado previamente (Ponomareva et al., 2017). Esta controversia sugiere que el impacto del gen *PICALM* puede variar según el estado cognitivo del sujeto o, como mínimo, según la severidad de la neurodegeneración.

En relación al análisis de SE, este parámetro presentó variaciones similares a las obtenidas con RP. Los valores de SE del grupo CS no mostraron diferencias estadísticamente significativas entre genotipos en ninguna banda, mientras que los pacientes con EA sí las revelaron en la banda beta. Se observó que los alelos protectores en el grupo de pacientes de EA se asociaron con una disminución de SE en las frecuencias delta y zeta, y un aumento en las frecuencias alfa, beta y gamma. Estudios previos han identificado regiones cerebrales con funciones especializadas, definidas por estructuras citoarquitectónicas (Bressler, 1995). Además, se ha sugerido que la sincronización local está relacionada principalmente con frecuencias más altas, mientras que las frecuencias más lentas tienen un papel predominante en las interacciones a larga distancia (Varela et al., 2001; von Stein and Sarnthein, 2000). Por lo tanto, es plausible suponer que las alteraciones en SE podrían reflejar cambios en la conectividad, dado que la sincronización entre diversas redes neuronales podría influir en la distribución de RP en diferentes bandas de frecuencia. Así pues, los resultados obtenidos sugieren que las variantes de riesgo de *PICALM* y *CLU* podrían estar vinculadas a alteraciones en el funcionamiento cerebral.

B.5.4 Alteraciones asociadas a variaciones *MAPT* en la red funcional cerebral mediante MNA

El último estudio desarrollado en esta Tesis Doctoral aborda las propiedades inter-banda de la red funcional cerebral en individuos con siete genotipos

distintos de *MAPT*. Estas variantes genéticas han sido previamente asociadas con neuropatologías o cambios en la presencia de tau en el CSF (Maturana-Candelas et al., 2024). Para este estudio, se empleó MNA con el objetivo de evaluar la actividad del EEG en sujetos CS y pacientes con EA, categorizados en portadores de alelos de riesgo y protección de los genotipos mencionados. El propósito principal fue investigar la uniformidad en la contribución de valores de conectividad proporcionada por cada red funcional específica de cada banda de frecuencia.

En un primer análisis, se observó que los portadores de alelos de riesgo estaban asociados a valores positivos de disrupción de P, mientras que aquellos con alelos protectores se asociaban a valores predominantemente negativos. Este hallazgo indica que los individuos del grupo de pacientes de EA portadores de alelos de riesgo proporcionan un coeficiente P mayor en comparación con los individuos con alelos protectores. En contraste, los sujetos CS muestran el patrón opuesto. Esta diferencia se debe al aumento significativo del coeficiente P obtenido a partir del grupo de EA con alelos de riesgo y, a su vez, al aumento significativo del coeficiente P dentro del grupo CS portadores de alelos protectores. Estos resultados sugieren que el impacto de las diferentes variantes del gen *MAPT* en la actividad cerebral puede variar según el estado clínico. Sin embargo, es destacable que el efecto de estas variantes es más notable en el grupo CS. Estos datos concuerdan con los resultados obtenidos del parámetro k, el cual no solo demostró diferencias estadísticamente significativas entre las variantes de riesgo y protección, sino que también reveló que los alelos de riesgo están asociados con una mayor disrupción de P global entre los pacientes con EA y los sujetos CS.

Los valores de P en la región izquierda de la *default mode network* (DMN) demostraron una mayor sensibilidad general a la expresión genotípica, presentando los valores más elevados en sujetos CS con alelos protectores. Los valores reducidos de P indican una conectividad más concentrada en una sola capa. Ello sugiere que los sujetos CS con alelos de riesgo sufren una posible carencia para integrar información de diferentes bandas de frecuencia en la DMN izquierda. Las razones subyacentes por las cuales la DMN es más sensible a las variaciones genéticas relacionadas con la proteína tau podría incluir aspectos de mielinización. Se ha demostrado una relación entre la mielina y la resistencia a los efectos citotóxicos de la tau (Rubinski et al., 2022), lo cual es compatible con la estrecha asociación entre bajos niveles de mielina en la DMN y mayores concentraciones de tau (Dean et al., 2017). Dado que la DMN se considera una región con mielinización tardía durante el desarrollo cerebral (Kernbach et al., 2018), podría ser más sensible a los

cambios en las propiedades de tau provocados por variantes del gen *MAPT*. Otra razón que puede explicar una mayor sensibilidad de la DMN a las disrupciones citotóxicas de tau es su predisposición a acumular mayores cantidades de esta proteína. Se ha comprobado que la propagación de los ovillos neurofibrilares y otros productos relacionados con la proteína tau por el tejido cerebral se da a través de mecanismos de transferencia priónica (Mudher et al., 2017). La probabilidad de activación de estos procesos de transporte es mayor en regiones caracterizadas por una alta densidad sináptica (Calafate et al., 2015), como es la DMN (Raichle, 2015).

Por último, se evaluó la contribución de cada ROI en cada capa de la red funcional múltiplex de manera individual calculando el grado de nodo. Este análisis reveló diferencias significativas consistentes entre genotipos, específicamente en las bandas de frecuencia zeta y beta. Estudios previos han destacado la asociación entre cambios en la actividad eléctrica en la banda de frecuencia zeta y alteraciones en las concentraciones o estructura de la proteína tau (Das et al., 2018; Stomrud et al., 2010). Por otro lado, se han demostrado relaciones entre cambios en las frecuencias rápidas y niveles anormales de tau, evidenciados mediante diferencias en la conectividad funcional (Canuet et al., 2015) y en la potencia global del EEG (Smailovic et al., 2018). Estos hallazgos podrían reflejar las manifestaciones más relevantes en la actividad cerebral inducidas por diferentes formas de tau.

B.5.5 Conclusiones

La presente Tesis Doctoral se ha centrado en proponer parámetros novedosos para la caracterización de la actividad eléctrica cerebral en estados neurodegenerativos atribuidos a la EA desde diferentes perspectivas. Se ha aplicado un enfoque de entropías multiescala para evaluar las alteraciones de la complejidad del EEG, una exploración de las interacciones de los componentes de frecuencia inter-banda, un análisis de las modificaciones en la densidad espectral de potencia en relación con variantes genéticas específicas, y un estudio que aborda la contribución de cada banda de frecuencia en la red funcional cerebral en función de los genotipos relacionados con tau. Estos enfoques han arrojado relaciones entre parámetros que pueden ser esenciales para comprender las alteraciones neurofisiológicas de la EA. Las conclusiones más importantes obtenidas en esta Tesis Doctoral se enumeran a continuación:

1. Se emplearon métricas de entropía multiescala como estimadores de la complejidad del EEG, demostrando ser indicadores fiables de estados

neurodegenerativos (Maturana-Candelas et al., 2019). En consecuencia, se evidencia que los métodos analíticos que incorporan métricas de entropía multiescala pueden resultar útiles para caracterizar los efectos subyacentes de la neurodegeneración a lo largo del continuo de la EA.

2. Se ha corroborado la presencia de perturbaciones en el acoplamiento inter-banda, constatando mayores alteraciones a medida que la EA avanza en severidad (Maturana-Candelas et al., 2020). Este hallazgo señala una disminución general en las relaciones entre las componentes frecuenciales que abarcan todas las bandas de frecuencia. Por lo tanto, se establece una asociación entre un funcionamiento cerebral saludable y la sincronización inter-banda, que podría servir como un indicador de deterioro neuronal, incluso en las fases iniciales de la neurodegeneración.

3. Las interacciones entre los componentes de frecuencia inter-banda parecen estar asociadas con la complejidad. Esta idea indica que las estructuras que expresan un comportamiento complejo, caótico y no lineal podrían tener su origen en interacciones entre componentes de frecuencia pertenecientes a diversas bandas. Por esta razón, la disminución del acoplamiento no lineal entre bandas podría ser un estimador útil de disfunción cerebral.

4. Los genes *PICALM* y *CLU*, asociados a la eliminación de Aβ, parecen desempeñar un papel importante en la actividad eléctrica cerebral. Se obtuvieron alteraciones del EEG en pacientes con EA portadores de alelos de riesgo en SNPs específicos inductores de EA de ambos genes (Maturana-Candelas et al., 2021). Además, la potencia en la banda beta mostró mayor sensibilidad a variaciones genéticas relacionadas con el metabolismo del Aβ (Maturana-Candelas et al., 2021).

5. La red funcional cerebral es diferente entre poblaciones portadoras de múltiples variantes del gen *MAPT* (Maturana-Candelas et al., 2024). Estas alteraciones se manifestaron como cambios en la contribución de conectividad atribuida a cada banda de frecuencia en el conjunto de la red. Además, la DMN izquierda en sujetos CS expresó una mayor sensibilidad a las variaciones de los genotipos, lo que sugiere que los factores genéticos pueden tener un impacto más prominente durante las etapas preclínicas en esta región del cerebro. Esta asociación podría estar inducida por la influencia de diversas propiedades estructurales de tau en la configuración de la red funcional cerebral.

6. Las implicaciones de las variaciones genotípicas sobre la actividad eléctrica cerebral son diferentes en función del estadio de progresión de la EA. Los genes implicados en mecanismos relacionados con el metabolismo del Aβ parecen tener un mayor impacto en estados patológicos, mientras que los efectos de los procesos relacionados con tau serían más evidentes en estados preclínicos.

7. Los factores genéticos que influyen en la acumulación de Aβ y tau hiperfosforilada podrían estar relacionados con las perturbaciones homeostáticas que regulan la excitación y la inhibición cortical. Estas anomalías pueden deberse a desequilibrios en la concentración y síntesis de neurotransmisores.

Bibliography

Abásolo, D., Hornero, R., Espino, P., et al., 2005. Analysis of regularity in the EEG background activity of Alzheimer's disease patients with Approximate Entropy. Clinical Neurophysiology 116 (8), 1826–1834.

Abásolo, D., Hornero, R., Gómez, C., et al., 2006a. Analysis of EEG background activity in Alzheimer's disease patients with Lempel–Ziv complexity and central tendency measure. Medical Engineering & Physics 28 (4), 315–322.

Abásolo, D., Hornero, R., Espino, P., et al., 2006b. Entropy analysis of the EEG background activity in Alzheimer's disease patients. Physiological Measurement 27 (3), 241–253.

Abásolo, D., Escudero, J., Hornero, R., et al., 2008. Approximate entropy and auto mutual information analysis of the electroencephalogram in Alzheimer's disease patients. Medical & Biological Engineering & Computing 46 (10), 1019–1028.

Abdellaoui, A., Yengo, L., Verweij, K. J., and Visscher, P. M., 2023. 15 years of GWAS discovery: Realizing the promise. The American Journal of Human Genetics 110 (2), 179–194.

Achard, S., Delon-Martin, C., Vértes, P. E., et al., 2012. Hubs of brain functional networks are radically reorganized in comatose patients. Proceedings of the National Academy of Sciences 109 (50), 20608–20613.

Aguet, F., Anand, S., Ardlie, K. G., et al., 2020. The GTEx Consortium atlas of genetic regulatory effects across human tissues. Science 369 (6509), 1318–1330.

Al-Haggar, M., Madej-Pilarczyk, A., Kozlowski, L., et al., 2012. A novel homozygous p.Arg527Leu LMNA mutation in two unrelated Egyptian families causes overlapping mandibuloacral dysplasia and progeria syndrome. European Journal of Human Genetics 20 (11), 1134–1140.

Alexander, G. C. and Karlawish, J., 2021. The Problem of Aducanumab for the Treatment of Alzheimer Disease. Annals of Internal Medicine 174 (9), 1303–1304.

Allen, M., Kachadoorian, M., Quicksall, Z., et al., 2014. Association of MAPT haplotypes with Alzheimer's disease risk and MAPT brain gene expression levels. Alzheimer's Research & Therapy 6 (4), 39.

Alzforum, 2023. Repository of variants in genes implicated in Alzheimer's disease. `https://www.alzforum.org/mutations`, accessed: 2023-06-20.

Alzheimer's Association, 2022. 2022 Alzheimer's disease facts and figures. Alzheimer's & Dementia 18 (4), 700–789.

Amin, H. U., Malik, A. S., Badruddin, N., and Chooi, W.-T., 2012. Brain activation during cognitive tasks: An overview of EEG and fMRI studies. In: 2012 IEEE-EMBS Conference on Biomedical Engineering and Sciences. IEEE, pp. 950–953.

Amzica, F. and Steriade, M., 1998. Electrophysiological correlates of sleep delta waves. Electroencephalography and Clinical Neurophysiology 107 (2), 69–83.

Anderson, C. A., Pettersson, F. H., Clarke, G. M., et al., 2010. Data quality control in genetic case-control association studies. Nature Protocols 5 (9), 1564–1573.

Antonakakis, M., Schrader, S., Ümit Aydin, et al., 2020. Inter-subject variability of skull conductivity and thickness in calibrated realistic head models. NeuroImage 223, 117353.

Arendt, D., 2021. Elementary nervous systems. Philosophical Transactions of the Royal Society B: Biological Sciences 376 (1821), 20200347.

Axmacher, N., Henseler, M. M., Jensen, O., et al., 2010. Cross-frequency coupling supports multi-item working memory in the human hippocampus. Proceedings of the National Academy of Sciences 107 (7), 3228–3233.

Azami, H., Moguilner, S., Penagos, H., et al., 2023. EEG Entropy in REM Sleep as a Physiologic Biomarker in Early Clinical Stages of Alzheimer's Disease. Journal of Alzheimer's Disease 91 (4), 1557–1572.

Azevedo, F. A., Carvalho, L. R., Grinberg, L. T., et al., 2009. Equal numbers of neuronal and nonneuronal cells make the human brain an isometrically scaled-up primate brain. Journal of Comparative Neurology 513 (5), 532–541.

Babiloni, C., Arakaki, X., Azami, H., et al., 2021. Measures of resting state EEG rhythms for clinical trials in Alzheimer's disease: Recommendations of an expert panel. Alzheimer's & Dementia 17 (9), 1528–1553.

Bachiller, A., Díez, A., Suazo, V., et al., 2014. Decreased spectral entropy modulation in patients with schizophrenia during a P300 task. European Archives of Psychiatry and Clinical Neuroscience 264 (6), 533–543.

Bai, Y., Xia, X., and Li, X., 2017. A review of resting-state electroencephalography analysis in disorders of consciousness. Frontiers in Neurology 8, 471.

Bao, X., Liu, G., Jiang, Y., et al., 2015. Cell adhesion molecule pathway genes are regulated by cis-regulatory SNPs and show significantly altered expression in Alzheimer's disease brains. Neurobiology of Aging 36 (10), 2904.e1–2904.e7.

Barthélemy, M., 2004. Betweenness centrality in large complex networks. The European Physical Journal B - Condensed Matter 38 (2), 163–168.

Basile, L. F. H., Sato, J. R., Alvarenga, M. Y., et al., 2013. Lack of Systematic Topographic Difference between Attention and Reasoning Beta Correlates. Plos One 8 (3), e59595.

Battiston, F., Nicosia, V., and Latora, V., 2014. Structural measures for multiplex networks. Physical Review E 89 (3), 032804.

Becker, J. T., Mintun, M. A., Aleva, K., et al., 1996. Compensatory reallocation of brain resources supporting verbal episodic memory in Alzheimer's disease. Neurology 46 (3), 692–700.

Belbin, O., Morgan, K., Medway, C., et al., 2019. The Epistasis Project: A Multi-Cohort Study of the Effects of BDNF, DBH, and SORT1 Epistasis on Alzheimer's Disease Risk. Journal of Alzheimer's Disease 68 (4), 1535–1547.

Bell, A. J. and Sejnowski, T. J., 1995. An information-maximization approach to blind separation and blind deconvolution. Neural Computation 7, 1129–1159.

Bellenguez, C., Grenier-Boley, B., and Lambert, J.-C., 2020. Genetics of Alzheimer's disease: where we are, and where we are going. Current Opinion in Neurobiology 61, 40–48.

Benjamini, Y. and Hochberg, Y., 1995. Controlling the False Discovery Rate: A Practical and Powerful Approach to Multiple Testing. Journal of the Royal Statistical Society: Series B (Methodological) 57 (1), 289–300.

Benwell, C. S., Davila-Pérez, P., Fried, P. J., et al., 2020. EEG spectral power abnormalities and their relationship with cognitive dysfunction in patients with Alzheimer's disease and type 2 diabetes. Neurobiology of Aging 85, 83–95.

Berger, H., 1929. Über das Elektrenkephalogramm des Menschen. Archiv für Psychiatrie und Nervenkrankheiten 87 (1), 527–570.

Bialek, W., Nemenman, I., and Tishby, N., 2001. Predictability, Complexity, and Learning. Neural Computation 13 (11), 2409–2463.

Bianchetti, A., Ranieri, P., Margiotta, A., and Trabucchi, M., 2006. Pharmacological treatment of Alzheimer's Disease. Aging Clinical and Experimental Research 18 (2), 158–162.

Bishop, C. M., 2007. Pattern Recognition and Machine Learning. Journal of Electronic Imaging 16 (4), 049901.

Biswal, B., Zerrin Yetkin, F., Haughton, V. M., and Hyde, J. S., 1995. Functional connectivity in the motor cortex of resting human brain using echo-planar MRI. Magnetic Resonance in Medicine 34 (4), 537–541.

Blanco, R., Koba, C., and Crimi, A., 2023. Resting State Brain Connectivity analysis from EEG and FNIRS signals. bioRxiv, 2023.04.11.536366.

Braak, E., Griffing, K., Arai, K., et al., 1999. Neuropathology of Alzheimer's disease: what is new since A. Alzheimer? European Archives of Psychiatry and Clinical Neurosciences 249 (S3), S14–S22.

Braak, H. and Braak, E., 1991. Neuropathological stageing of Alzheimer-related changes. Acta Neuropathologica 82 (4), 239–259.

Braak, H. and Braak, E., 1996. Development of Alzheimer-related neurofibrillary changes in the neocortex inversely recapitulates cortical myelogenesis. Acta Neuropathologica 92 (2), 197–201.

Bressler, S. L., 1995. Large-scale cortical networks and cognition. Brain Research Reviews 20 (3), 288–304.

Brier, M. R., Thomas, J. B., Snyder, A. Z., et al., 2012. Loss of Intranetwork and Internetwork Resting State Functional Connections with Alzheimer's Disease Progression. Journal of Neuroscience 32 (26), 8890–8899.

Brookes, M. J., Tewarie, P. K., Hunt, B. A., et al., 2016. A multi-layer network approach to MEG connectivity analysis. NeuroImage 132, 425–438.

Bullmore, E. and Sporns, O., 2009. Complex brain networks: graph theoretical analysis of structural and functional systems. Nature Reviews Neuroscience 10 (3), 186–198.

Cacace, R., Sleegers, K., and Van Broeckhoven, C., 2016. Molecular genetics of early-onset Alzheimer's disease revisited. Alzheimer's & Dementia 12 (6), 733–748.

Cai, L., Wei, X., Liu, J., et al., 2020. Functional Integration and Segregation in Multiplex Brain Networks for Alzheimer's Disease. Frontiers in Neuroscience 14, 51.

Calafate, S., Buist, A., Miskiewicz, K., et al., 2015. Synaptic Contacts Enhance Cell-to-Cell Tau Pathology Propagation. Cell Reports 11 (8), 1176–1183.

Canuet, L., Pusil, S., Lopez, M. E., et al., 2015. Network Disruption and Cerebrospinal Fluid Amyloid-Beta and Phospho-Tau Levels in Mild Cognitive Impairment. Journal of Neuroscience 35 (28), 10325–10330.

Cao, Y., Cai, L., Wang, J., et al., 2015. Characterization of complexity in the electroencephalograph activity of Alzheimer's disease based on fuzzy entropy. Chaos: An Interdisciplinary Journal of Nonlinear Science 25 (8), 083116.

Carr, D., Goate, A., Phil, D., and Morris, J., 1997. Current Concepts in the Pathogenesis of Alzheimer's Disease. The American Journal of Medicine 103 (3), 3S–10S.

Carrillo-Mora, P., Luna, R., and Colín-Barenque, L., 2014. Amyloid Beta: Multiple Mechanisms of Toxicity and Only Some Protective Effects? Oxidative Medicine and Cellular Longevity 2014, 1–15.

Cash, R. F. H., Noda, Y., Zomorrodi, R., et al., 2017. Characterization of Glutamatergic and GABAA-Mediated Neurotransmission in Motor and Dorsolateral Prefrontal Cortex Using Paired-Pulse TMS–EEG. Neuropsychopharmacology 42 (2), 502–511.

Cassani, R., Estarellas, M., San-Martin, R., et al., 2018. Systematic Review on Resting-State EEG for Alzheimer's Disease Diagnosis and Progression Assessment. Disease Markers 2018, 1–26.

CenterWatch, 2023. FDA approved drugs. `https://www.centerwatch.com/directories/1067-fda-approved-drugs/topic/137-alzheimer-s-disease`, accessed: 2023-06-20.

Chakraborty, S., Lennon, J. C., Malkaram, S. A., et al., 2019. Serotonergic system, cognition, and BPSD in Alzheimer's disease. Neuroscience Letters 704, 36–44.

Chang, W.-T., Jääskeläinen, I. P., Belliveau, J. W., et al., 2015. Combined MEG and EEG show reliable patterns of electromagnetic brain activity during natural viewing. NeuroImage 114, 49–56.

Chatrian, G. E., Lettich, E., and Nelson, P. L., 1985. Ten Percent Electrode System for Topographic Studies of Spontaneous and Evoked EEG Activities. American Journal of EEG Technology 25 (2), 83–92.

Cheng, I. H., Scearce-Levie, K., Legleiter, J., et al., 2007. Accelerating Amyloid-β Fibrillization Reduces Oligomer Levels and Functional Deficits in Alzheimer Disease Mouse Models. Journal of Biological Chemistry 282 (33), 23818–23828.

Chi, H., Sang, T.-K., and Chang, H.-Y., 2019. Tauopathy. In: Cognitive Disorders. IntechOpen.

Chua, K. C., Chandran, V., Acharya, U. R., and Lim, C. M., 2010. Application of higher order statistics/spectra in biomedical signals—A review. Medical Engineering & Physics 32 (7), 679–689.

Coben, L. A., Danziger, W. L., and Berg, L., 1983. Frequency analysis of the resting awake EEG in mild senile dementia of Alzheimer type. Electroencephalography and Clinical Neurophysiology 55 (4), 372–380.

Coben, L. A., Danziger, W., and Storandt, M., 1985. A longitudinal EEG study of mild senile dementia of Alzheimer type: changes at 1 year and at 2.5 years. Electroencephalography and Clinical Neurophysiology 61 (2), 101–112.

Cohen, M., Hudson, D., and Deedwania, P., 1996. Applying continuous chaotic modeling to cardiac signal analysis. IEEE Engineering in Medicine and Biology Magazine 15 (5), 97–102.

Cohen, M. X., Axmacher, N., Lenartz, D., et al., 2009. Good Vibrations: Cross-frequency Coupling in the Human Nucleus Accumbens during Reward Processing. Journal of Cognitive Neuroscience 21 (5), 875–889.

Cohen, M. X., 2014. Analyzing Neural Time Series Data. The MIT Press.

Cooper, N. R., Burgess, A. P., Croft, R. J., and Gruzelier, J. H., 2006. Investigating evoked and induced electroencephalogram activity in task-related alpha power increases during an internally directed attention task. NeuroReport 17 (2), 205–208.

Cordovado, S., Hendrix, M., Greene, C., et al., 2012. CFTR mutation analysis and haplotype associations in CF patients. Molecular Genetics and Metabolism 105 (2), 249–254.

Coronel, C., Garn, H., Waser, M., et al., 2017. Quantitative EEG Markers of Entropy and Auto Mutual Information in Relation to MMSE Scores of Probable Alzheimer's Disease Patients. Entropy 19 (3), 130.

Costa, M., Goldberger, A. L., and Peng, C.-K., 2002. Multiscale Entropy Analysis of Complex Physiologic Time Series. Physical Review Letters 89 (6), 068102.

Costa, M., Goldberger, A. L., and Peng, C.-K., 2005. Multiscale entropy analysis of biological signals. Physical Review E 71 (2), 021906.

Creel, D. J., 2019. Visually evoked potentials. In: Handbook of Clinical Neurology. 160. Elsevier, pp. 501–522.

Das, M., Maeda, S., Hu, B., et al., 2018. Neuronal levels and sequence of tau modulate the power of brain rhythms. Neurobiology of Disease 117, 181–188.

Dauwels, J., Vialatte, F., and Cichocki, A., 2010. Diagnosis of Alzheimers Disease from EEG Signals: Where Are We Standing? Current Alzheimer Research 7 (6), 487–505.

de Haan, W., Mott, K., van Straaten, E. C. W., et al., 2012. Activity Dependent Degeneration Explains Hub Vulnerability in Alzheimer's Disease. PLOS Computational Biology 8 (8), e1002582.

Dean, D. C., Hurley, S. A., Kecskemeti, S. R., et al., 2017. Association of Amyloid Pathology With Myelin Alteration in Preclinical Alzheimer Disease. JAMA Neurology 74 (1), 41.

Deco, G., Jirsa, V. K., and McIntosh, A. R., 2013. Resting brains never rest: computational insights into potential cognitive architectures. Trends in Neurosciences 36 (5), 268–274.

Delorme, A. and Makeig, S., 2004. EEGLAB: an open source toolbox for analysis of single-trial EEG dynamics including independent component analysis. Journal of Neuroscience Methods 134 (1), 9–21.

DeMattos, R. B., O'dell, M. A., Parsadanian, M., et al., 2002. Clusterin promotes amyloid plaque formation and is critical for neuritic toxicity in a mouse model of Alzheimer's disease. Proceedings of the National Academy of Sciences 99 (16), 10843–10848.

Desikan, R. S., Ségonne, F., Fischl, B., et al., 2006. An automated labeling system for subdividing the human cerebral cortex on MRI scans into gyral based regions of interest. NeuroImage 31 (3), 968–980.

Dickerson, B. C., Salat, D. H., Greve, D. N., et al., 2005. Increased hippocampal activation in mild cognitive impairment compared to normal aging and AD. Neurology 65 (3), 404–411.

Dien, J., 2010. Evaluating two-step pca of erp data with geomin, infomax, oblimin, promax, and varimax rotations. Psychophysiology 47, 170–183.

Dominguez, L. G., 2009. On the risk of extracting relevant information from random data. Journal of Neural Engineering 6 (5), 058001.

Douw, L., Nieboer, D., Stam, C. J., et al., 2018. Consistency of magnetoencephalographic functional connectivity and network reconstruction using a template versus native MRI for co-registration. Human Brain Mapping 39, 104–119.

Drubin, D. G. and Kirschner, M. W., 1986. Tau protein function in living cells. The Journal of Cell Biology 103 (6), 2739–2746.

Dujardin, S., Bégard, S., Caillierez, R., et al., 2018. Different tau species lead to heterogeneous tau pathology propagation and misfolding. Acta neuropathologica communications 6 (1), 132.

Eberhart, R., 1989. Chaos theory for the biomedical engineer. IEEE Engineering in Medicine and Biology Magazine 8 (3), 41–45.

Elgendi, M., Vialatte, F., Cichocki, A., et al., 2011. Optimization of EEG frequency bands for improved diagnosis of Alzheimer disease. In: 2011 Annual International Conference of the IEEE Engineering in Medicine and Biology Society. IEEE, pp. 6087–6091.

Engel, A. K. and Fries, P., 2010. Beta-band oscillations - signalling the status quo? Current Opinion in Neurobiology 20 (2), 156–165.

Engels, M., van der Flier, W., Stam, C., et al., 2017. Alzheimer's disease: The state of the art in resting-state magnetoencephalography. Clinical Neurophysiology 128 (8), 1426–1437.

Engels, M. M., Yu, M., Arjan, H., et al., 2016. P4-179: MEG Cross-Frequency Analysis in Patients With Alzheimer's Disease. Alzheimer's & Dementia 12 (7), P1087–P1088.

English, B. A., Hahn, M. K., Gizer, I. R., et al., 2009. Choline transporter gene variation is associated with attention-deficit hyperactivity disorder. Journal of Neurodevelopmental Disorders 1 (4), 252–263.

Escudero, J., Abásolo, D., Hornero, R., et al., 2006. Analysis of electroencephalograms in Alzheimer's disease patients with multiscale entropy. Physiological Measurement 27 (11), 1091–1106.

Fadason, T., Farrow, S., Gokuladhas, S., et al., 2022. Assigning function to SNPs: Considerations when interpreting genetic variation. Seminars in Cell & Developmental Biology 121, 135–142.

Farias, G., Cornejo, A., Jimenez, J., et al., 2011. Mechanisms of Tau Self-Aggregation and Neurotoxicity. Current Alzheimer Research 8 (6), 608–614.

Farrer, L. A., 1997. Effects of Age, Sex, and Ethnicity on the Association Between Apolipoprotein E Genotype and Alzheimer Disease. JAMA 278 (16), 1349.

Fath, T., Eidenmüller, J., and Brandt, R., 2002. Tau-Mediated Cytotoxicity in a Pseudohyperphosphorylation Model of Alzheimer's Disease. The Journal of Neuroscience 22 (22), 9733–9741.

Ferrari, R., Moreno, J. H., Minhajuddin, A. T., et al., 2012. Implication of common and disease specific variants in CLU, CR1, and PICALM. Neurobiology of Aging 33, 1846.e7–1846.e18.

Ferreira-Vieira, T. H., Guimaraes, I. M., Silva, F. R., and Ribeiro, M. F., 2016. Alzheimer's disease: Targeting the Cholinergic System. Current Neuropharmacology 14 (1), 101–115.

Folstein, M. F., Folstein, S. E., and McHugh, P. R., 1975. "Mini-mental state": a practical method for grading the cognitive state of patients for the clinician. Journal of Psychiatric Research 12 (3), 189–198.

Fraga, F. J., Falk, T. H., Kanda, P. A., and Anghinah, R., 2013. Characterizing Alzheimer's Disease Severity via Resting-Awake EEG Amplitude Modulation Analysis. Plos One 8 (8), e72240.

Fraser, A. M. and Swinney, H. L., 1986. Independent coordinates for strange attractors from mutual information. Physical Review A 33 (2), 1134–1140.

Freedman, D. and Diaconis, P., 1981. On the histogram as a density estimator: L2 theory. Zeitschrift für Wahrscheinlichkeitstheorie und Verwandte Gebiete 57 (4), 453–476.

García-Pretelt, F. J., Suárez-Relevo, J. X., Aguillon-Niño, D. F., et al., 2022. Automatic Classification of Subjects of the PSEN1-E280A Family at Risk of Developing Alzheimer's Disease Using Machine Learning and Resting State Electroencephalography. Journal of Alzheimer's Disease 87 (2), 817–832.

Gaubert, S., Raimondo, F., Houot, M., et al., 2019. EEG evidence of compensatory mechanisms in preclinical Alzheimer's disease. Brain 142 (7), 2096–2112.

Gauthier, S., Rosa-Neto, P., Morais, J., and Webster, C., 2021. World alzheimer report 2021: Journey through the diagnosis of dementia. Alzheimer's Disease International.

Ghaderi, A. H., Moradkhani, S., Haghighatfard, A., et al., 2018. Time estimation and beta segregation: An EEG study and graph theoretical approach. Plos One 13 (4), e0195380.

Glenner, G. G. and Wong, C. W., 1984. Alzheimer's disease and Down's syndrome: Sharing of a unique cerebrovascular amyloid fibril protein. Biochemical and Biophysical Research Communications 122 (3), 1131–1135.

Goedert, M., Spillantini, M., Jakes, R., et al., 1989. Multiple isoforms of human microtubule-associated protein tau: sequences and localization in neurofibrillary tangles of Alzheimer's disease. Neuron 3 (4), 519–526.

Grassberger, P., 1991. Information and Complexity Measures in Dynamical Systems. Springer US, Boston, MA.

Guillon, J., Attal, Y., Colliot, O., et al., 2017. Loss of brain inter-frequency hubs in Alzheimer's disease. Scientific Reports 7 (1), 10879.

Gutiérrez-de Pablo, V., Gómez, C., Poza, J., et al., 2020. Relationship between the Presence of the ApoE $\epsilon 4$ Allele and EEG Complexity along the Alzheimer's Disease Continuum. Sensors 20 (14), 3849.

Haass, C. and Selkoe, D. J., 2007. Soluble protein oligomers in neurodegeneration: lessons from the Alzheimer's amyloid β-peptide. Nature Reviews Molecular Cell Biology 8 (2), 101–112.

Hallinan, G. I., Vargas-Caballero, M., West, J., and Deinhardt, K., 2019. Tau Misfolding Efficiently Propagates between Individual Intact Hippocampal Neurons. The Journal of Neuroscience 39 (48), 9623–9632.

Hardy, J. A. and Higgins, G. A., 1992. Alzheimer's Disease: The Amyloid Cascade Hypothesis. Science 256 (5054), 184–185.

Harold, D., Abraham, R., Hollingworth, P., et al., 2009. Genome-wide association study identifies variants at CLU and PICALM associated with Alzheimer's disease. Nature Genetics 41 (10), 1088–1093.

Hasegawa, M., Smith, M. J., and Goedert, M., 1998. Tau proteins with FTDP-17 mutations have a reduced ability to promote microtubule assembly. FEBS Letters 437 (3), 207–210.

Hillebrand, A., Barnes, G. R., Bosboom, J. L., et al., 2012. Frequency-dependent functional connectivity within resting-state networks: An atlas-based MEG beamformer solution. NeuroImage 59 (4), 3909–3921.

Horvath, A., 2018. EEG and ERP biomarkers of Alzheimer's disease: a critical review. Frontiers in Bioscience 23 (1), 4587.

Hsu, C.-C., Cheng, C.-W., and Chiu, Y.-S., 2017. Analyze the beta waves of electroencephalogram signals from young musicians and non-musicians in major scale working memory task. Neuroscience Letters 640, 42–46.

Hughes, C. P., Berg, L., Danziger, W., et al., 1982. A New Clinical Scale for the Staging of Dementia. British Journal of Psychiatry 140 (6), 566–572.

Humeau-Heurtier, A., Wu, C.-W., Wu, S.-D., et al., 2016. Refined Multiscale Hilbert–Huang Spectral Entropy and Its Application to Central and Peripheral Cardiovascular Data. IEEE Transactions on Biomedical Engineering 63 (11), 2405–2415.

Hyman, B., 2023. All the Tau We Cannot See. Annual Review of Medicine 74 (1), 503–514.

Ibáñez-Molina, A. J., Iglesias-Parro, S., Soriano, M. F., and Aznarte, J. I., 2015. Multiscale Lempel–Ziv complexity for EEG measures. Clinical Neurophysiology 126 (3), 541–548.

Ieracitano, C., Mammone, N., Hussain, A., and Morabito, F. C., 2020. A novel multi-modal machine learning based approach for automatic classification of EEG recordings in dementia. Neural Networks 123, 176–190.

Im, C.-H., 2018. Computational EEG Analysis. Biological and Medical Physics, Biomedical Engineering. Springer Singapore, Singapore.

Itoh, A., Nitta, A., Nadai, M., et al., 2002. Dysfunction of Cholinergic and Dopaminergic Neuronal Systems in β-Amyloid Protein-Infused Rats. Journal of Neurochemistry 66 (3), 1113–1117.

Jack, C. R., Bennett, D. A., Blennow, K., et al., 2016. A/T/N: An unbiased descriptive classification scheme for Alzheimer disease biomarkers. Neurology 87 (5), 539–547.

Jack, C. R., Bennett, D. A., Blennow, K., et al., 2018. NIA-AA Research Framework: Toward a biological definition of Alzheimer's disease. Alzheimer's & Dementia 14 (4), 535–562.

Janelidze, S., Zetterberg, H., Mattsson, N., et al., 2016. CSF Aβ42/Aβ40 and Aβ42/Aβ38 ratios: better diagnostic markers of Alzheimer disease. Annals of Clinical and Translational Neurology 3 (3), 154–165.

Jelic, V., Johansson, S.-E., Almkvist, O., et al., 2000. Quantitative electroencephalography in mild cognitive impairment: longitudinal changes and possible prediction of Alzheimer's disease. Neurobiology of Aging 21 (4), 533–540.

Jelles, B., van Birgelen, J., Slaets, J., et al., 1999. Decrease of non-linear structure in the EEG of Alzheimer patients compared to healthy controls. Clinical Neurophysiology 110 (7), 1159–1167.

Jeong, J., Gore, J. C., and Peterson, B. S., 2001a. Mutual information analysis of the EEG in patients with Alzheimer's disease. Clinical Neurophysiology 112 (5), 827–835.

Jeong, J., Chae, J., Kim, S. Y., and Han, S., 2001b. Nonlinear Dynamic Analysis of the EEG in Patients with Alzheimer's Disease and Vascular Dementia. Journal of Clinical Neurophysiology 18 (1), 58–67.

Jeong, J., 2004. EEG dynamics in patients with Alzheimer's disease. Clinical Neurophysiology 115 (7), 1490–1505.

Jones, S., 2002. Clusterin. The International Journal of Biochemistry & Cell Biology 34 (5), 427–431.

Jutten, C. and Karhunen, J., 2004. Advances in blind source separation (bss) and independent component analysis (ica) for nonlinear mixtures. International Journal of Neural Systems 14, 267–292.

Kandimalla, R. and Reddy, P. H., 2017. Therapeutics of Neurotransmitters in Alzheimer's Disease. Journal of Alzheimer's Disease 57 (4), 1049–1069.

Kauwe, J. S. K., Cruchaga, C., Mayo, K., et al., 2008. Variation in MAPT is associated with cerebrospinal fluid tau levels in the presence of amyloid-beta deposition. Proceedings of the National Academy of Sciences 105 (23), 8050–8054.

Kernbach, J. M., Yeo, B. T. T., Smallwood, J., et al., 2018. Subspecialization within default mode nodes characterized in 10,000 UK Biobank participants. Proceedings of the National Academy of Sciences 115 (48), 12295–12300.

Khanna, A., Pascual-Leone, A., Michel, C. M., and Farzan, F., 2015. Microstates in resting-state EEG: Current status and future directions. Neuroscience & Biobehavioral Reviews 49, 105–113.

Kikuchi, M., Wada, Y., Koshino, Y., et al., 2000. Effects of Scopolamine on Interhemispheric EEG Coherence in Healthy Subjects: Analysis during Rest and Photic Stimulation. Clinical Electroencephalography 31 (2), 109–115.

Kimura, N. and Yanagisawa, K., 2018. Traffic jam hypothesis: Relationship between endocytic dysfunction and Alzheimer's disease. Neurochemistry International 119, 35–41.

Kinsley, A. C., Rossi, G., Silk, M. J., and VanderWaal, K., 2020. Multilayer and Multiplex Networks: An Introduction to Their Use in Veterinary Epidemiology. Frontiers in Veterinary Science 7, 596.

Kirkitadze, M. D., Bitan, G., and Teplow, D. B., 2002. Paradigm shifts in Alzheimer's disease and other neurodegenerative disorders: The emerging role of oligomeric assemblies. Journal of Neuroscience Research 69 (5), 567–577.

Kisilevsky, R., 2000. Review: Amyloidogenesis—Unquestioned Answers and Unanswered Questions. Journal of Structural Biology 130 (2-3), 99–108.

Kissin, I., 2000. Depth of Anesthesia and Bispectral Index Monitoring. Anesthesia & Analgesia 90 (5), 1114–1117.

Kivela, M., Arenas, A., Barthelemy, M., et al., 2014. Multilayer networks. Journal of Complex Networks 2 (3), 203–271.

Klein, W., Stine, W., and Teplow, D., 2004. Small assemblies of unmodified amyloid β-protein are the proximate neurotoxin in Alzheimer's disease. Neurobiology of Aging 25 (5), 569–580.

Klepl, D., He, F., Wu, M., et al., 2023. Cross-Frequency Multilayer Network Analysis with Bispectrum-based Functional Connectivity: A Study of Alzheimer's Disease. Neuroscience 521, 77–88.

Klimesch, W., 2012. Alpha-band oscillations, attention, and controlled access to stored information. Trends in Cognitive Sciences 16 (12), 606–617.

Knyazev, G. G., 2007. Motivation, emotion, and their inhibitory control mirrored in brain oscillations. Neuroscience & Biobehavioral Reviews 31 (3), 377–395.

Kolmogorov, A. N., 1968. Three approaches to the quantitative definition of information. International Journal of Computer Mathematics 2 (1-4), 157–168.

Koltai, T., 2014. Clusterin: a key player in cancer chemoresistance and its inhibition. OncoTargets and Therapy 7, 447.

Kosko, B., 1986. Fuzzy entropy and conditioning. Information Sciences 40 (2), 165–174.

Labate, D., Foresta, F. L., Morabito, G., et al., 2013. Entropic Measures of EEG Complexity in Alzheimer's Disease Through a Multivariate Multiscale Approach. IEEE Sensors Journal 13 (9), 3284–3292.

Lacasa, L. and Toral, R., 2010. Description of stochastic and chaotic series using visibility graphs. Physical Review E 82 (3), 036120.

Lalo, E., Gilbertson, T., Doyle, L., et al., 2007. Phasic increases in cortical beta activity are associated with alterations in sensory processing in the human. Experimental Brain Research 177 (1), 137–145.

Lambert, J.-C., Heath, S., Even, G., et al., 2009. Genome-wide association study identifies variants at CLU and CR1 associated with Alzheimer's disease. Nature Genetics 41 (10), 1094–1099.

Lambert, J.-C., Ibrahim-Verbaas, C. A., Harold, D., et al., 2013. Meta-analysis of 74,046 individuals identifies 11 new susceptibility loci for Alzheimer's disease. Nature Genetics 45 (12), 1452–1458.

Lau, Z. J., Pham, T., Chen, S. H. A., and Makowski, D., 2022. Brain entropy, fractal dimensions and predictability: A review of complexity measures for EEG in healthy and neuropsychiatric populations. European Journal of Neuroscience 56 (7), 5047–5069.

Li, G., Pan, T., Guo, D., and Li, L.-C., 2014. Regulatory Variants and Disease: The E-Cadherin -160C/A SNP as an Example. Molecular Biology International 2014, 1–9.

Li, M. and Vitányi, P., 2008. An Introduction to Kolmogorov Complexity and Its Applications. Texts in Computer Science. Springer New York, New York, NY.

Li, X., Zhu, Z., Zhao, W., et al., 2018. Decreased resting-state brain signal complexity in patients with mild cognitive impairment and Alzheimer's disease: a multi-scale entropy analysis. Biomedical Optics Express 9 (4), 1916.

Long, J. M. and Holtzman, D. M., 2019. Alzheimer Disease: An Update on Pathobiology and Treatment Strategies. Cell 179 (2), 312–339.

Lucka, F., Pursiainen, S., Burger, M., and Wolters, C. H., 2012. Hierarchical bayesian inference for the eeg inverse problem using realistic fe head models: Depth localization and source separation for focal primary currents. NeuroImage 61, 1364–1382.

Macedo, A., Gómez, C., Rebelo, M. Â., et al., 2021. Risk Variants in Three Alzheimer's Disease Genes Show Association with EEG Endophenotypes. Journal of Alzheimer's Disease 80 (1), 209–223.

Machiela, M. J. and Chanock, S. J., 2015. LDlink: a web-based application for exploring population-specific haplotype structure and linking correlated alleles of possible functional variants. Bioinformatics 31 (21), 3555–3557.

Maestú, F., Cuesta, P., Hasan, O., et al., 2019. The Importance of the Validation of M/EEG With Current Biomarkers in Alzheimer's Disease. Frontiers in Human Neuroscience 13, 17.

Makeig, S., Jung, T.-P., Bell, A. J., et al., 1997. Blind separation of auditory event-related brain responses into independent components. Proceedings of the National Academy of Sciences 94 (20), 10979–10984.

Makowka, S., Mory, L.-N., Mouthon, M., et al., 2023. EEG Beta functional connectivity decrease in the left amygdala correlates with the affective pain in fibromyalgia: A pilot study. Plos One 18 (2), e0281986.

Marucci, G., Buccioni, M., Ben, D. D., et al., 2021. Efficacy of acetylcholinesterase inhibitors in Alzheimer's disease. Neuropharmacology 190, 108352.

Massoud, F. and Léger, G. C., 2011. Pharmacological Treatment of Alzheimer Disease. The Canadian Journal of Psychiatry 56 (10), 579–588.

Mathur, R., Rana, B. S., and Jha, A. K., 2018. Single Nucleotide Polymorphism (SNP). In: Encyclopedia of Animal Cognition and Behavior. Springer International Publishing, Cham, pp. 1–4.

Maturana-Candelas, A., Gómez, C., Poza, J., et al., 2019. EEG Characterization of the Alzheimer's Disease Continuum by Means of Multiscale Entropies. Entropy 21 (6), 544.

Maturana-Candelas, A., Gómez, C., Poza, J., et al., 2020. Inter-band Bispectral Analysis of EEG Background Activity to Characterize Alzheimer's Disease Continuum. Frontiers in Computational Neuroscience 14, 70.

Maturana-Candelas, A., Gómez, C., Poza, J., et al., 2021. Influence of PICALM and CLU risk variants on beta EEG activity in Alzheimer's disease patients. Scientific Reports 11 (1), 20465.

Maturana-Candelas, A., Hornero, R., Poza, J., et al., 2024. Effect of MAPT gene variations on the brain electrical activity: a multiplex network study (UNDER REVIEW). Computer Methods and Programs in Biomedicine.

Mcintosh, A. R., Kovacevic, N., Lippe, S., et al., 2010. The Development of a Noisy Brain. Archives Italiennes de Biologie 148 (3), 323–337.

Mesulam, M., Shaw, P., Mash, D., and Weintraub, S., 2004. Cholinergic nucleus basalis tauopathy emerges early in the aging-MCI-AD continuum. Annals of Neurology 55 (6), 815–828.

Miljevic, A., Bailey, N. W., Vila-Rodriguez, F., et al., 2022. Electroencephalographic Connectivity: A Fundamental Guide and Checklist for Optimal Study Design and Evaluation. Biological Psychiatry: Cognitive Neuroscience and Neuroimaging 7 (6), 546–554.

Mitternacht, S., Staneva, I., Härd, T., and Irbäck, A., 2010. Comparing the folding free-energy landscapes of Aβ42 variants with different aggregation properties. Proteins: Structure, Function, and Bioinformatics 78 (12), 2600–2608.

Mizuno, T., Takahashi, T., Cho, R. Y., et al., 2010. Assessment of EEG dynamical complexity in Alzheimer's disease using multiscale entropy. Clinical Neurophysiology 121 (9), 1438–1446.

Moretti, D., Paternicò, D., Binetti, G., et al., 2014. Electroencephalographic Upper/Low Alpha Frequency Power Ratio Relates to Cortex Thinning in Mild Cognitive Impairment. Neurodegenerative Diseases 14 (1), 18–30.

Mudher, A., Colin, M., Dujardin, S., et al., 2017. What is the evidence that tau pathology spreads through prion-like propagation? Acta Neuropathologica Communications 5 (1), 99.

Nasrolahzadeh, M., Mohammadpoory, Z., and Haddadnia, J., 2018. Higher-order spectral analysis of spontaneous speech signals in Alzheimer's disease. Cognitive Neurodynamics 12 (6), 583–596.

Natal, J., Ávila, I., Tsukahara, V. B., et al., 2021. Entropy: From thermodynamics to information processing. Entropy 23, 1340.

National Institute of Aging, 2023. How is Alzheimer's disease treated? `https://www.nia.nih.gov/health/how-alzheimers-disease-treated`, accessed: 2023-06-20.

Newson, J. J. and Thiagarajan, T. C., 2019. EEG Frequency Bands in Psychiatric Disorders: A Review of Resting State Studies. Frontiers in Human Neuroscience 12, 521.

Nicholls, M. M. and Whelan, R. R., 1998. Hemispheric Asymmetries for the Temporal Resolution of Brief Tactile Stimuli. Journal of Clinical and Experimental Neuropsychology 20 (4), 445–456.

Nikias, C. and Mendel, J., 1993. Signal processing with higher-order spectra. IEEE Signal Processing Magazine 10 (3), 10–37.

Nixon, R. A., 2013. The role of autophagy in neurodegenerative disease. Nature Medicine 19 (8), 983–997.

Nunez, P. L. and Srinivasan, R., 2006. Electric Fields of the Brain. Oxford University Press.

O'Neill, G. C., Barratt, E. L., Hunt, B. A. E., et al., 2015. Measuring electrophysiological connectivity by power envelope correlation: a technical review on MEG methods. Physics in Medicine and Biology 60 (21), R271–R295.

Palva, J. M., Palva, S., and Kaila, K., 2005. Phase Synchrony among Neuronal Oscillations in the Human Cortex. The Journal of Neuroscience 25 (15), 3962–3972.

Palva, S. and Palva, J. M., 2007. New vistas for α-frequency band oscillations. Trends in Neurosciences 30 (4), 150–158.

Palva, S. and Palva, J. M., 2012. Discovering oscillatory interaction networks with M/EEG: challenges and breakthroughs. Trends in Cognitive Sciences 16 (4), 219–230.

Pan, X., Kaminga, A. C., Wen, S. W., et al., 2019. Dopamine and Dopamine Receptors in Alzheimer's Disease: A Systematic Review and Network Meta-Analysis. Frontiers in Aging Neuroscience 11, 175.

Park, H.-J. and Friston, K., 2013. Structural and functional brain networks: From connections to cognition. Science 342.

Pascual-Marqui, R. D., 2002. Standardized low-resolution brain electromagnetic tomography (sLORETA): technical details. Methods and findings in experimental and clinical pharmacology 24 Suppl D, 5–12.

Paulraj, M. P., Subramaniam, K., Yaccob, S. B., et al., 2015. Auditory Evoked Potential Response and Hearing Loss: A Review. The Open Biomedical Engineering Journal 9 (1), 17–24.

Petersen, R. C., 2004. Mild cognitive impairment as a diagnostic entity. Journal of Internal Medicine 256 (3), 183–194.

Pincus, S., 1995. Approximate entropy (ApEn) as a complexity measure. Chaos: An Interdisciplinary Journal of Nonlinear Science 5 (1), 110–117.

Pini, L., Salvalaggio, A., De Filippo De Grazia, M., et al., 2021. A novel stroke lesion network mapping approach: improved accuracy yet still low deficit prediction. Brain Communications 3 (4).

Ponomareva, N., Andreeva, T., Protasova, M., et al., 2013. Age-dependent effect of Alzheimer's risk variant of CLU on EEG alpha rhythm in non-demented adults. Frontiers in Aging Neuroscience 5, 86.

Ponomareva, N., Andreeva, T., Protasova, M., et al., 2020. Genetic Association Between Alzheimer's Disease Risk Variant of the PICALM Gene and EEG Functional Connectivity in Non-demented Adults. Frontiers in Neuroscience 14, 324.

Ponomareva, N. V., Andreeva, T. V., Protasova, M. S., et al., 2017. Quantitative EEG during normal aging: association with the Alzheimer's disease genetic risk variant in PICALM gene. Neurobiology of Aging 51, 177.

Ponomareva, N. V., Andreeva, T. V., Protasova, M. S., et al., 2023. Neuronal Hyperactivation in EEG Data during Cognitive Tasks Is Related to the Apolipoprotein J/Clusterin Genotype in Nondemented Adults. International Journal of Molecular Sciences 24 (7), 6790.

Porjesz, B., Almasy, L., Edenberg, H. J., et al., 2002. Linkage disequilibrium between the beta frequency of the human EEG and a GABA A receptor gene locus. Proceedings of the National Academy of Sciences 99 (6), 3729–3733.

Powell, G. E. and Percival, I. C., 1979. A spectral entropy method for distinguishing regular and irregular motion of Hamiltonian systems. Journal of Physics A: Mathematical and General 12 (11), 2053–2071.

Poza, J., Hornero, R., Abásolo, D., et al., 2007. Extraction of spectral based measures from meg background oscillations in alzheimer's disease. Medical Engineering & Physics 29, 1073–1083.

Prichep, L., John, E., Ferris, S., et al., 1994. Quantitative EEG correlates of cognitive deterioration in the elderly. Neurobiology of Aging 15 (1), 85–90.

Prinz, P. N. and Vitiell, M. V., 1989. Dominant occipital (alpha) rhythm frequency in early stage Alzheimer's disease and depression. Electroencephalography and Clinical Neurophysiology 73 (5), 427–432.

Pritchard, W. S. and Duke, D. W., 1992. Measuring Chaos in the Brain: A Tutorial Review of Nonlinear Dynamical EEG Analysis. International Journal of Neuroscience 67 (1-4), 31–80.

Purcell, S., Neale, B., Todd-Brown, K., et al., 2007. PLINK: A Tool Set for Whole-Genome Association and Population-Based Linkage Analyses. The American Journal of Human Genetics 81 (3), 559–575.

Putcha, D., Brickhouse, M., O'Keefe, K., et al., 2011. Hippocampal Hyperactivation Associated with Cortical Thinning in Alzheimer's Disease Signature Regions in Non-Demented Elderly Adults. The Journal of Neuroscience 31 (48), 17680–17688.

Putman, P., van Peer, J., Maimari, I., and van der Werff, S., 2010. EEG theta/beta ratio in relation to fear-modulated response-inhibition, attentional control, and affective traits. Biological Psychology 83 (2), 73–78.

Raichle, M. E., 2015. The Brain's Default Mode Network. Annual Review of Neuroscience 38 (1), 433–447.

Rampil, I. J., 1998. A Primer for EEG Signal Processing in Anesthesia. Anesthesiology 89 (4), 980–1002.

Rangaswamy, M., Porjesz, B., Chorlian, D. B., et al., 2002. Beta power in the EEG of alcoholics. Biological Psychiatry 52 (8), 831–842.

Reisberg, B., 1986. Dementia: a systematic approach to identifying reversible causes. Geriatrics 41 (4), 30–46.

Renna, M., Handy, J., and Shah, A., 2003. Low Baseline Bispectral Index of the Electroencephalogram in Patients with Dementia. Anesthesia & Analgesia 96 (5), 1380–1385.

Richman, J. S. and Moorman, J. R., 2000. Physiological time-series analysis using approximate entropy and sample entropy. American Journal of Physiology-Heart and Circulatory Physiology 278 (6), H2039–H2049.

Riddle, J., Alexander, M. L., Schiller, C. E., et al., 2022. Reward-based decision-making engages distinct modes of cross-frequency coupling. Cerebral cortex (New York, N.Y. : 1991) 32, 2079–2094.

Roach, B. J. and Mathalon, D. H., 2008. Event-Related EEG Time-Frequency Analysis: An Overview of Measures and An Analysis of Early Gamma Band Phase Locking in Schizophrenia. Schizophrenia Bulletin 34 (5), 907–926.

Robbie, J. C., Clarke, A. R., Barry, R. J., et al., 2016. Coherence in children with AD/HD and excess alpha power in their EEG. Clinical Neurophysiology 127 (5), 2161–2166.

Rosenblatt, M. and Ness, J. W. V., 1965. Estimation of the Bispectrum. The Annals of Mathematical Statistics 36 (4), 1120–1136.

Rubinov, M. and Sporns, O., 2010. Complex network measures of brain connectivity: Uses and interpretations. NeuroImage 52 (3), 1059–1069.

Rubinski, A., Franzmeier, N., Dewenter, A., et al., 2022. Higher levels of myelin are associated with higher resistance against tau pathology in Alzheimer's disease. Alzheimer's Research & Therapy 14 (1), 139.

Rudenko, L. K., Wallrabe, H., Periasamy, A., et al., 2019. Intraneuronal Tau Misfolding Induced by Extracellular Amyloid-β Oligomers. Journal of Alzheimer's Disease 71 (4), 1125–1138.

Ruiz-Gómez, S., Gómez, C., Poza, J., et al., 2018a. Automated Multiclass Classification of Spontaneous EEG Activity in Alzheimer's Disease and Mild Cognitive Impairment. Entropy 20 (1), 35.

Ruiz-Gómez, S. J., Gómez, C., Poza, J., et al., 2018b. Measuring Alterations of Spontaneous EEG Neural Coupling in Alzheimer's Disease and Mild Cognitive Impairment by Means of Cross-Entropy Metrics. Frontiers in neuroinformatics 12, 76.

Ruiz-Gómez, S. J., Hornero, R., Poza, J., et al., 2019. Computational modeling of the effects of EEG volume conduction on functional connectivity metrics. Application to Alzheimer's disease continuum. Journal of Neural Engineering 16 (6), 066019.

Ruiz-Gómez, S. J., Hornero, R., Poza, J., et al., 2021. A new method to build multiplex networks using canonical correlation analysis for the characterization of the Alzheimer's disease continuum. Journal of Neural Engineering 18 (2), 026002.

Saby, J. N. and Marshall, P. J., 2012. The Utility of EEG Band Power Analysis in the Study of Infancy and Early Childhood. Developmental Neuropsychology 37 (3), 253–273.

Schoenemann, P. T., 2006. Evolution of the Size and Functional Areas of the Human Brain. Annual Review of Anthropology 35 (1), 379–406.

Schoffelen, J.-M. and Gross, J., 2009. Source connectivity analysis with MEG and EEG. Human Brain Mapping 30 (6), 1857–1865.

Schomer, D. L. and Lopes da Silva, F. H., 2017. Niedermeyer's Electroencephalography: Basic Principles, Clinical Applications, and Related Fields. Oxford University Press.

Schrijvers, E. M. C., 2011. Plasma Clusterin and the Risk of Alzheimer Disease. JAMA 305 (13), 1322.

Schutter, D. J., Leitner, C., Kenemans, J. L., and Honk, J. V., 2006. Electrophysiological correlates of cortico-subcortical interaction: A cross-frequency spectral EEG analysis. Clinical Neurophysiology 117 (2), 381–387.

Seitzman, B. A., Snyder, A. Z., Leuthardt, E. C., and Shimony, J. S., 2019. The State of Resting State Networks. Topics in Magnetic Resonance Imaging 28 (4), 189–196.

Sergeant, N., Delacourte, A., and Buée, L., 2005. Tau protein as a differential biomarker of tauopathies. Biochimica et Biophysica Acta (BBA) - Molecular Basis of Disease 1739 (2-3), 179–197.

Shannon, C. E., 1948. A Mathematical Theory of Communication. Bell System Technical Journal 27 (3), 379–423.

Shaw-Taylor, L., 2020. An introduction to the history of infectious diseases, epidemics and the early phases of the long-run decline in mortality†. The Economic History Review 73 (3), E1–E19.

Shcherbatykh, I. and Carpenter, D. O., 2007. The Role of Metals in the Etiology of Alzheimer's Disease. Journal of Alzheimer's Disease 11 (2), 191–205.

Sherry, S. T., 2001. dbSNP: the NCBI database of genetic variation. Nucleic Acids Research 29 (1), 308–311.

Siegel, M., Donner, T. H., and Engel, A. K., 2012. Spectral fingerprints of large-scale neuronal interactions. Nature Reviews Neuroscience 13 (2), 121–134.

Simons, S., Abasolo, D., and Escudero, J., 2015. Classification of Alzheimer's disease from quadratic sample entropy of electroencephalogram. Healthcare Technology Letters 2 (3), 70–73.

Sloan, E. P., Fenton, G. W., and Standage, K. P., 1992. Anticholinergic drug effects on quantitative electroencephalogram, visual evoked potential, and verbal memory. Biological Psychiatry 31 (6), 600–606.

Smailovic, U., Koenig, T., Kåreholt, I., et al., 2018. Quantitative EEG power and synchronization correlate with Alzheimer's disease CSF biomarkers. Neurobiology of Aging 63, 88–95.

Smitha, K., Akhil Raja, K., Arun, K., et al., 2017. Resting state fMRI: A review on methods in resting state connectivity analysis and resting state networks. The Neuroradiology Journal 30 (4), 305–317.

Sochocka, M., Zwolińska, K., and Leszek, J., 2017. The Infectious Etiology of Alzheimer's Disease. Current Neuropharmacology 15 (7), 996–1009.

Son, J., Schantell, M., Taylor, B., et al., 2022. P428. Altered Trajectory of dMPFC Connectivity in Youth With Subclinical Anxiety and PTSD Symptoms. Biological Psychiatry 91 (9), S260–S261.

Spitzer, B. and Haegens, S., 2017. Beyond the Status Quo: A Role for Beta Oscillations in Endogenous Content (Re)Activation. eNeuro 4 (4), e0170.

Stam, C., Jones, B., Nolte, G., et al., 2006. Small-World Networks and Functional Connectivity in Alzheimer's Disease. Cerebral Cortex 17 (1), 92–99.

Stam, C. and van Straaten, E., 2012. The organization of physiological brain networks. Clinical Neurophysiology 123 (6), 1067–1087.

Stam, C. J., Van Der Made, Y., Pijnenburg, Y. A. L., and Scheltens, P., 2003. EEG synchronization in mild cognitive impairment and Alzheimer's disease. Acta Neurologica Scandinavica 108 (2), 90–96.

Stam, C. J., Montez, T., Jones, B. F., et al., 2005. Disturbed fluctuations of resting state EEG synchronization in Alzheimer's disease. Clinical neurophysiology : official journal of the International Federation of Clinical Neurophysiology 116 (3), 708–715.

Stam, C. J., Nolte, G., and Daffertshofer, A., 2007. Phase lag index: Assessment of functional connectivity from multi channel EEG and MEG with diminished bias from common sources. Human Brain Mapping 28 (11), 1178–1193.

Stam, C. J., 2014. Modern network science of neurological disorders. Nature Reviews Neuroscience 15 (10), 683–695.

Stewart, R., 2012. Subjective cognitive impairment. Current Opinion in Psychiatry 25 (6), 445–450.

Stomrud, E., Hansson, O., Minthon, L., et al., 2010. Slowing of EEG correlates with CSF biomarkers and reduced cognitive speed in elderly with normal cognition over 4 years. Neurobiology of Aging 31 (2), 215–223.

Strittmatter, W. J., Saunders, A. M., Schmechel, D., et al., 1993. Apolipoprotein E: high-avidity binding to beta-amyloid and increased frequency of type 4 allele in late-onset familial Alzheimer disease. Proceedings of the National Academy of Sciences 90 (5), 1977–1981.

Sun, J., Wang, B., Niu, Y., et al., 2020. Complexity Analysis of EEG, MEG, and fMRI in Mild Cognitive Impairment and Alzheimer's Disease: A Review. Entropy 22 (2), 239.

Tábuas-Pereira, M., Santana, I., Guerreiro, R., and Brás, J., 2020. Alzheimer's Disease Genetics: Review of Novel Loci Associated with Disease. Current Genetic Medicine Reports 8 (1), 1–16.

Tadel, F., Baillet, S., Mosher, J. C., et al., 2011. Brainstorm: A user-friendly application for MEG/EEG analysis. Computational Intelligence and Neuroscience 2011, 1–13.

Takashima, A., 2013. Tauopathies and Tau Oligomers. Journal of Alzheimer's Disease 37 (3), 565–568.

Tanzi, R. E., 2012. The Genetics of Alzheimer Disease. Cold Spring Harbor Perspectives in Medicine 2 (10), a006296–a006296.

Terwel, D., Dewachter, I., and Van Leuven, F., 2002. Axonal Transport, Tau Protein, and Neurodegeneration in Alzheimer's Disease. NeuroMolecular Medicine 2 (2), 151–166.

Tewarie, P., Hillebrand, A., van Dijk, B. W., et al., 2016. Integrating cross-frequency and within band functional networks in resting-state MEG: A multi-layer network approach. NeuroImage 142, 324–336.

Thambisetty, M., Simmons, A., Velayudhan, L., et al., 2010. Association of Plasma Clusterin Concentration With Severity, Pathology, and Progression in Alzheimer Disease. Archives of General Psychiatry 67 (7), 739.

Tononi, G., Edelman, G. M., and Sporns, O., 1998. Complexity and coherency: integrating information in the brain. Trends in Cognitive Sciences 2 (12), 474–484.

Trabace, L., Kendrick, K., Castrignanò, S., et al., 2007. Soluble amyloid beta1-42 reduces dopamine levels in rat prefrontal cortex: Relationship to nitric oxide. Neuroscience 147 (3), 652–663.

Tranel, D., Cooper, G., and Rodnitzky, R. L., 2003. Higher Brain Functions. In: Neuroscience in Medicine. Humana Press, Totowa, NJ, pp. 621–639.

Trougakos, I. P., So, A., Jansen, B., et al., 2004. Silencing Expression of the Clusterin/Apolipoprotein J Gene in Human Cancer Cells Using Small Interfering RNA Induces Spontaneous Apoptosis, Reduced Growth Ability, and Cell Sensitization to Genotoxic and Oxidative Stress. Cancer Research 64 (5), 1834–1842.

Uhlhaas, P. J., Haenschel, C., Nikolic, D., and Singer, W., 2008. The Role of Oscillations and Synchrony in Cortical Networks and Their Putative Relevance for the Pathophysiology of Schizophrenia. Schizophrenia Bulletin 34 (5), 927–943.

van der Hiele, K., Vein, A., Reijntjes, R., et al., 2007. EEG correlates in the spectrum of cognitive decline. Clinical Neurophysiology 118 (9), 1931–1939.

Vaquerizo-Villar, F., Álvarez, D., Kheirandish-Gozal, L., et al., 2018. Utility of bispectrum in the screening of pediatric sleep apnea-hypopnea syndrome using oximetry recordings. Computer Methods and Programs in Biomedicine 156, 141–149.

Varela, F., Lachaux, J.-P., Rodriguez, E., and Martinerie, J., 2001. The brainweb: Phase synchronization and large-scale integration. Nature Reviews Neuroscience 2 (4), 229–239.

Vaz-Drago, R., Custódio, N., and Carmo-Fonseca, M., 2017. Deep intronic mutations and human disease. Human Genetics 136 (9), 1093–1111.

Vecchio, F., Babiloni, C., Lizio, R., et al., 2013. Resting state cortical EEG rhythms in Alzheimer's disease. In: Supplements to Clinical Neurophysiology. 62. Elsevier, pp. 223–236.

Vinogradova, O., 1995. Expression, control, and probable functional significance of the neuronal theta-rhythm. Progress in Neurobiology 45 (6), 523–583.

von Stein, A. and Sarnthein, J., 2000. Different frequencies for different scales of cortical integration: from local gamma to long range alpha/theta synchronization. International Journal of Psychophysiology 38 (3), 301–313.

Wang, J., Barstein, J., Ethridge, L. E., et al., 2013. Resting state EEG abnormalities in autism spectrum disorders. Journal of Neurodevelopmental Disorders 5 (1), 24.

Wang, R., Wang, J., Li, S., et al., 2015. Multiple feature extraction and classification of electroencephalograph signal for Alzheimers' with spectrum and bispectrum. Chaos 25 (1), 013110.

Wang, X.-J., 2010. Neurophysiological and Computational Principles of Cortical Rhythms in Cognition. Physiological Reviews 90 (3), 1195–1268.

Watts, D. J. and Strogatz, S. H., 1998. Collective dynamics of 'small-world' networks. Nature 393 (6684), 440–442.

Wegmann, S., Maury, E. A., Kirk, M. J., et al., 2015. Removing endogenous tau does not prevent tau propagation yet reduces its neurotoxicity. The EMBO Journal 34 (24), 3028–3041.

Weng, W. C., Jiang, G. J., Chang, C. F., et al., 2015. Complexity of Multi-Channel Electroencephalogram Signal Analysis in Childhood Absence Epilepsy. Plos One 10 (8), e0134083.

Wolk, D. and Vaishnavi, S., 2016. Mild cognitive impairment and Alzheimer's disease. In: International Neurology. 12. John Wiley & Sons, Ltd, Chichester, UK, pp. 133–139.

Wróbel, A., 2000. Beta activity: a carrier for visual attention. Acta neurobiologiae experimentalis 60 (2), 247–60.

Xia, M., Wang, J., and He, Y., 2013. BrainNet Viewer: A Network Visualization Tool for Human Brain Connectomics. Plos One 8 (7), e68910.

Xu, W., Tan, L., and Yu, J.-T., 2015. The Role of PICALM in Alzheimer's Disease. Molecular Neurobiology 52 (1), 399–413.

Yang, A. C., Wang, S.-J., Lai, K.-L., et al., 2013. Cognitive and neuropsychiatric correlates of EEG dynamic complexity in patients with Alzheimer's disease. Progress in Neuro-Psychopharmacology and Biological Psychiatry 47, 52–61.

Yates, D., 2011. Frontal cortex biopsy samples can predict Alzheimer disease. Nature Reviews Neurology 7 (1), 5–5.

Yeh, C., Jones, D. K., Liang, X., et al., 2021. Mapping Structural Connectivity Using Diffusion MRI: Challenges and Opportunities. Journal of Magnetic Resonance Imaging 53 (6), 1666–1682.

Yeo, B. T. T., Krienen, F. M., Sepulcre, J., et al., 2011. The organization of the human cerebral cortex estimated by intrinsic functional connectivity. Journal of Neurophysiology 106 (3), 1125–1165.

Yu, J.-T. and Tan, L., 2012. The Role of Clusterin in Alzheimer's Disease: Pathways, Pathogenesis, and Therapy. Molecular Neurobiology 45 (2), 314–326.

Yu, M., Engels, M. M. A., Hillebrand, A., et al., 2017. Selective impairment of hippocampus and posterior hub areas in Alzheimer's disease: an MEG-based multiplex network study. Brain 140 (5), 1466–1485.

Yu, M., Sporns, O., and Saykin, A. J., 2021. The human connectome in Alzheimer disease — relationship to biomarkers and genetics. Nature Reviews Neurology 17 (9), 545–563.

Yuvaraj, R., Rajendra Acharya, U., and Hagiwara, Y., 2018. A novel Parkinson's Disease Diagnosis Index using higher-order spectra features in EEG signals. Neural Computing and Applications 30 (4), 1225–1235.

Zádori, D., Veres, G., Szalárdy, L., et al., 2014. Glutamatergic Dysfunctioning in Alzheimer's Disease and Related Therapeutic Targets. Journal of Alzheimer's Disease 42 (s3), S177–S187.

Zhang, H. and Jacobs, J., 2015. Traveling Theta Waves in the Human Hippocampus. Journal of Neuroscience 35 (36), 12477–12487.

Zhao, Z., Sagare, A. P., Ma, Q., et al., 2015. Central role for PICALM in amyloid-β blood-brain barrier transcytosis and clearance. Nature Neuroscience 18 (7), 978–987.

Zhou, P., Wu, Q., Zhan, L., et al., 2023. Alpha peak activity in resting-state EEG is associated with depressive score. Frontiers in Neuroscience 17, 1057908.

Zlokovic, B., Martel, C., Mackic, J., et al., 1994. Brain Uptake of Circulating Apolipoproteins J and E Complexed to Alzheimer's Amyloid β. Biochemical and Biophysical Research Communications 205 (2), 1431–1437.

Index